THREE DIMENSIONAL NUMERICAL MODELLING OF RECHARGE: CASE STUDY: EĞRİ CREEK SUB-BASIN, İZMİR

A Thesis Submitted to
the Graduate School of Engineering and Sciences of
İzmir Institute of Technology
in Partial Fulfillment of the Requirements for the Degree of

DOCTOR OF PHILOSOPHY

in Civil Engineering

by
Yavuz ŞAHİN

May 2022
İZMİR

ACKNOWLEDGMENTS

First and foremost, I would like to express my sincere gratitude to my advisor and co-advisor, Prof. Gökmen Tayfur and Prof. Alper Baba for their guidance and constant motivation throughout this study. I have learned so much from them, both as a person and a researcher.

I also would like to thank the members of my dissertation committee, Prof. Orhan Gündüz and Prof. Şebnem Elçi, for their support and guidance at times I lost my way and for their significant contributions to the study.

I also thank the members of my defense jury, Assoc. Prof. Ayşegül Özgenç Aksoy and Assoc. Prof. Gökçen Bombar, for generously offering their time and valuable comments.

My highest appreciation goes to my parents Deniz & Yüksel Şahin and my beloved brother Oğuz Şahin for their endless support and sacrifice throughout my life. If it weren't for you, I wouldn't be where and who I am today.

And for my mother Deniz Şahin, thank you for being endlessly patient and believing in me, even when I could not believe in myself.

ABSTRACT

THREE DIMENSIONAL NUMERICAL MODELLING OF RECHARGE: CASE STUDY: EĞRİ CREEK SUB-BASIN, İZMİR

Although the science of water management has experienced significant improvements over the past century, many issues still require the attention of the scientific community. Global change, growing population and increasing pressure on existing water supplies have intensified the need for further improvement of water resources management practice. The purpose of this special issue is to present some of the latest research carried out in the area of water resources management under uncertain and changing conditions. Study in this issue highlight recent consuming in this basin covering all the surface & groundwater of the hydrologic cycle. The large demand for drinking, irrigation and industrial water in the region of K. Menderes Basin. The main objective of the study is to emerge capacity of surface and groundwater. Also, notice that decreasing groundwater level in basin. This river basin agricultural dominant has fertile land and range of harvest diversity in all season. In dry periods, Groundwater level has been facing decreases for past 30 years. Every private farm has private wells that were drilled without permission. These cause depletion of groundwater and restraining the usage of groundwater. Another subject is industrial usage of groundwater and increasing population in area. For this purpose, surface artificial recharge methods in conjunction with underground dam construction were investigated in Egri Creek sub-basin. Thus, their contributions to the groundwater levels were investigated with the help of a numerical model.

Keywords: Groundwater; Artificial Recharge; Numerical Modeling; Surface Spreading Methods; Design Optimization; Hydraulic Engineering.

ÖZET

BESLEME ÜÇ BOYUTLU SAYISAL MODELLEMESİ: ÖRNEK ÇALIŞMA: EĞRİ DERE ALT-HAVZASI, İZMİR

Su yönetimi bilimi geçen yüzyılda önemli gelişmeler yaşamış olsa da, birçok konu hala bilim camiasının dikkatini gerektirmektedir. Küresel değişim, artan nüfus ve mevcut su kaynakları yönetimi uygulamasının daha da iyileştirilmesi ihtiyacını yoğunlaştırdı. Bu özel durumun amacı, belirsiz ve değişen koşullar altında su kaynakları yönetimi alanında yapılan en son araştırmalardan bazılarını sunmaktır. Bu çalışma, hidrolojik döngünün tüm yüzey ve yeraltı suyunu kapsayan bu havzadaki son tüketimi vurgulamaktadır. K. Menderes Havzası'ndaki içme-kullanma, tarımsal sulama ve sanayi suyuna yönelik olan büyük talebi. Çalışmanın temel amacı, yüzey ve yeraltı sularının kapasitesini ortaya çıkarmaktır. Bu nehir havzası tarımsal üretim yoğunluğuna, verimli topraklara ve her mevsimde hasat çeşitliliğine sahiptir. Kurak dönemlerde, yeraltı suyu seviyesi son 30 yılda ciddi bir düşüş yaşamıştır. Her tarımsal üretim yapan çiftliğin izinsiz açılmış kuyuları bulunmaktadır. Bunlar yeraltı suyunun tükenmesine ve yeraltı sularının gelecek dönemlerde kullanılabilmesini kısıtlamaktadır. Diğer bir husus ise yeraltı sularına endüstriyel kullanım ve artan nüfus karşısında olan taleptir. Bu amaçla, yeraltı barajı inşaatı ile birlikte yüzeysel yapay besleme yöntemleri Eğri Dere alt havzasında araştırılmıştır. Böylece sayısal bir modelleme yardımıyla, yeraltı suyu seviyelerine katkıları araştırılmıştır.

Anahtar Kelimeler: Yeraltı Suyu; Yapay Besleme; Nümerik Modelleme; Yüzey Yayılım Metodu; Tasarım Optimizasyonu; Hidrolik Mühendisliği.

To the woman who shaped me with her presence: my mother Deniz

TABLE OF CONTENTS

LIST OF FIGURES ix

LIST OF TABLES xi

CHAPTER 1. INTRODUCTION……..…….1

1.1. Statement of the Problem 1

1.2. Objective and Scope 2

1.3. Outline of the Thesis 3

CHAPTER 2. LITERATURE REVIEW.....5

2.1. Introduction 5

2.2. Selected Literature 5

2.3. Surface Spreading Method 6

2.4. Direct Injection 8

2.5. Underground Dam 8

2.6. Modeling of Artificial Groundwater Recharge 9

CHAPTER 3. STUDY AREA……..11

3.1. Introduction 11

3.2. Climate 12

3.3. Geology 15

3.3.1. Regional Geology 15

3.3.2. Local Geology 16

3.4. Hydrology and Hydrogeology 19

3.4.1. Surface Water Resources 19

3.4.2. Hydraulic Parameters 22

3.4.2.1. Saturated Zone 22

3.4.2.2. Unsaturated Zone 22

3.4.3. Groundwater Levels & Contours in Site 24

CHAPTER 4. METHODOLOGY……27

4.1. Introduction 27

4.2. Field Tests 28

4.2.1. Research Well 28

4.2.2. Evaluation of Field Tests 29
4.2.2.1. Pumping Tests 29
4.2.2.2. Kriging Method 31
4.2. Investigation of Alluvium Aquifer 33
4.2.2.Laboratory Studies 33
4.2.2.1. Type of Soil 33
4.2.2.2. Water Content and Specific Gravity 35
4.2.2.3. Porosity 36
4.2.2.4. Permeability 37
4.2.3. Unsaturated Hydraulic Conductivity 37
4.2.3.1. Hysteresis in Soil Water Retention Curve 39
4.3. Model Description 40
CHAPTER 5. RECHARGE MODELING……41
5.1. Conceptual Model 41
5.2. Numerical Model 42
5.2.1. Finite Element Mesh 43
5.2.2. Boundary Conditions 44
5.2.3. Initial Conditions 46
5.2.4. Model Calibration and Validation 47
5.2.4.1. Model Validation 51
CHAPTER 6. ARTIFICIAL RECHARGE SCENARIOS……56
6.1. Introduction 56
6.2. Recharge Basin Design 56
6.3. Artificial Recharge Scenarios 57
6.4. Underground Dam 60
6.4.1. Modeling of Underground Dam 62
6.4.2. Finite Element Grid 64
6.4.3. Boundary Conditions 64
6.4.4. Underground Dam Model Results 65
6.5. Discussion of the Results 67
CHAPTER 7. GROUNDWATER TABLE HYDRAULIC IMPACT……69
7.1. Introduction 69
7.2. Analytical Modeling 69
7.2.1. An Overview of The Hantush Spreadsheet 70

7.3. Mounding Scenarios 71
7.3.1. Adjustment of Basin Size, Hydraulic Properties and Recharge Rate 73
7.4. Discussion of the Results 75
CHAPTER 8. ECONOMICAL FEASIBILITY OF EGRI CREEK……76
8.1. Introduction 76
8.2. Annual Interest and Amortization Expenses 78
8.3. Annual Operating and Maintenance Expenses 78
8.3.1. Renovation Factor 79
8.4. Revenue of The Project 80
8.5. Rantability 80
8.6.Construction Work Schedule and Interest Application Periods 81
8.7. Economic Feasibility of Underground Dam 81
8.7.1. The Cost of an Underground Dam 82
8.7.2. The Facility Costs 83
8.7.3. Annual Operating and Maintenance Expenses 83
8.7.4. Renovation Factor 83
8.8. Revenue of the Underground Dam 84
8.9. Discussion of the Results 85
CHAPTER 9. SUMMARY, CONCLUSIONS AND FUTURE STUDIES…….86
REFERENCES 93
APPENDIX A 99
APPENDIX B 113

LIST OF FIGURES

Figure **Page**

Figure 1. Location map of the KMRB and the Eğri Creek Sub-basin 2
Figure 2. Examples of water spreading structures (Reddy, 2008) 7
Figure 3. The location of Eğri Creek subbasin in Küçük Menderes River Basin. 11
Figure 4. The location of Ödemiş Station 12
Figure 5. Average, min. and max. monthly temperature values for Ödemiş Station 13
Figure 6. Seasonal distribution of average annual precipitation for Ödemiş Station. 13
Figure 7. Average, min. and max. monthly precipitation values for Ödemiş Station 14
Figure 8. Average, minimum and maximum evaporation values for Ödemiş Station. .. 14
Figure 9. Regional location of the Küçük Menderes River Basin (DSİ, 2018). 16
Figure 10. Generalized columnar section of KMRB (DSİ, 2016). 17
Figure 11. Geological map of Gökçen region, study area (after Yazıcıgil et. al., 2000) 18
Figure 12. Flow measurement stations in the Küçük Menderes River Basin. 20
Figure 13. Distribution of wells drilled by DSİ in the study area. 23
Figure 14. Cross-section of X-X 24
Figure 15. Cross-section of Y-Y' 24
Figure 16. Location of irrigation wells in the study area. 25
Figure 17. Monthly groundwater level change in the study area (1966-2018). 25
Figure 18. The groundwater level distribution map (October-April, 2018-2019)……26
Figure 19. Flowchart of the steps in artificial recharge of groundwater. 28
Figure 20. Research wells in the study area. 29
Figure 21. Representation of pumping test results of observation wells. 32
Figure 22. Representation of SK-14 borehole 35
Figure 23. Main drying and wetting soil water retention curves because of hysteresis . 40
Figure 24. Schematic view of artificial recharge from Eğri Creek 42
Figure 25. Distribution of finite element mesh along the (W-E) domain 43
Figure 26. Cross-section W-E location and 2D view with boundary conditions. 45
Figure 27. Boundary conditions used in the model. 45
Figure 28. Time variable boundary conditions data from the Ödemiş Station. 48
Figure 29. Material properties for water flow in the model domain. 49

Figure **Page**

Figure 30. Location of observation wells. 50
Figure 31. SK_K27 simulated and observed GWL. 50
Figure 32. Relationship between the observed and simulated groundwater levels. 51
Figure 33. SK_K6 simulated and observed GWL. 52
Figure 34. AK_5 simulated and observed GWL. 52
Figure 35. Relationship between observed and simulated groundwater levels. 53
Figure 36. Relationship between observed and simulated groundwater levels. 54
Figure 37. Location of the recharge basin. 57
Figure 38. Location of the observation points in the HYDRUS-3D. 59
Figure 39. Cumulative water recharge (m^3) for various artificial recharge scenarios. ... 59
Figure 40. Average increase in GWL (m) for various artificial recharge scenarios. 60
Figure 41. Underground dam location (the map from Google Earth) 60
Figure 42. Location of underground dam. 61
Figure 43. A schematic view of subsurface material types in the model domain 62
Figure 44. Underground dam reservoir elevation (m) – volume (m^3) graph 63
Figure 45. Distribution of finite element mesh along the dam axis 64
Figure 46. The observation points in the model domain 65
Figure 47. Modeling of the underground dam with HYDRUS-3D 66
Figure 48. Calculated water budget of underground dam simulation 66
Figure 49. Water table elevation corresponds to observation points 67
Figure 50. Representation of groundwater mound beneath the rectangular area……70
Figure 51. The Hantush results of groundwater level 71
Figure 52. Modeling results of groundwater mounding with HYDRUS-3D 72
Figure 53. The Hantush and HYDRUS-3D mounding results 72
Figure 54. The relationship between HYDRUS-3D&Hantush mounding results 73

LIST OF TABLES

Table **Page**

Table 1. Eğri Creek upstream developed (predicted) flows (m^3/sec.) 21
Table 2. K and S values of observation well in the study area. 33
Table 3. Sieve analysis results of SK-14. 34
Table 4. SK-14 laboratory soil experiment results 37
Table 5. Daily discharge of Eğri Creek in simulation period (m^3/sec.). 46
Table 6. Values of R^2, root mean square error and mean absolute error 55
Table 7. Depth of recharge water & corresponding hydraulic level in basins……58
Table 8. Underground dam volume (m^3) – elevation (m) values 63
Table 9. The scenarios of groundwater mounding depend on different parameter 74
Table 10. Bill of quantity Eğri Creek artificial recharge pool project (**1$=14.65**) 77
Table 11. Renovation period and renovation factors 79
Table 12. The renovation, operating and maintenance expenses 79
Table 13. The annual income and expense ratio (R) 81
Table 14. The work schedule and construction interest application period 81
Table 15. The estimated costs of the underground dam 82
Table 16. The facility costs of the underground dam 83
Table 17. The renovation factors for each facility 84
Table 18. The revenue of the underground dam 84
Table 19. Annual income and outcome ratio (rantability) 85

CHAPTER 1

INTRODUCTION

1.1. Statement of the Problem

Groundwater is one of the important resources in agriculture, industry, and domestic consumption. About 43% of the groundwater is used in agricultural activities (Siebert et. al., 2010). Due to climate change and unconscious human activities, groundwater resources are threatened. In addition, decreasing rainfall rates within past decades have led to an increase in groundwater usage. More wells were drilled to meet this demand, which resulted in a significant decrease in groundwater storage. Although groundwater resources are renewable, it is not easy to replenish groundwater storage. The rate of groundwater replenishment depends on several factors, such as climate, and anthropogenic effect. When natural recharge processes become inadequate, artificial methods used to accelerate the recharge process.

The purpose of this study is to assess the potential for artificial recharge of groundwater in the Küçük Menderes River Basin (KMRB) in Western Turkey. (KMRB) has been faced continuous groundwater level decreases for the past 30 years. Most of the groundwater in the basin is used for irrigation in the summer season when the Küçük Menderes River and its tributary streams are mostly dry. Streams in the basin generally run from October through April in response to precipitation received in this period. Thus, extensive pumping in summer seasons reduces groundwater levels significantly, thereby allowing a groundwater storage potential to be recharged in the wet seasons when the streams are running. The groundwater storage increases by utilizing this excess water obtained in wet periods to recharge the underlying aquifer. A reasonable way to achieve this is to apply the methods of artificial recharge of groundwater. These methods aim to store water for later use when water is inadequate.

This study aimed to explore and augment the potential for artificial groundwater storage in one of the sub-basins of the Küçük Menderes River Basin, known as the Eğri-Creek Basin (Figure 1). For this purpose, surface artificial recharge methods in conjunction with underground dam construction were investigated. So, their contributions to the groundwater levels were investigated with the help of a numerical model.

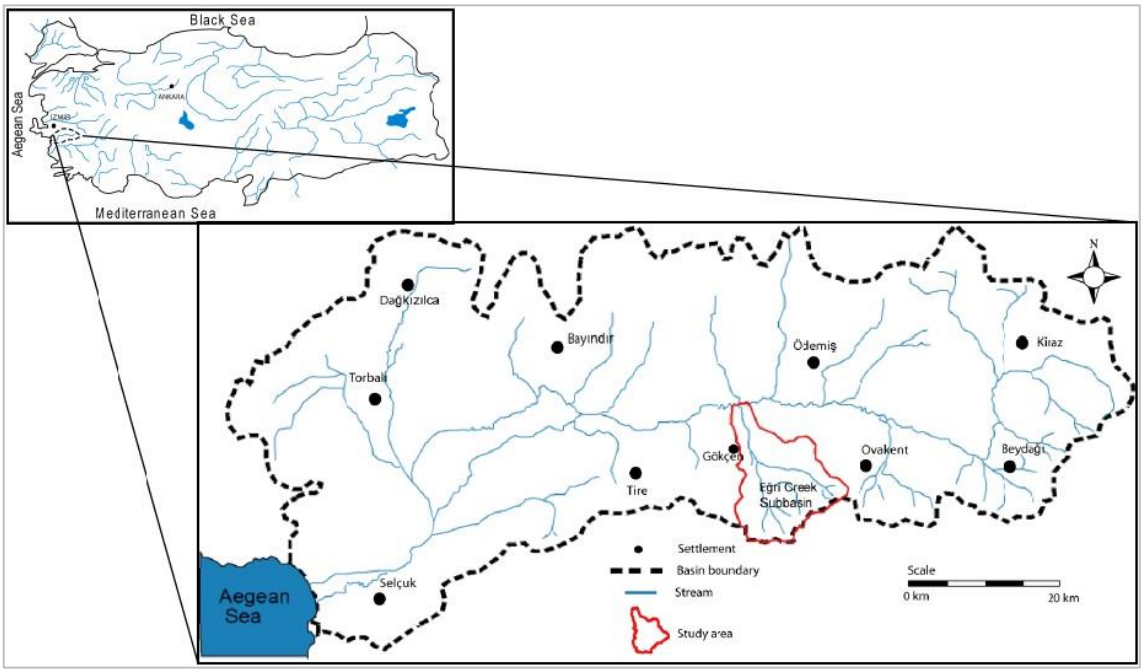

Figure 1. Location map of the Küçük Menderes River Basin and the Eğri Creek Sub basin

1.2. Objective and Scope

The main objective of this study is to develop a method for augmenting the groundwater budget. To predict groundwater recharge of the alluvium aquifer using surface spreading methods. For this study, the following research is completed

- Sixteen research wells were drilled through the aquifer in the study area. The depth of the wells ranges from 26m to 148m.
- The hydraulic properties of the alluvium aquifer determine by using research well data and laboratory tests.
- Long-term meteorological data collected.
- Long-term groundwater level monitoring data collected.
- HYDRUS 3D program used to determine recharge capacity.
- According to study area test results, GIS-based recharge distribution and hydraulic conductivity were maps prepared.
- Alternative artificial recharge pool scenarios and their effects on groundwater levels were examined.

- One of the aquifer recharge methods is an underground dam analyzed in the southern part of the study area.
- Economic feasibility is calculated and the most feasible option recommended.

These are analyzing steps for monitoring the change in groundwater level by designing an artificial recharge pool on the surface. It is to find the artificial recharge pool scenario in dimensions and economy that provide the most effective benefit with alternatives.

1.3. Outline of the Thesis

This thesis consists of nine chapters. The first chapter presents a general approach to the content of the thesis.

Chapter 2 gives an overview of the studies in the literature that aim to develop alternative design procedures to be used for improving the groundwater. The shortcomings of the summarized work are pointed out in this chapter.

Chapter 3 is to determine the characteristics of the study area with many field tests and observations carried out. In addition, the information given about the latest state of the groundwater level in the study area.

Chapter 4 is to determine the modeling methodology. Initial conditions, boundary conditions, and geological/hydrogeological features of the study area were appointed. After defining these features, the model was run with governing equations for numerical solutions.

Chapter 5 presents the calibration and verification process. Groundwater levels were observed with three observation wells (SK_K27, SK_K6 and AK_5) over 180-days in the study area. **SK_K27**, measured and simulated results used for the calibration step. The observation wells **SK_K6** and **AK_5** were used for the validation process.

Chapter 6 consists of alternative scenarios which depend on Chapter 5 calibrated parameters. Moreover, the effects of the scenarios on the groundwater level were analyzed. The parameters that most affected the results were revealed using regression analysis methods.

Another groundwater recharge method, the underground dam, was studied in this chapter. The underground dam was modeled with HYDRUS 3D. The budget of water the underground dam can store upstream of the domain with natural precipitation data under appropriate topographic/geologic conditions was analyzed.

In Chapter 7, to determine the height and range of groundwater mounding used an Excel Spreadsheet to solve the Hantush (1967) equation. The groundwater mounding model result of the scenarios in Chapter 6 was compared with the data obtained from the Hantush (1967) analytical equation.

In chapter 8 presents, after selecting the appropriate groundwater recharge scenario in Chapter 6, the economic feasibility of the scenario was detailed.

The summary of the study and the conclusions inferred are presented in Chapter 9.

CHAPTER 2

LITERATURE REVIEW

2.1. Introduction

The increasing demand for water in many regions worldwide, including Turkey, has motivated the implementation of more intensive water management measures to achieve more efficient utilization of the limited available water supplies. To increase the natural replenishment of groundwater, artificial recharge of groundwater has become increasingly important across Turkey. Artificial recharge is accomplished by pumping excess water from rivers and lakes to suitable aquifer system either by surface infiltration in basins or by pumping directly into the underground. The discharge in rivers usually varies over the season. Therefore, an artificial recharge scheme can be operated so that the diversion of surface water for infiltration primarily takes place during the season with sufficient discharge, increasing the underground storage of water during that time.

2.2. Selected Literature

Artificial recharge of groundwater is defined by Reddy (2008) as an engineered system designed to introduce and store water beneath the ground. In other words, it refers to the increase in the amount of water that is introduced into the ground, artificially (Philips, 2003).

In many parts of the world especially arid and semi-arid regions, groundwater extractions are exceeded groundwater recharge. The groundwater level decreased by over-exploitation of groundwater resources. Artificial recharge provided more recharge than natural conditions. The main objective of artificial recharge is to augment groundwater resources for later usage.

Artificial recharge systems are considered hydrological, source water, operation-maintenance, legal and regulatory issues. Banks et al. (1954) suggested factors for designing a suitable artificial recharge project. These are; hydrogeological considerations, source water considerations, operation-maintenance considerations, legal and regulatory

issues. Soil textures and geology, availability of sufficient land, silt control, maintenance of percolation rates, and quality of the recharged water can be given as some examples. Bouwer (2002) pointed out the type of the aquifer, the permeability of geological formations lying on the aquifer, characteristics of the vadose zone, and homogeneity are affected the recharge rate and design procedure of the recharge system. If the vadose zone is thin, groundwater mounding will occur during the recharge and cause pooling, leading to a decrease in the recharge rate. On the other hand, if the vadose is too deep, the vertical transit time to the aquifer may be too long. Heterogenous soils increase lateral dispersion of recharge water, and therefore increase time and distance; however, very uniform soils increase air entrainment in the vadose zone, thus reducing recharge (Reddy, 2008).

In addition, the temperature of the water can affect the recharge rate. Since cold water is more viscous, its recharge rate will be lower than warm water (Lytle, 1994).

Sources of recharge water include surface water from streams or lakes, reclaimed wastewater, rainfall and storm runoff, imported water from other areas, groundwater from other aquifers and treated drinking water. Water quality plays a critical role in direct injection methods. For water spreading, since the unsaturated zone and the material in the aquifer act as natural filters and clean water, additional treatment is not necessary (Peters, 1994).

The annotated bibliographies by Todd (1959) and Signor et al. (1970) can be given as the basic references on the subject of the artificial recharge of groundwater. Recently, the interest in artificial recharge has increased due to the growing population, decreasing rainfall rates and increasing demand for freshwater.

Generally, the demands for the water are not uniform; i.e., it increases in dry seasons, while decreasing in wet seasons, resulting in fluctuations in the water table.

2.3. Surface Spreading Method

The most common method of artificial recharge of groundwater is the surface spreading method, where recharge water is allowed to infiltrate down to the water table from natural or man-made depressions (Phillips, 2003). The aquifer should be unconfined in order to give response to the infiltrated water. Based on the permeability of the underlying units in the unsaturated zone, water spreading methods can be divided into two subgroups, surface spreading and subsurface spreading methods. Recharge pools and

pits are some examples of surface spreading methods, whereas infiltration galleries can be classified as subsurface spreading methods (Figure 2). In subsurface spreading, a layer that prevents recharge (such as a clay layer) exists at the near ground surface, hence recharge water is introduced at some depth beneath the land surface but above the water table (within the vadose zone) and then allowed to infiltrate into the unconfined aquifer.

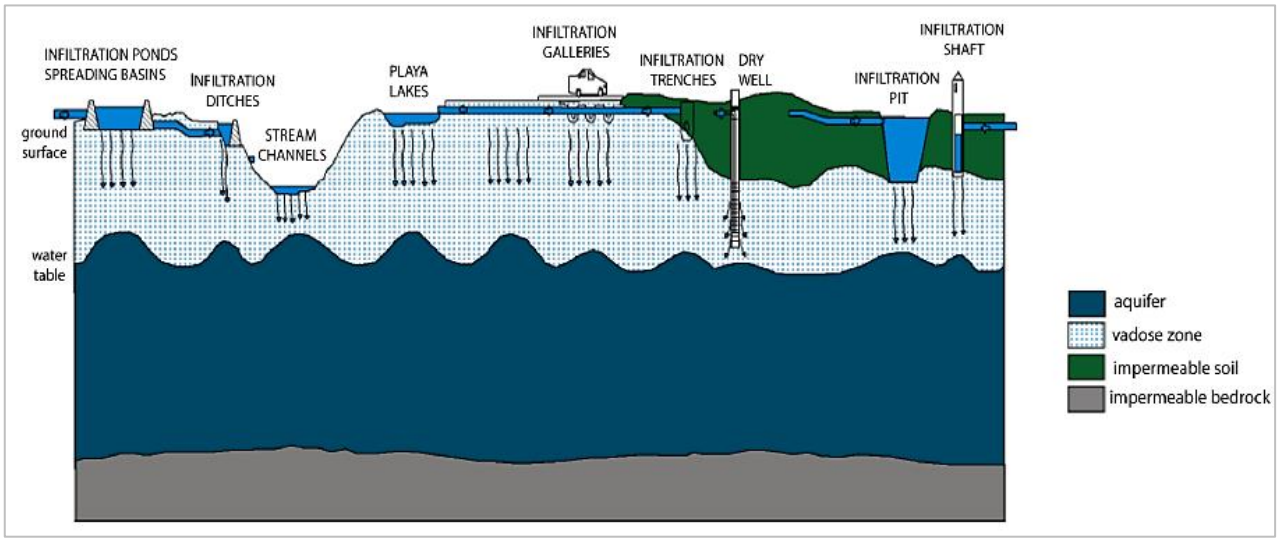

Figure 2. Examples of water spreading structures (Reddy, 2008)

Maximizing the infiltration rate beneath structures is the main concern in water spreading. Infiltration rates are closely related to the physical and chemical characteristics of soil and subsurface conditions. Ground shape, surface soils and physiography can be used as a guide for the prediction of these conditions (Richter and Chun, 1959; Schiff and Dyer, 1964).

Clogging appears to be the most limiting technical problem in artificial recharge. The phenomenon is known but the processes are triggering clogging and their interrelations are still not fully understood and particularly. It is noted that even small air entry in the water or operation can lead to clogging. To overcome this situation, desilting of floodwater before spreading is recommended (Berend, 1967). Also, the maintenance and cleaning of the recharge pool prevent clogging from siltation during rainy periods.

Surface spreading methods require extensive land areas, permeable surface materials with high vertical permeability, periodic maintenance to prevent clogging, and little or no water pretreatment (Kimrey, 1989). On the other hand, high evaporation losses and groundwater vulnerability to surface contamination make these methods inapplicable

for nearby land use. In the case of subsurface spreading, evaporation losses and required land area are minimized, but initial costs are increased. Besides, it is difficult to clean these structures (Reddy, 2008).

2.4. Direct Injection

Another method of artificial recharge is direct injection. Recharge wells and aquifer storage and recovery (ASR) wells are examples of direct injection methods, where water is injected into the aquifer (Phillips, 2003). The recharge well and its purpose were briefly described with equations derived from idealized boundary and permeability conditions by Thiem (1923). Simpson (1948) described the factors affecting recharge rates in wells. Dewey (1933) summarized the conditions where recharge wells can be used successfully.

The ASR wells are the other type of direct injection method, where water is stored and recovered from the same well. The benefits of the ASR wells were introduced by Pyne (1994). Requirement of small land area, frequent maintenance, and monitoring, the need of pretreatment are the characteristics of the direct injection methods (Kimrey, 1989).

2.5. Underground Dam

Another artificial recharge method is named underground dam. This method prevents running off groundwater beneath the ground. The water is stored upstream of the dam (Nilsson, 1988). The underground dam prevents losses of high evaporation rates, reservoir contamination and siltation risks, etc. (Boochs and Billib, 1994).

The underground dams are usually constructed in arid regions, where irregular rainfall is observed. Well defined and narrow valleys, natural dikes are preferred for locating underground dams. In a hydrogeological point of view, the river beds consisting of sand and gravel are considered as best localities, where suitable storage and flow characteristics are observed.

In Turkey, studying underground dam construction is a new topic. İzmir (Çeşme) is the first location application to prevent the saltiness of water and storage purposes.

Other than Çeşme, experiments on the underground dams were conducted in Yahşihan, Kırıkkale, and Malıboğazı, Ankara (Apaydın, 2009; Apaydın et al., 2005).

2.6. Modeling of Artificial Groundwater Recharge

Anderson et. al. (2015) defined a model as "any device that represents an approximation of the field situation". Scientists and water resources engineers use computer models to better understand the groundwater flow conditions and get an insight into the future of the ground reservoirs. The emergence of high-speed computers has encouraged the using computer simulations as a water management tool.

Optimization techniques are widely used in the artificial recharge of groundwater for the determination of the optimal recharge rate. The main objective is to determine maximum infiltration. Numerical models provide convenient long-term (dry or wet periods) analysis.

The crucial point is determined infiltration from the recharge basin after water collecting.

SEEP/W, MODFLOW, SEAWAT, and HYDRUS are the most commonly used programs for groundwater recharge modeling. In this study, the HYDRUS-3D program was utilized.

The HYDRUS program numerically solves the Richard equation (2.1) for saturated and unsaturated water flow.

$$\frac{\partial \theta}{\partial t} = \frac{\partial}{\partial z}\left[K(\theta)\left(\frac{\partial h}{\partial z} + 1\right)\right] \tag{2.1}$$

K is the hydraulic conductivity,

h is the matric head induced by capillary action,

z is the elevation above a vertical datum,

Ɵ is the volumetric water content,

t is time.

The governing flow equations are solved numerically using the Galerkin-type finite element method. Depending upon the size of the problem, the matrix equations resulting from the discretization of the governing equations are solved using either

Gaussian elimination for banded matrices or the conjugate gradient method for symmetric matrices and the orthomin method for asymmetric matrices (Mendoza et. al., 1991).

CHAPTER 3

STUDY AREA

3.1. Introduction

The study area is the Egri Creek sub-basin, which is one of the sub-basins of the Küçük Menderes River Basin. It is surrounded by the K. Menderes River in the north and steep mountain ridges in the other direction. The map of the Küçük Menderes River Basin and the location of the Egri Creek sub-basin is shown in Figure 3. The range of sea level is 100msl to 1550msl. The presence of alluvial fans at the front of the mountains is the distinguished character of the area. The Egri Creek, which originates in the mountains in the south of Gökçen, drains the area. The total drainage area of the Egri Creek subbasin is 130.32 km^2.

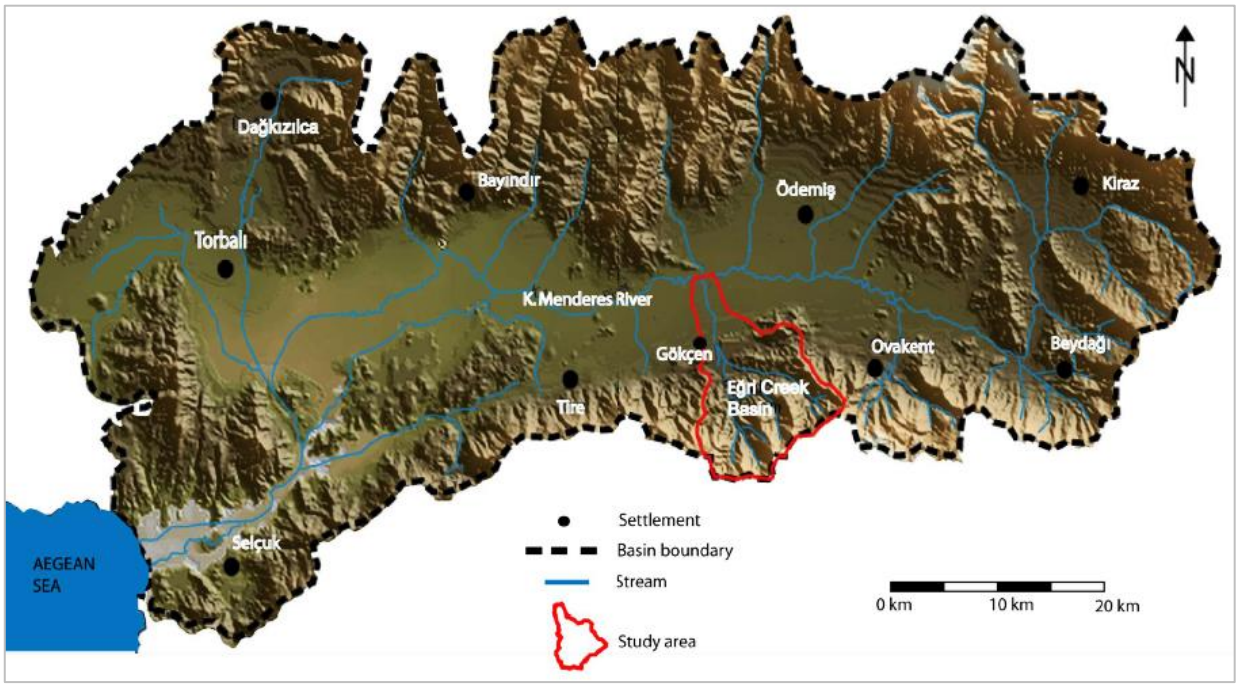

Figure 3. The location of Eğri Creek subbasin in Küçük Menderes River Basin.

3.2. Climate

The study area is under the influence of the Mediterranean (Aegean) climate, where summers are hot and dry, while winters are mild and rainy. Two types of rainfalls are observed in the area. Convective type at depressions in the lands and orographic type at high elevations (Yazıcıgil et. al., 2000).

In Turkey, meteorological data is obtained from DMİ (State Meteorological Works). Meteorological data such as the amount of precipitation, wind direction and speed, humidity, and air temperature were measured from these stations. In K. Menderes River Basin, there are 10 meteorological stations, however, only three of them are located adjacent to the study area, namely Tire, Ödemiş, and Ovakent. Ödemiş Station is the closest station to the model area (about 12 km) and topographically at the same elevation as the model domain. Therefore, the meteorological data used in this study have been obtained from the Ödemiş Station, which is still operated and best represents the model area (Figure 4).

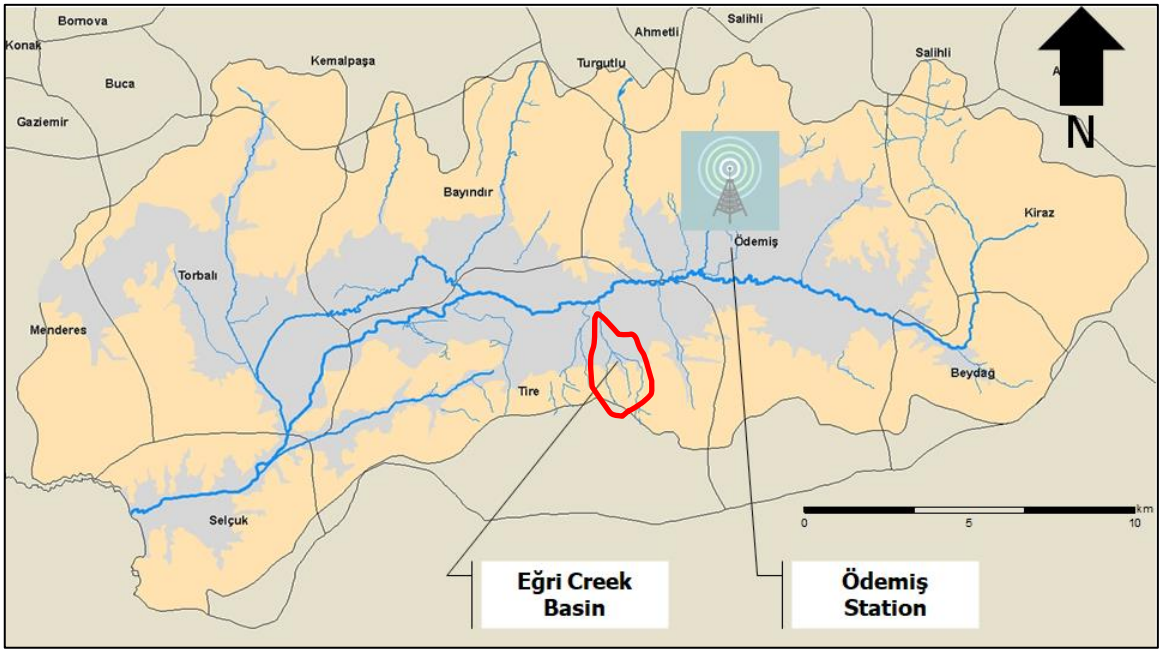

Figure 4. The location of Ödemiş Station

In the Ödemiş Station, from May to September, measured monthly temperatures are above the average. The maximum temperature is measured as 30 °C, whereas the minimum temperature is measured in January as about 3 °C. The annual average

temperature is about 16 °C. Monthly average, maximum and minimum temperature values obtained for the years 1960 – 2018 are shown in Figure 5.

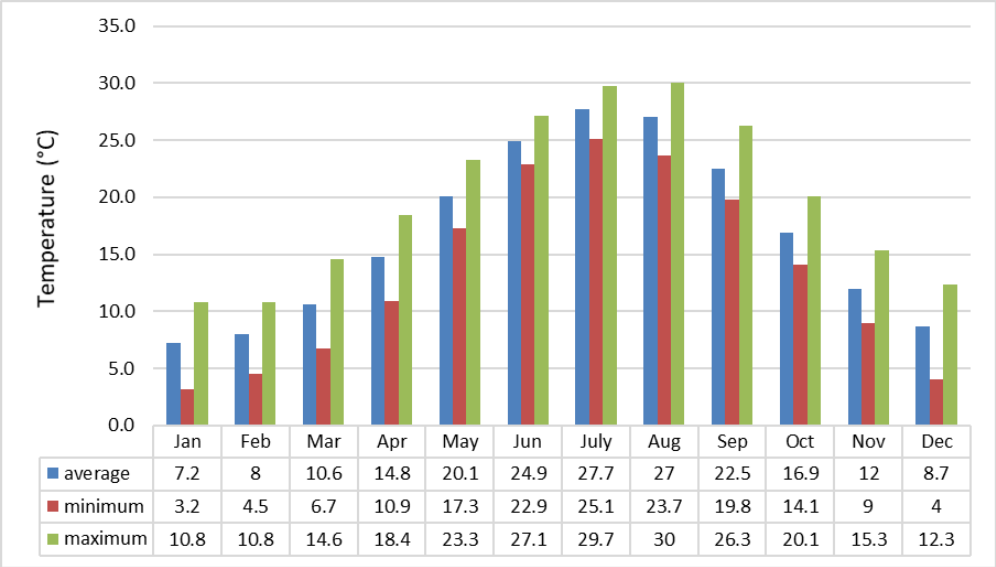

	Jan	Feb	Mar	Apr	May	Jun	July	Aug	Sep	Oct	Nov	Dec
average	7.2	8	10.6	14.8	20.1	24.9	27.7	27	22.5	16.9	12	8.7
minimum	3.2	4.5	6.7	10.9	17.3	22.9	25.1	23.7	19.8	14.1	9	4
maximum	10.8	10.8	14.6	18.4	23.3	27.1	29.7	30	26.3	20.1	15.3	12.3

Figure 5. Average, minimum and maximum monthly temperature values for Ödemiş Station.

As a characteristic of the Mediterranean climate, precipitation is high in winter, but low in summer. The seasonal distribution of average annual precipitation is given in Figure 6. The average monthly precipitation is about 52 mm. The annual total precipitation is about 620,5 mm. Based on the long-term data from the Ödemiş station, the maximum and minimum monthly precipitations are measured as 333.7 mm and 0 mm, respectively. Figure 7. illustrates the monthly average, maximum and minimum precipitation results obtained for the years 1960-2018.

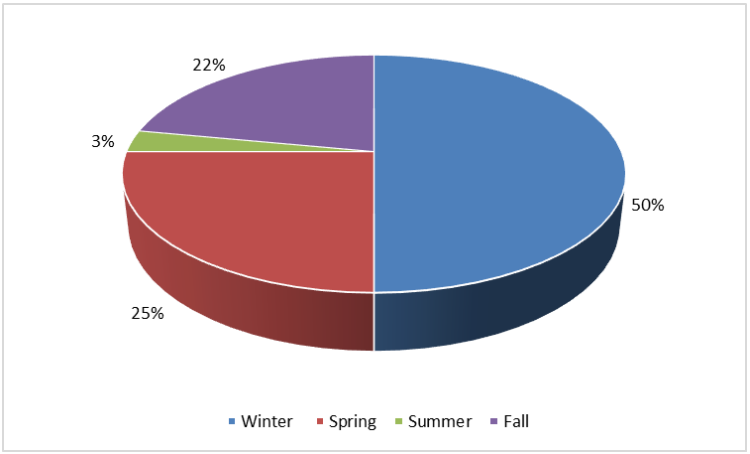

Figure 6. Seasonal distribution of average annual precipitation for Ödemiş Station.

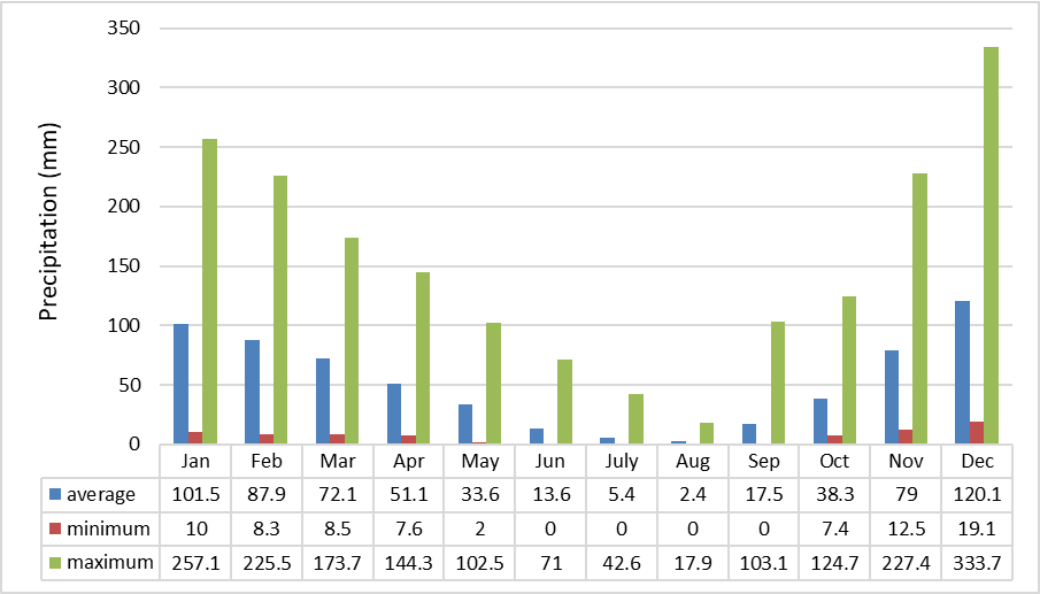

	Jan	Feb	Mar	Apr	May	Jun	July	Aug	Sep	Oct	Nov	Dec
average	101.5	87.9	72.1	51.1	33.6	13.6	5.4	2.4	17.5	38.3	79	120.1
minimum	10	8.3	8.5	7.6	2	0	0	0	0	7.4	12.5	19.1
maximum	257.1	225.5	173.7	144.3	102.5	71	42.6	17.9	103.1	124.7	227.4	333.7

Figure 7. Average, minimum and maximum monthly precipitation values for Ödemiş Station

The monthly maximum evaporation value is measured as 415.4 mm in July, which is the hottest month. The long-term data indicate that the annual total evaporation is measured as 1509.3 mm. The monthly average, minimum and maximum evaporation data obtained from 1960 to 2018 are shown in Figure 8.

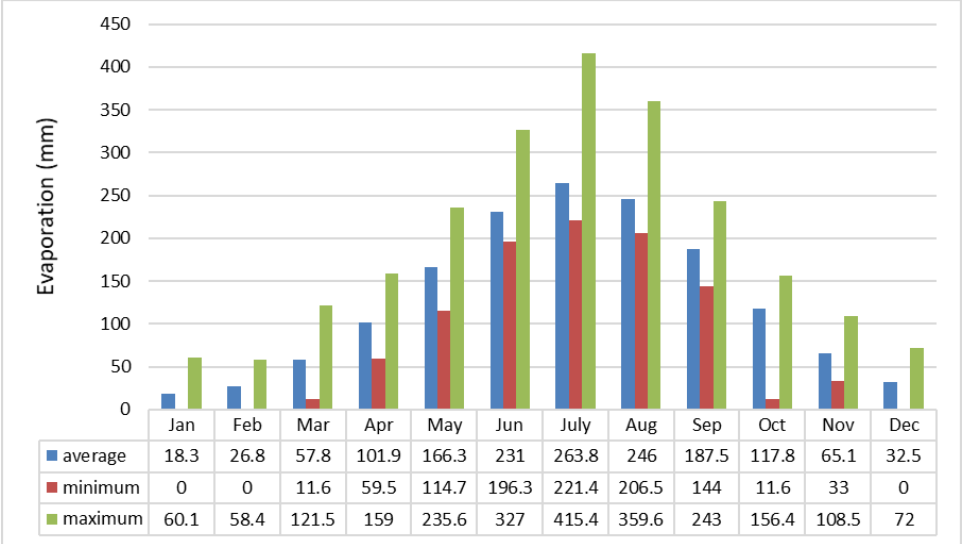

	Jan	Feb	Mar	Apr	May	Jun	July	Aug	Sep	Oct	Nov	Dec
average	18.3	26.8	57.8	101.9	166.3	231	263.8	246	187.5	117.8	65.1	32.5
minimum	0	0	11.6	59.5	114.7	196.3	221.4	206.5	144	11.6	33	0
maximum	60.1	58.4	121.5	159	235.6	327	415.4	359.6	243	156.4	108.5	72

Figure 8. Average, minimum and maximum evaporation values for Ödemiş Station.

3.3. Geology

The geological information related to the Küçük Menderes River Basin and the Eğri Creek sub-basin were synthesized from the final report of ‘’Investigation and Management of Groundwater Resources in Küçük Menderes River Basin” (Yazıcıgil et al., 2000) and ‘’Küçük Menderes River Basin Master Plan Report” (DSİ, 2016).

3.3.1. Regional Geology

Western Anatolia is a region characterized by approximately N-S directed continental extension. E-W and WNW-ESE grabens and their related active normal faults are the most distinctive neo-tectonic features in the region. The Küçük Menderes River Basin is one of the grabens stretching in the east-west direction. It is surrounded by the Gediz and the Büyük Menderes Grabens in the north and south, respectively (Figure 9). In Western Anatolia, metamorphic rocks of Menderes Massif and Neogene sediments are widely observed.

The Küçük Menderes River Basin includes metamorphic assemblages of the Menderes Massif as the basement rocks. It is overlain by the Late Cretaceous-Paleocene Bornova flysch that is represented by limestone blocks, Neogene units and Quaternary sediments. The generalized columnar section and geological map of the Küçük Menderes River Basin (DSİ, 2016) are shown in Figure 10.

The Neogene sedimentary sequence is characterized by the alternation of conglomerate-sandstone-mudstone and clayey limestone and it is mainly observed in the western part of the study area. The volcanics are rarely seen in the Küçük Menderes Basin. Quaternary alluvium and talus unconformably overlie these volcanic.

Quaternary alluvium, alluvial cone, talus, Plio-Quaternary River deposits and red pebbles characterize the Plio-Quaternary unit. The contact between the Plio-Quaternary units and the underlying units is defined as an angular unconformity.

Alluvial fans, composed mainly of boulder, gravel, and sand alternating with clay, are widely observed, especially in the margins of the Küçük Menderes Plain. The thickness of these fans generally exceeds 90m. Their great thicknesses and steep slopes are considered fault indicators. Alluvial fill is another deposit that covers most of the plain. It is composed of an alternation of gravel, sand, silt and clay. Changes in discharge

rate and migration of the river channel are responsible for the deposition of different lithologic units. Faults located in the northern and southern margins of the plain control deposition of the alluvial fills.

The Küçük Menderes River Basin is characterized by E-W trending normal faults due to the N-S extension of the Western Anatolia. The most evident E-W trending normal fault can be observed along the Beydağı-Gökçen-Tire-Belevi belt and is parallel to the longitudinal axis of the basin.

3.3.2. Local Geology

The study area is located near the Gökçen region, which lies between Tire in the west and Adagüme in the east. As seen from the geological map of the study area represented in Figure 11. There are two main lithologic units: alluvial fan deposits and Menderes Massif metamorphic.

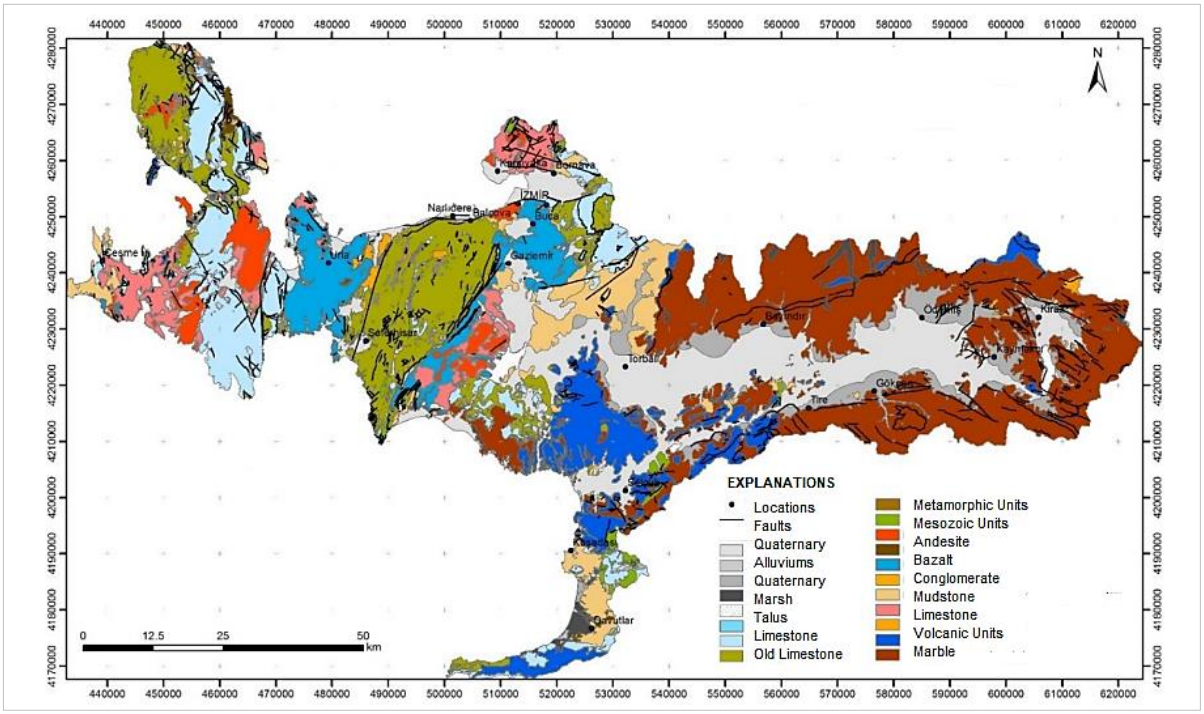

Figure 9. Regional location of the Küçük Menderes River Basin (DSİ, 2018).

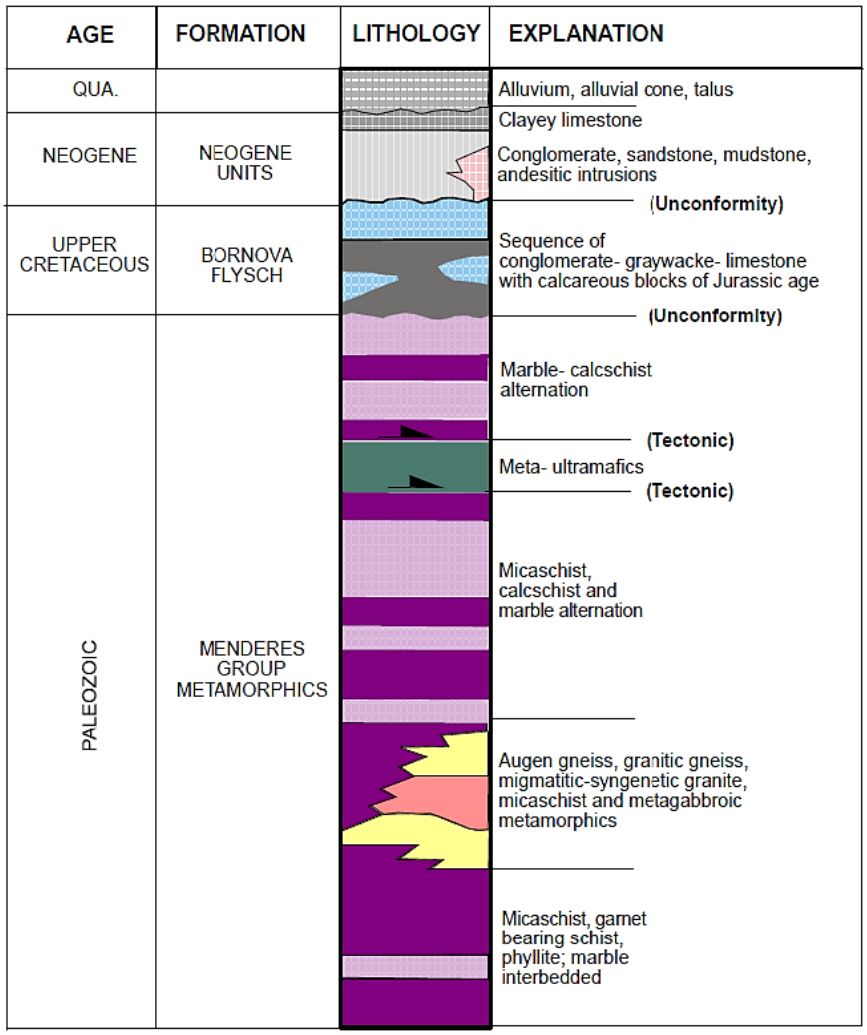

Figure 10. Generalized columnar section of Küçük Menderes River Basin (DSİ, 2016).

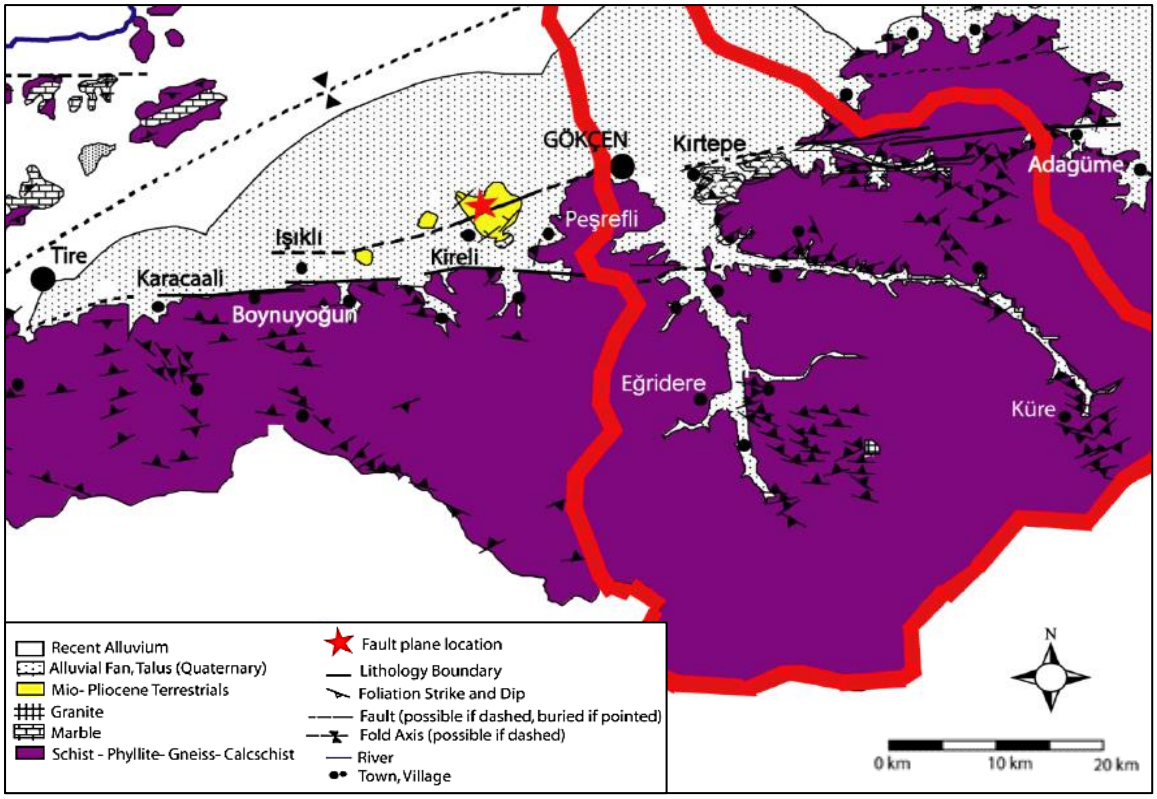

Figure 11. Geological map of Gökçen region, study area (after Yazıcıgil et. al., 2000)

The most characteristic feature of the area is the presence of alluvial fans. The thickness and slope of the fans seem to increase from the Tire towards the eastern parts. The thickness appears to be about 180 m. In addition, the fan material has been transported over long distances into the plain. The main mechanism controlling the formation of the alluvial fans is faulting.

Along the margins of the area, the Menderes Massif metamorphics are widely observed. Especially in the Gökçen region, alternation of schists and gneiss are dominant, whereas marble is not found.

The faults examined in the Gökçen region stretch in the E-W direction. The largest fault can be followed along the Çamlıca, Sarılar, Işıklı, Boynuyoğun and Karacaali villages, not continuously but discretely. To the west, this joins with another fault that reaches to Belevi. Fault steepness, the presence of thick alluvial deposits and Neogene units are the main indicators for the occurrence of the fault. Based on the lineation studies, the fault appears as a left-lateral normal fault.

3.4. Hydrology and Hydrogeology

3.4.1. Surface Water Resources

The Küçük Menderes River Basin is drained by the Küçük Menderes River and its tributaries. One of these tributaries, the Eğri Creek drains the study area. Eğri Creek flows in a northerly direction and joins the Küçük Menderes River at the north.

In artificial recharge projects, the aim is to utilize excess water (that is the rest of the water budget with other projects) as a source to recharge the aquifer. Hence, the potential volume of water that can be collected should be first determined from flow measurements.

In Küçük Menderes River Basin, stream gauging stations operated by DSİ (State Hydraulic Works) and EİEİ (General Directorate of Electrical Power Resources Survey and Development Administration) measure flow data. Along the basin, there are eight-stream gauging stations, where seven stations belong to DSİ and one station belongs to EİEİ. The distribution of the stations in the basin is given in Figure 12.

The two DSİ stream gauging stations operating adjacent to Eğri Creek, namely the Kızılkaya-Eğri Creek (06-42) and Rahmanlar (06-11) stations, were used to determine the discharge pattern in the study area. In order to determine the Eğri Creek flow data, a correlation analysis is conducted between Kızılkaya-Eğri Creek and Rahmanlar stations. Correlation analysis is started to calculate missing monthly flow data for the years (1980-1989 and 1991-2010). Then to obtain a relation (Equ. 3.1) between the flow data for the period between 1986 and 2019. Based on the correlation equation (3.1), Eğri Creek's monthly flow values were calculated. The design flow rate was calculated according to the volume of water remaining from the other projects (Beydağ Dam, Burgaz and Rahmanlar Dam additional water supply) developed upstream. Correlation results of monthly average discharge is shown in Table 1.

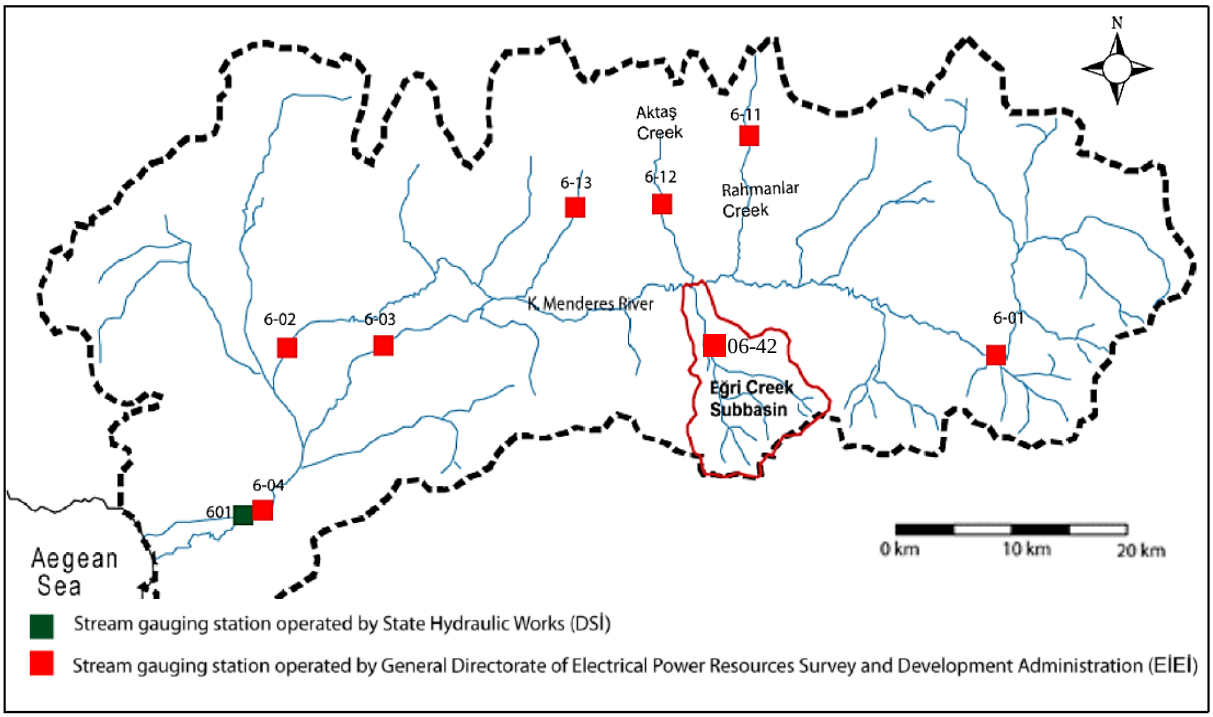

Figure 12. Flow measurement stations in the Küçük Menderes River Basin.

2011-2019 period flows are observed flow values of stream gauge station no. 06-42. The underline 1980-1989 and 1991-2010 period flows were completed with daily correlation with stream gauge station no. 06-11.

$$Q_{06\text{-}42}=0.8844x\ Q_{06\text{-}11}+0.0506 \quad (3.1)$$

Correlation coefficient is $(R^2) = 0.91$

Table 1. Eğri Creek upstream developed (predicted) flows (m^3/sec.)

YEAR	(m^3)												Σ
	OCT.	NOV.	DEC.	JAN.	FEB.	MARCH	APRIL	MAY	JUNE	JULY	AUGUST	SEPT.	
1986	0.069	0.140	0.966	3.231	1.818	3.290	1.257	1.137	1.133	0.000	0.072	0.070	**1.099**
1987	0.040	0.800	2.906	12.354	1.118	1.001	0.374	0.641	0.310	0.077	0.083	0.084	**1.649**
1988	0.074	0.184	12.928	3.445	1.533	4.653	1.870	1.245	0.514	0.010	0.044	0.053	**2.213**
1989	0.006	0.143	0.232	0.882	0.891	1.376	1.411	0.464	0.577	0.036	0.081	0.083	**0.515**
1990	0.074	0.598	0.412	2.792	6.410	1.164	0.799	0.296	0.167	0.083	0.083	0.083	**1.080**
1991	0.072	0.134	0.187	0.610	0.568	0.489	0.434	0.235	0.180	0.000	0.000	0.000	**0.242**
1992	0.077	0.138	0.155	1.081	2.610	1.128	0.371	0.203	0.186	0.084	0.084	0.084	**0.517**
1993	0.077	0.118	0.702	2.500	1.570	1.627	2.169	0.547	0.235	0.081	0.083	0.083	**0.816**
1994	0.068	0.144	0.618	0.330	0.626	4.740	1.351	0.622	0.318	0.082	0.084	0.083	**0.755**
1995	0.078	0.185	0.959	0.375	0.348	0.390	0.214	0.167	0.141	0.087	0.087	0.087	**0.260**
1996	0.011	0.288	0.418	0.758	1.184	1.411	1.081	0.507	0.230	0.000	0.000	0.000	**0.491**
1997	0.077	0.114	0.820	0.432	0.489	0.463	0.721	0.535	0.334	0.081	0.083	0.083	**0.353**
1998	0.078	0.125	0.167	0.211	0.191	0.210	0.425	0.151	0.160	0.076	0.084	0.083	**0.163**
1999	0.077	0.200	0.244	0.555	1.402	1.430	1.394	0.703	0.238	0.080	0.085	0.085	**0.541**
2000	0.076	0.127	0.181	0.259	0.385	0.470	0.379	0.234	0.141	0.084	0.085	0.085	**0.209**
2001	0.077	0.119	0.236	1.447	0.463	1.925	1.843	0.597	0.197	0.083	0.084	0.084	**0.596**
2002	0.077	0.117	0.223	0.258	1.583	0.846	1.206	0.477	0.201	0.083	0.083	0.083	**0.437**
2003	0.078	0.126	0.218	0.280	0.317	0.520	0.871	0.352	0.188	0.085	0.084	0.084	**0.267**
2004	0.076	0.126	0.513	0.902	1.475	1.227	0.992	1.952	0.606	0.073	0.083	0.068	**0.674**
2005	0.052	0.300	0.432	1.508	7.901	1.619	0.903	0.370	0.195	0.084	0.084	0.084	**1.128**
2006	0.078	0.120	0.157	0.215	0.810	0.523	0.394	0.225	0.176	0.084	0.084	0.084	**0.246**
2007	0.077	0.125	0.156	0.252	0.310	0.269	0.272	0.204	0.153	0.081	0.084	0.084	**0.172**
2008	0.078	0.327	1.408	0.971	0.721	1.763	1.542	0.499	0.253	0.080	0.083	0.104	**0.652**
2009	0.053	0.164	0.197	0.649	3.576	1.198	1.017	0.269	0.277	0.082	0.083	0.083	**0.637**
2010	0.070	0.134	0.316	1.470	1.327	0.903	0.692	0.409	0.178	0.084	0.083	0.083	**0.479**
2011	0.078	0.121	0.302	0.129	0.555	1.259	0.347	0.105	0.138	0.087	0.086	0.085	**0.274**
2012	0.085	0.116	0.189	0.351	2.757	4.877	3.376	0.452	0.252	0.084	0.084	0.084	**1.059**
2013	0.069	0.394	0.200	0.240	0.284	0.265	0.209	0.158	0.143	0.087	0.087	0.087	**0.185**
2014	0.086	0.280	0.514	0.518	0.744	0.826	0.663	0.191	0.100	0.087	0.087	0.087	**0.349**
2015	0.087	0.101	0.182	0.804	3.948	2.936	2.464	0.435	0.182	0.087	0.087	0.087	**0.950**
2016	0.053	0.419	0.643	0.567	4.263	2.005	0.893	0.395	0.185	0.087	0.086	0.086	**0.807**
2017	0.049	0.114	0.221	0.661	0.559	0.460	0.345	0.234	0.170	0.008	0.000	0.000	**0.235**
2018	0.157	0.018	0.218	1.304	1.780	1.186	1.301	0.540	0.215	0.004	0.000	0.000	**0.560**
2019	0.000	0.062	0.192	1.143	2.264	1.978	1.802	0.589	0.211	0.000	0.000	0.000	**0.687**
AVE.	**0.069**	**0.198**	**0.836**	**1.279**	**1.670**	**1.483**	**1.041**	0.475	0.261	0.065	0.070	0.071	0.626

The discharge rates of the Eğri Creek were calculated to determine the maximum and minimum flow rates obtained for each year. The minimum flow rate is necessary to design a regulatory project system.

Eğri Creek discharge showed that 1 (one) hm^3 volume of water could utilize for groundwater recharge in six months (rainy period).

When the Eğri Creek upstream flows are examined. The results showed that Eğri Creek artificial recharge project could be operated for six months. The design discharge value is 70 l/sec.

3.4.2. Hydraulic Parameters

Estimation of hydraulic parameters is a critical issue and directly affects the characterization of the system. Since hydrogeological models usually deal with aquifer simulations, estimation of saturated zone parameters is generally sufficient. However, in artificial recharge models, both saturated and unsaturated parameters should be taken into consideration.

3.4.2.1. Saturated Zone

Hydraulic parameters of the saturated zone include the determination of specific yield, saturated hydraulic conductivity and storativity values, as well as the aquifer top and bottom elevations and water table elevations. Detailed maps, well logs and pumping test results are used for the estimation of the parameters.

Saturated hydraulic conductivity values derived from 13 pumping test results performed in the study area vary from 1.3 to 7.2 m/day. The pumping test results are explained in Chapter 4. DSİ drilled 21 exploration wells to determine the areal extent of the hydrogeological units and soil type (Appendix A).

3.4.2.2. Unsaturated Zone

The unsaturated zone is characterized by alluvial fan materials, which consist of an alternation of talus, gravel, sand, silt and clay. Since the aquifer is unconfined in the study area.

The depth of the unsaturated zone is observed to decrease from north to south. The depth ranges from 60m to 20m throughout the Eğri Creek subbasin, with an average depth of 35m in the study area. Hydraulic parameters for the unsaturated zone are available in the site tests. Van Genuchten's (1980) Soil-Water Retention Curve numerical solution helped determine hydraulic conductivity relationship with water content in HYDRUS 3D.

In the Eğri Creek basin, there are 21 wells drilled by DSİ for exploration of the study area (Appendix A). The distribution of the wells in the study area is shown in Figure

13. The cross sections drawn from two locations along the study area are shown in Figure 14 and 15.

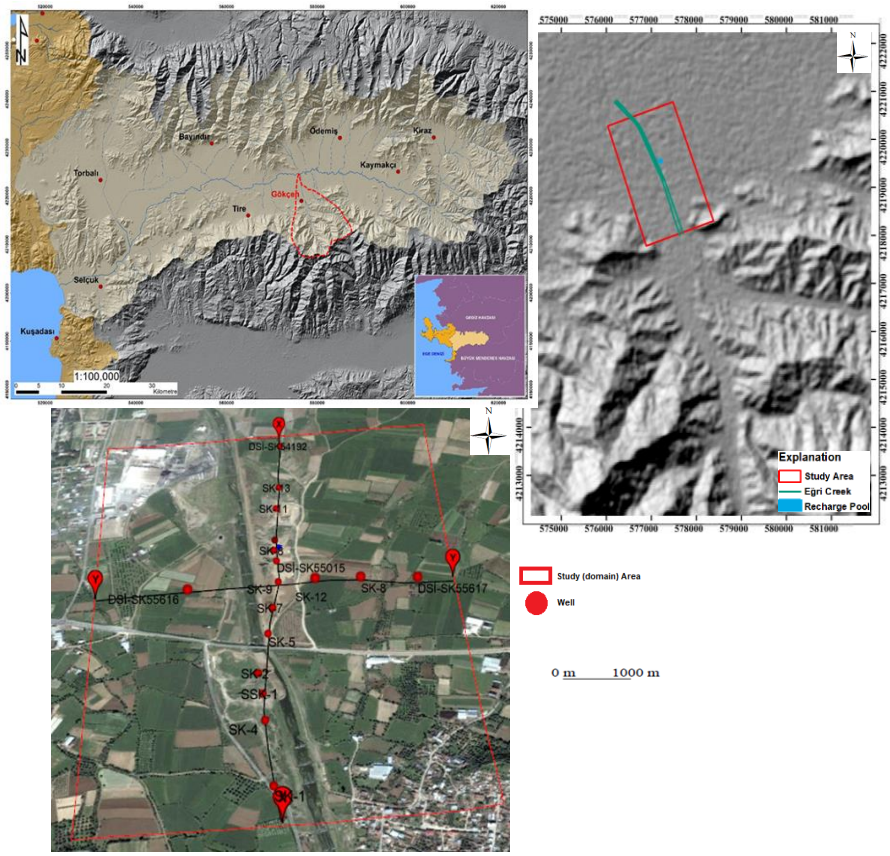

Figure 13. Distribution of wells drilled by DSİ in the study area.

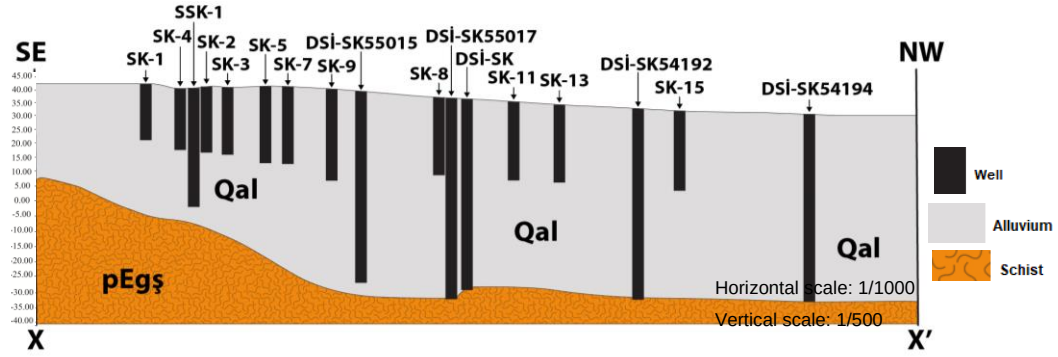

Figure 14. Cross-section of X-X

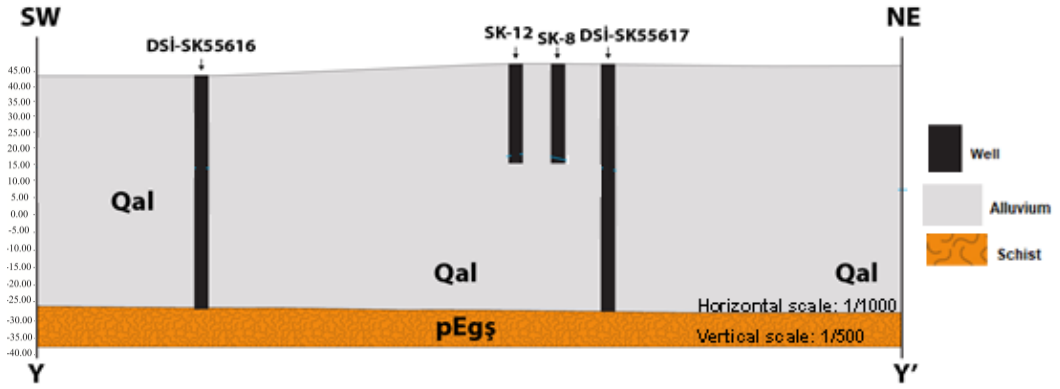

Figure 15. Cross-section of Y-Y'

3.4.3. Groundwater Levels & Contours in Site

Agricultural irrigation and domestic activities from groundwater alluvial aquifers have caused a dramatic decline in groundwater levels over the years. In '60, the groundwater level ranged from 13-25m and reached 35-60m in 1960-2018. In the study area, the groundwater level is approximately 35m. Figure 16 shows the location of irrigation wells, while Figure 17 presents monthly groundwater level change in the study area.

Groundwater levels were measured during rainy and dry periods in the project site and its vicinity. In order to be able to interpret how groundwater levels are distributed within the basin in the study area, a spatial distribution map of point groundwater level values was prepared (October-April in 2018-2019) Figure 18.

Figure 16. Location of irrigation wells in the study area.

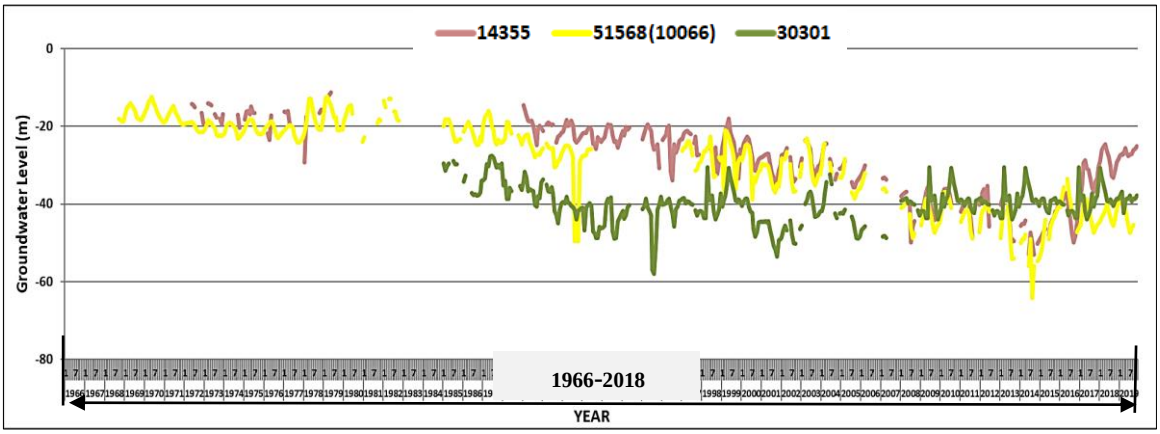

Figure 17. Monthly groundwater level change in the study area (1966-2018).

In the study area, many site tests were performed to understand the character of the area. Previous DSİ site analysis and observations helped us understand saturated and unsaturated zone features. The field and laboratory test results were interpreted in Chapter 4. which was entitled 'Methodology'. Field and laboratory results of the research wells were presented in Appendix A.

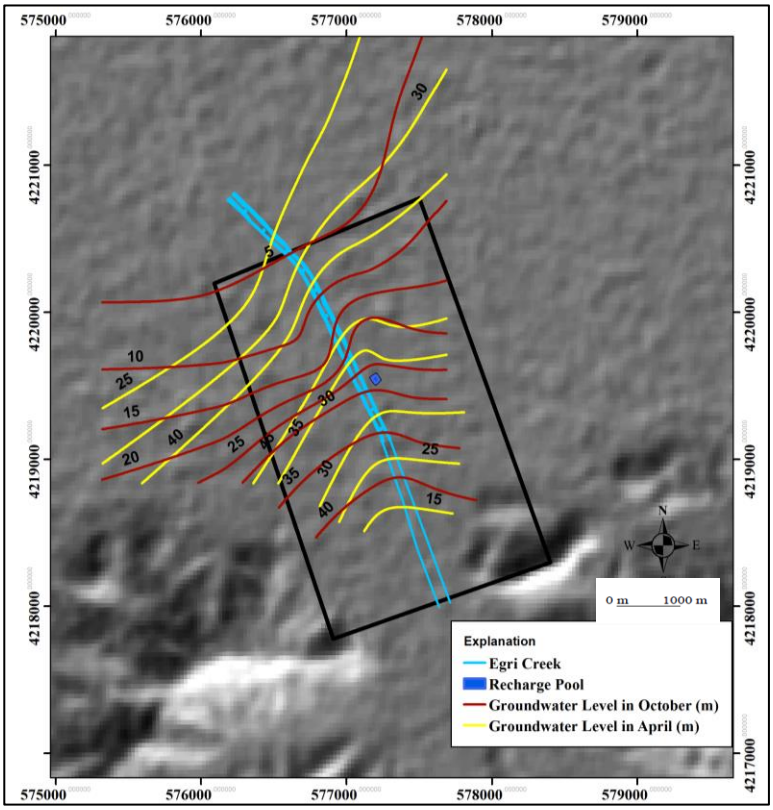

Figure 18. The groundwater level distribution map was created according to site tests (October-April, 2018-2019).

The groundwater level ranges from 15m to 40m. The groundwater levels show that the alluvium aquifer of the project site and its vicinity are recharging from Eğri Creek. The groundwater flow direction is towards the Küçük Menderes River in the north.

CHAPTER 4

METHODOLOGY

4.1. Introduction

A Model is a simplified representation of the real world by using mathematical equations (Wang and Anderson, 1982). The success of a model depends on the degree of how closely the mathematical equations approximate the physical system being modeled.

The methodology of the recharge system design is defined by the American Society of Civil Engineers (Reddy, 2008). The recharge system design starts with preliminary activities such as data collection, determination of processes involved in the system and conceptual model development. Then, in order to gain a better understanding of the system, field investigations and tests are performed. In the design phase, recharge system design, groundwater modeling, economic analysis and environmental assessments are completed. The design phase is followed by construction, operation, and maintenance.

This study aims to show the applicability of artificial recharge methods in the Eğri Creek Sub-basin. Therefore, it includes preliminary activities and recharge system modeling. Before the implementation of any recharge system, a more detailed characterization of the site supported with field and laboratory tests is required (Figure 19).

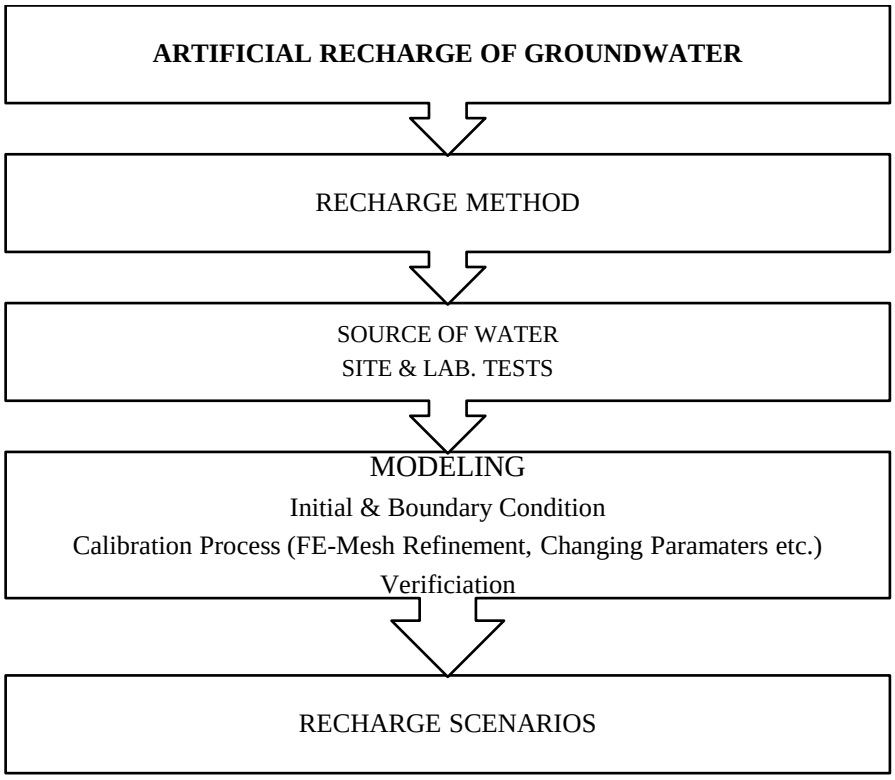

Figure 19. Flowchart of the steps in artificial recharge of groundwater.

4.2. Field Tests

4.2.1. Research Well

1020 m total depth research wells were drilled at 16 points to define the alluvium aquifer lithology of the study area (SK-1 to SK-16) (Figure 20). These drills were used to determine the hydraulic properties of the vadose zone. The depth of the research wells ranges from 26 m to 148 m. Research wells correctly reflect the properties of the alluvium aquifer in the study area. All lithological properties of these well were determined and long-term groundwater level monitoring studies were carried out in the study area.

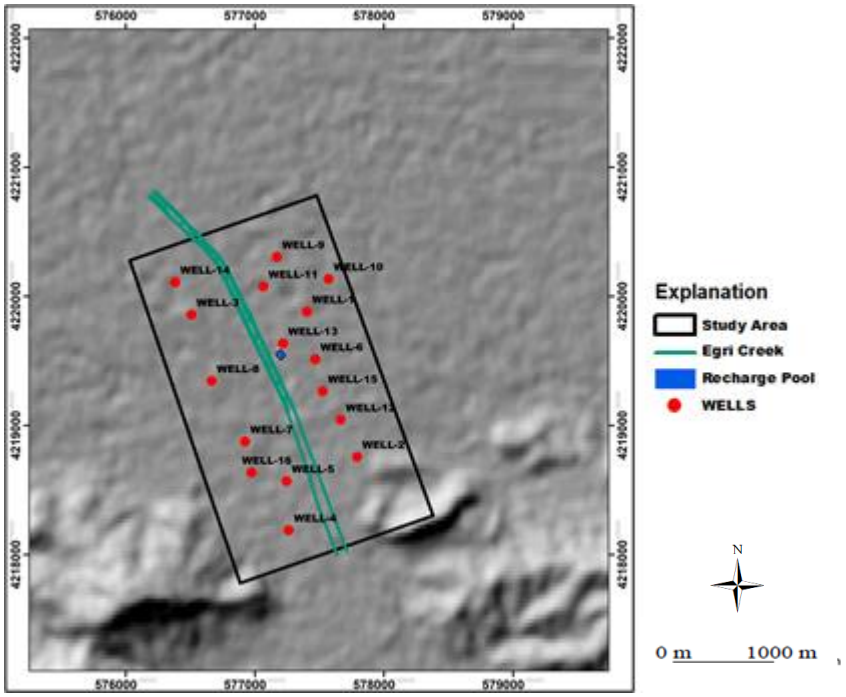

Figure 20. Research wells in the study area.

4.2.2. Evaluation of Field Tests

4.2.2.1. Pumping Tests

Alluvial aquifer tests with pumping tests are long-term, the entire thickness of the aquifer with the results of observation wells are shown in Figure 21. The average hydraulic conductivity and storage coefficients of 13 tests with observation wells within study area and its vicinity were calculated by the Aquifer Test Pro program. In aquifer tests, methods for unconfined aquifer analysis usually are Neumann or Theis with Jacob correction also be used for late-time of the pumping tests. In this study, Neuman model and Theis with Jacob correction for unconfined aquifer are used to fit the water level variation curve of the pumping process. Jacob (1940) proposed the following correction Equation (4.1) for suggesting the use of corrected drawdown (s_{cor}), by measuring the drawdown at the top and bottom of the aquifer separately at a radial distance (D) using a pair of observation wells. The corrected drawdown is calculated as the arithmetic average of top and bottom drawdowns. Saturated hydraulic conductivity values were derived from

13 pumping test results performed in the study area. The range of results is varied from 1.3 to 7.2 m/day. The results are shown in Table 2.

$$s_{cor.} = s - (s^2 \div 2D) \tag{4.1}$$

The equation developed by Neumann representing drawdown in an unconfined aquifer is given by (Neumann, 1975) Equation (4.2.)

$$s = \frac{Q}{4\pi T} W(u_A, u_B, \beta) \tag{4.2}$$

Where W (u_A,u_B,β) is known as the unconfined well function: $u_A = r^2 s / 4Tt$ is the Type A curve for early time steps, $u_B = r^2 S_y / 4Tt$ is the Type B curve for later time steps, $\beta = r^2 K_v / K_H$, K_v , K_H are vertical and horizontal permeability, r is the distance to the observation well, S is storativity, S_y is the specific yield and T is transmissivity. The Theis equation can be performed as follows Equation (4.3).

$$s = \frac{Q}{4\pi T} W(u) \tag{4.3}$$

s: drawdown (m)

Q: pumping rate (m^3/day)

T: Transmissivity (m^2/day)

W(u) is Theis well function, abbreviated w(u). Therefore, we may write Theis equation in compact notation as follows Equation (4.4).

$$W(u) = \int_u^\infty \frac{e^{-y}}{y} \partial y = -\gamma - \log_e u + u - \frac{u^2}{2\times 2!} + \frac{u^3}{3\times 3!} - \cdots \tag{4.4}$$

γ: Euler's constant = 0.577215

The Theis well function may be evaluated using the following infinite series expression. Jacob found that the Theis well function may be approximated using only the first two terms. The critical value of *u* required to achieve reasonable accuracy with the Jacob approximation is alternately given as $u \leq 0.05$. Converting to decimal logarithms, the Jacob equation is to apply in solution plot ***s*** as a function of log t on semi-logarithmic axes and draw a straight line through the datas. To determine T and S (storativity) equations are follows Equation (4.5-4.6). The details can be obtained from Tayfur and Sen (2018).

$$T = \frac{2{,}303Q}{4\pi\Delta s} \tag{4.5}$$

$$S = \frac{2{,}25Tt_0}{r^2} \tag{4.6}$$

4.2.2.2. Kriging Method

To determine the distribution of hydraulic conductivity (K) values in the study area, which were data is obtained from Aquifer Test Pro with pumping field tests. The Kriging (Spatial Analyst) was used. Kriging is a geostatistics method that predicts the value in a geographic area given a set of measurements. Kriging assumes that the distance or direction between sample points reflects a spatial correlation that can be used to explain variation in the surface. The Kriging fits a mathematical function to a specified number of points, or all points within a specified radius, to determine the output value for each location. Kriging is most appropriate when you know there is a spatially correlated distance or directional bias in the data. It is often used in soil science and geology.

Kriging is similar to IDW in that it weights the surrounding measured values to derive a prediction for an unmeasured location. The general formula for both interpolators is formed as a weighted sum of the data Equation 4.7.

$$Z(s_0) = \sum_{i=1}^{N} \lambda_i Z(s_i) \tag{4.7}$$

Where;

$Z(s_i)$: the measured value at the *i*th location.

λ_i: an unknown weight for the measured value at the *i*th location.

s_0: the prediction location.

N: the number of measured values.

To make a prediction with the Kriging interpolation method, two tasks are necessary: uncovered the dependency rules and make the prediction.

To realize these two tasks, kriging goes through a two-step process: it creates the variograms and covariance functions to estimate the statistical dependence (called spatial autocorrelation) values that depend on the model of autocorrelation (fitting model) and it predicts the unknown values (making a prediction). There are two kriging methods, ordinary and universal. Ordinary kriging is the most general and widely used of the kriging methods and is the default. In this study, the ordinary kriging method was used.

The results of pumping tests of observation wells are demonstrated in Figure 21 with helping of the Kriging method.

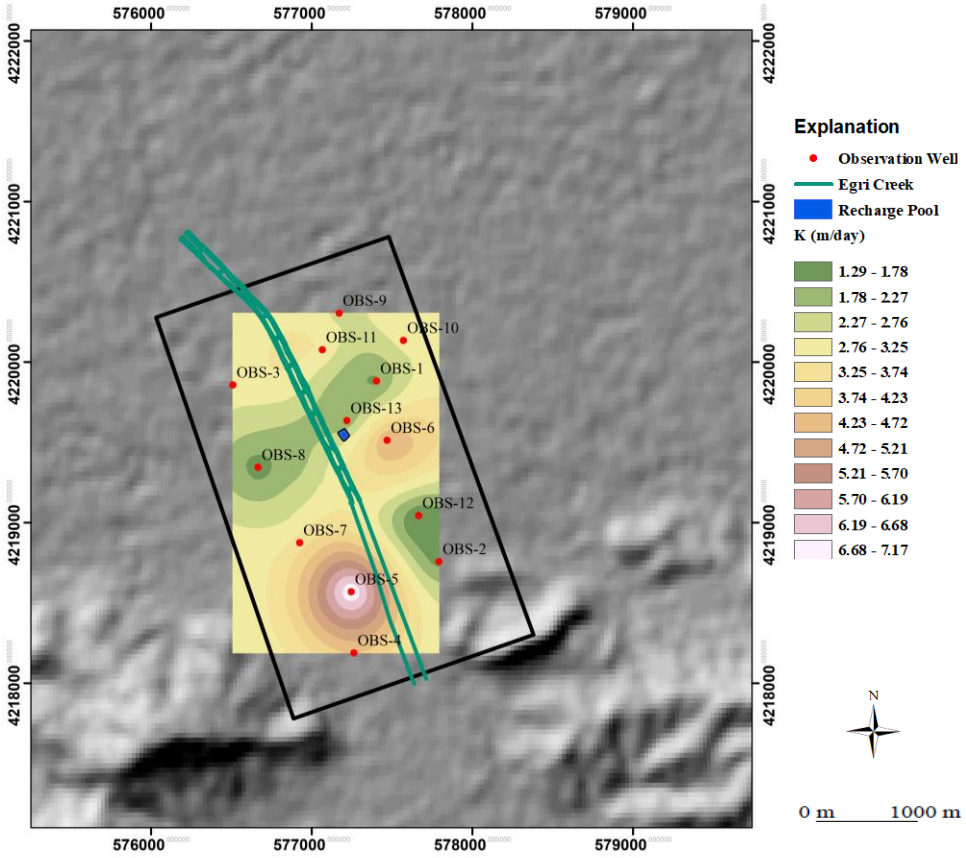

Figure 21. Representation of pumping test results of observation wells.

Table 2. K and S values of observation well in the study area.

Observation Well	S	K (m/d)	T (m^2/d)
1	0.11	3.2	275.2
2	0.086	4.84	412
3	0.1	2.6	221
4	0.0219	1.6	129
5	0.34	3	335
6	0.23	1.5	171
7	0.22	1.7	192.1
8	0.32	3.5	392
9	0.13	4.3	527.5
10	0.095	7.2	878.5
11	0.24	4.6	561.2
12	0.21	1.3	171
13	0.079	3	335
Ave.	**0.15**	**3.26**	**372.07**

4.2. Investigation of Alluvium Aquifer

Characterization of the alluvium aquifer in the study area was carried out by establishing laboratory and field studies.

4.2.2. Laboratory Studies

In the laboratory, soil hydraulic properties of the alluvium aquifer were determined.

4.2.2.1. Type of Soil

The aquifer soil properties affect the permeability, porosity and hydraulic parameters of the aquifer and thus control the recharge rate. In this context, sieve analysis has been carried out in order to classify the soil on the core samples taken from research wells in the alluvium aquifer in the study area. The aim here is to determine how the coarse and fine-grained soils of the alluvial material in the study area present variability. With this method, the samples were passed through a series of standard sieve with

different sizes were determined. All experiments were done in the DSİ laboratory. The research well (SK-14) results are shown in Table 3. The laboratory test results were determined soil type is poor-sand/silty-sand (SP-SM) (Figure 22). The rest of the research well results are presented in Appendix A. The sieve analysis results obtained from wells were used in the HYDRUS 3D package program.

Table 3. Sieve analysis results of SK-14.

1	2	3			4			5	6	7
No	Sample No	Particle Dist.			Consistency Limit			Soil Class	Clay	Silt
		0.075	4.75	75						
		mm	mm	mm	LL	PL	PI			
		Passed %	Passed %	Passed %	%	%	%		%	%
1	SK-14 (0.00 – 10.00 m)	18.2	81.8	100,00	-	-	-	SP-SM	0.3	1.2
2	SK-14 (10.00 – 15.00 m)	13,4	86.6	100,00	-	-	-	SP-SM	0.00	0.00
3	SK-14 (15.00 – 25.00 m)	11.8	88.2	100,00	-	-	-	SP-SM	0.00	2.1
4	SK-14 (25.00 – 35.00 m)	10.6	89.4	100,00	-	-	-	SP-SM	0.00	0.00
5	SK-14 (35.50 – 45.00 m)	8.6	91.4	100,00	-	-	-	SP-SM	0.00	0.00
6	SK-14 (45.00 – 55.00 m)	9.3	100	100,00	-	-	-	SP-SM	0.00	0.00
7	SK-14 (55.00 – 60.00 m)	11.2	100	100,00	-	-	-	SP-SM	0.00	0.00
8	SK-14 (60.00 – 65.50 m)	7.2	99.7	100,00	-	-	-	SP-SM	0.00	0.00
9	SK-14 (65.50 – 68.50 m)	10.2	100	100,00	-	-	-	SP-SM	0.00	0.00
10	SK-14 (68.50 – 70.00 m)	9.3	91.7	100,00	-	-	-	SP-SM	0.00	0.00

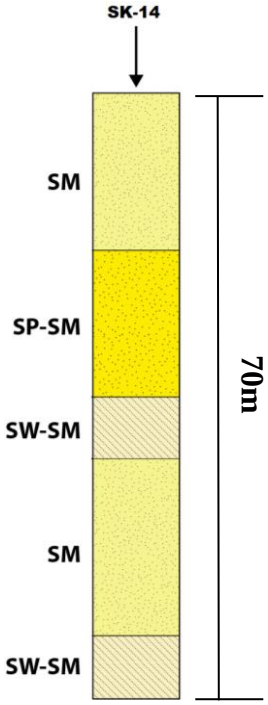

Figure 22. Representation of SK-14 borehole

4.2.2.2. Water Content and Specific Gravity

Water content experiments are one of the first experiments in the laboratory in core samples taken from research wells. Particularly, in order to find out the amount of water that is infiltrated directly from the precipitation, the results of the water content of the soils are needed. The water content is a parameter that can vary with time because it is indexed to precipitation and can be calculated by Equation (4.8).

$$\theta = \frac{\theta_{wet} - \theta_{dry}}{\theta_{\text{dry}}} \text{X}100 \tag{4.8}$$

In addition, in the drilling samples in the laboratory, the specific gravity (G_s) of soil samples was also determined. For this, firstly the dry density (γ_{dry}) values of the samples were calculated using Equation 4.9. then the specific weights were found using Equation 4.10.

$$\gamma_{\text{dry}} = \frac{\gamma}{(1+\theta)} \tag{4.9}$$

$$G_s = \frac{(1+e)X\gamma_{dry}}{\gamma_{water}} \quad (4.10)$$

Where e is void ratio [-], γ is density [ML^{-3}] (γ_{water} =1000 kg/m^3). The specific gravity experiment was carried out to check whether the water saturation rates are in contradiction to the natural condition of the soil. To illustrate, it is expected that the percentage of water saturation of a soil below the groundwater level (saturated zone) will be around 100%. However, in case of not obtaining values close to these values as the result of the experiment, the experiments were performed again and progress was made in a controlled manner. The range of results is between 1.5% to 14.9%. The SK-14 research well results (Θ&G_s) are shown in Table 4. The rest of the research well results are presented in Appendix A.

4.2.2.3. Porosity

The porosity, which is defined as the total volume ratio of the void volume, can be found with the help of Equation 4.11. porosity is one of the properties that reflect the void condition of the soil. The porosity is expressed in decimal or percentage.

$$n = \frac{V_{void}}{V_{total}} \quad (4.11)$$

where, n is the porosity [-] and V is the volume [L^3]. In the study, porosity values could be obtained from soil core samples from research wells. The range of results is between 0.34 to 0.42. Porosity results of SK-14 are shown in Table 4. The rest of the research well results are presented in Appendix A.

Table 4. SK-14 laboratory soil experiment results

Depth (m)	Water Content (%)	Natural Mass (g/cm^3)	Specific Gravity	Porosity
(0.00 – 10.00 m)	2.9	1.90	2.71	0.39
(10.00 – 15.00 m)	4.6	1.97	2.71	0.34
(15.00 – 25.00 m)	1.5	1.95	2.71	0.36
(25.00 – 35.00 m)	2.8	2.12	2.73	0.36
(35.50 – 45.00 m)	5.8	1.6	2.7	0.41
(45.00 – 55.00 m)	6.6	1.8	2.73	0.40
(55.00 – 60.00 m)	4.9	1.7	2.69	0.38
(60.00 – 65.50 m)	5.2	2.01	2.7	0.42
(65.50 – 68.50 m)	8.5	1.9	2.72	0.39
(68.50 – 70.00 m)	9.2	1.8	2.71	0.39

4.2.2.4. Permeability

Permeability is a measure of the water transmission capacity of soils. Permeability is a parameter that can be determined in the laboratory and in the field. Permeability tests in the laboratory are carried out with constant head permeability tests on coarse-grained soils, while falling head permeability tests are applied on fine-grained units such as sand and clay. In the field, permeability can be calculated borehole tests (sending water to soil). In this study, permeability values were obtained by constant head tests in the DSİ laboratory.

The range of results is between 2.55×10^{-5} to 5.30×10^{-4} m/sec. Details of the results are presented in Appendix A.

4.2.3. Unsaturated Hydraulic Conductivity

When the soil is saturated, all pores are fitted and conducted. The water phase is continuous and conductivity is at maximum. When the soil desaturates, some pores become air-filled, thus the conductive portion of the soil's volume diminishes, and tortuosity increases. When suction develops, the first pores to be emptied are the largest ones, which is the most potentially conductive. Therefore, unsaturated hydraulic conductivity is less than saturated conductivity and it is a function of matric suction and

also related to water content (Hillel, 2008). Unsaturated hydraulic conductivity mainly depends on soil textures.

Direct measurement of unsaturated hydraulic conductivity is difficult, time-consuming, expensive and requires simplified assumptions. To overcome this situation, mathematical models are formed by using measured or predicted volumetric water content function (Nielsen et al., 1986). The closed-form equations derived by Fredlund et al. (1994), Green and Corey (1971) and Van Genuchten (1980) are widely used for the estimation of unsaturated hydraulic conductivity. In literature, Van Genuchten (1980) closed-form equation is the most common method.

Van Genuchten equation estimates unsaturated hydraulic conductivity function from saturated hydraulic conductivity and two curve fitting parameters. The equations are expressed as:

$$\theta(h) = \begin{cases} \theta_r + \frac{\theta_s - \theta_r}{[1+|\alpha h|^n]^m} & h < 0 \\ \theta_s & h \geq 0 \end{cases} \qquad (4.12)$$

$$K(h) = K_s S_e^l [1 - (1 - S_e^{1/m})^m]^2 \qquad (4.13)$$

Where;

$$m = 1 - 1/n \qquad n > 1 \qquad (4.14)$$

The above equations contain six independent parameters: Θ_r , Θ_s , α , n , K_s and l. The pore-conductivity parameter l in the hydraulic conductivity function was estimated (Mualem, 1976) to be about 0.5 as an average for many soils. Θ_r and Θ_s denote the residual and saturated water content, respectively. K_s is the saturated hydraulic conductivity, α is the inverse of the air-entry value (or bubbling pressure). HYDRUS implements the soil-hydraulic functions of Van Genuchten (1980) to obtain a predictive equation for the unsaturated hydraulic conductivity function in terms of soil water retention parameters.

4.2.3.1. Hysteresis in Soil Water Retention Curve

In saturated soils, since all pores are filled with water, the volumetric water content (VWC) of soil equals to its porosity. In unsaturated soils, the volume of water stored in the voids varies due to matric suction (i.e., negative pore water pressure) within pore-water.

The soil moisture characteristic curve is described by two inflection points: Air-entry suction and residual water content. When a slight suction is applied to a saturated soil, the suction reaches a point where the largest surface pore begins to empty and its water content is displaced by air. This critical point is known as air-entry suction. Air entry suction is generally small in coarse-textured and well-aggregated soils having large pores, whereas relatively large in fine-textured, poorly aggregated soils. The point where the increase in suction causes no more decrease in water content is defined as residual water content.

The VWC function can be obtained by two ways: desorption (i.e., starting from a saturated soil and applying increasing suction to gradually extract water while taking continuous measurements of remaining soil moisture) or sorption (i.e., by gradually wetting an initially dry soil while reducing the suction). In the soil water retention curves, the wetting curve is usually drawn below the drying curve (Figure 23). This situation is known as Hysteresis. In the HYDRUS-3D software program, it is assumed that the value of Θ_r, Θ_s and n remain constant in dry and wet conditions in order to determine the hysteresis (Simunek et al., 2008). Only the α parameter changes (Anlauf et al., 2012). For this reason, no hysteresis option was selected in HYDRUS-3D under the soil hydraulic properties parameter.

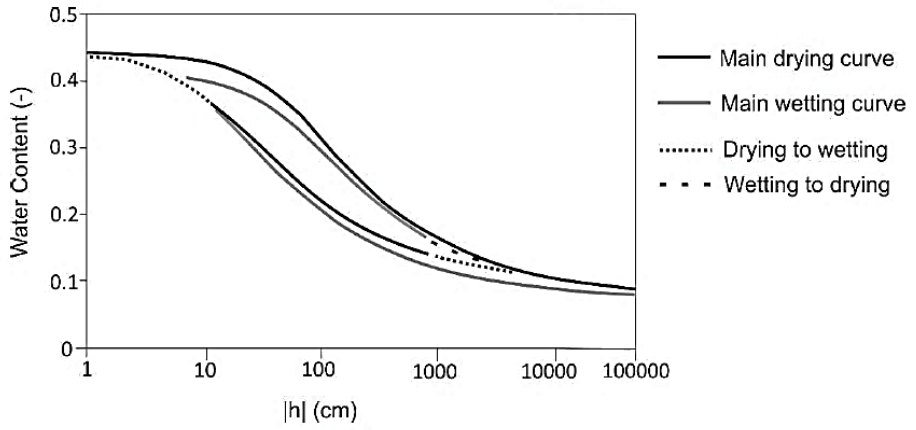

Figure 23. Main drying and wetting soil water retention curves because of hysteresis

4.3. Model Description

A model is a simplified version of a physical system and the key advantage of using a model is enhancing engineering judgment. Since hydrogeological relations within a system is defined in the form of mathematical equations, a mathematical model is used to describe the flow process. A set of partial differential equations, together with the determination of system geometry, parameters and boundary and/or initial conditions are required for the modeling (Chaipus, 2001).

Numerical solutions are used for more complex situations which is usually the case in the real world. In the unsaturated zone, the dependence of both water content and hydraulic conductivity on matric suction results in highly nonlinear conditions, which requires numerical methods for the solution of the flow equation (Equ. 2.1).

Numerical methods involve subdividing the domain into small, finite pieces which is known as discretization. Each sub-domain is called an element and they are composed of a series of nodal points. In numerical models, governing equations can be solved by either finite difference or finite element methods. In this study, the Galerkin finite element method with linear basis functions is used to obtain a solution of the flow equation (2.1) in HYDRUS-3D.

CHAPTER 5

RECHARGE MODELING

5.1. Conceptual Model

Conceptual model development is the main and most important step in modeling procedure. The conceptual model enables a detailed characterization of the system, extent of the model geometry and distribution of materials.

As indicated in the previous chapter, the study area consists of two main geological units. The basement rocks of schist and gneiss, and the overlying alluvial fan deposits. In terms of water-bearing capacities, the alluvial fan deposits are the main unit that allow flow of groundwater due to high porosity. The other unit, which is composed pf schist and gneiss form an impervious boundary, where no flow is observed. Hence, the flow takes place within alluvial fan deposits which consist of a combination of coarse materials. Exploration well logs indicate that the subsurface geology is not contained any impending layers with a significant thickness or extent. The aquifer in the study area is defined as unconfined.

Conditions of a thick unsaturated zone, the presence of alluvium and permeable material, as well as the existence of an unconfined aquifer suggest that artificial recharge of groundwater can be achieved via surface spreading methods (Chapter 2.3). With the implementation of a numerical method, the success of artificial recharge of groundwater in the Eğri Creek subbasin will be discussed. In this study, artificial recharge of groundwater in the Eğri Creek subbasin is applied to the study area for six months of October-April, in which the surplus streamflow from Eğri Creek can be diverted to the artificial recharge basin to augment aquifers, Figure 24.

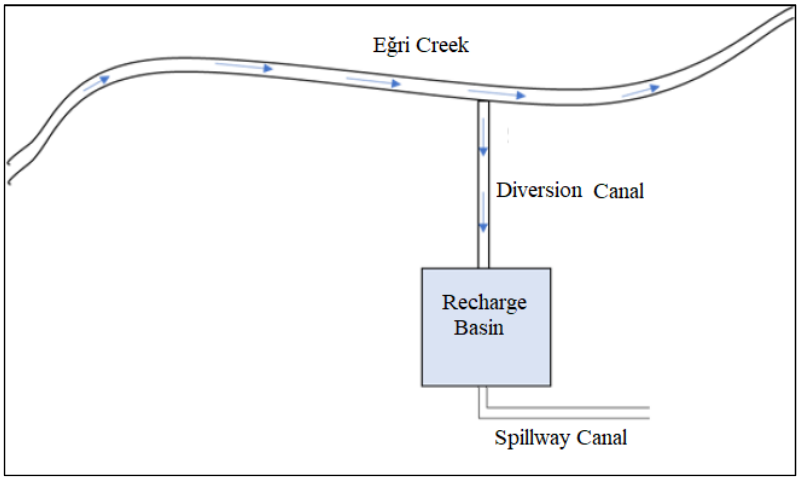

Figure 24. Schematic view of artificial recharge from Egri Creek

5.2. Numerical Model

Hydrogeological investigations reveal that the Eğri Creek subbasin is suitable for surface artificial recharge applications. An optimally suitable site would be one that consists of highly permeable soils, have the capacity for horizontal flow at the aquifer boundary and lacks of impending layers and a thick unsaturated zone. Since HYDRUS-3D uses a 3D representation of the subsurface, in this study a length of about 1 km along the recharge pool center in north-south and east directions. Eğri Creek is defined natural boundary on the west side. The distance of Eğri Creek to the center of the recharge pool is accepted 90m. The thickness of the domain ranges from 26m to 148m (see also Chapter 4).

In the selection of the model domain, some factors were taken into consideration. As a source of recharge water, excess flows of the Eğri Creek were chosen. Therefore, the model domain should be located on the downstream side, along with a gentle topography to divert (regulate) and infiltrate water. Also, the model area should be away from settlements to make the construction to recharge basins possible. Besides, the area should not contain any confining layers.

5.2.1. Finite Element Mesh

Discretization or meshing is a critical step in numerical modeling. Discretization involves the division of the system that is being modeled into small pieces where the governing equations are solved to obtain the overall solution. In terms of the finite element method, the model domain is divided into small parts, known as elements, the shape of which can be rectangular, triangular or mixed. In each element block, hydrogeological parameters are assumed to be uniform.

The number of finite equations to be solved is equal to the number of nodes located along element edges. Although smaller elements result in more accurate simulations, more time and computer memory are required to obtain the solution.

Determination of the size and shape of elements depends on the model geometry and aim of the study. In order to obtain the most suitable mesh size and shape, the trial and error method was used, where the effect of each mesh type on the solution was investigated. As a result, the mixed type gave the best results, and hence was selected. The element size in the model was assigned as 5m with a width of 0.5 m, which resulted in 3606 nodes and 14815 3D-elements. Figure 25 shows the west to east cross-section distribution of finite element mesh along with the domain. Since the flow equations are linear and the response of the water table to recharge is critical, a smaller mesh size was used. It may be necessary to generate a finer FE mesh, especially in the vicinity of the infiltration basin or to use anisotropic FE-mesh with finer discretization in the vertical than the horizontal direction. In vadose zone application vertical fluxes usually dominate over horizontal fluxes and thus, the spatial discretization should be much finer in the vertical direction than in the horizontal direction. HYDRUS can generate such FE meshes using the so-called FE-mesh stretching. In the study the stretching factor F_s to 0.5 and the stretching direction to Z. FE-mesh refinements were utilized for the bottom of the recharge basin and Egri-Creek (S=1.7).

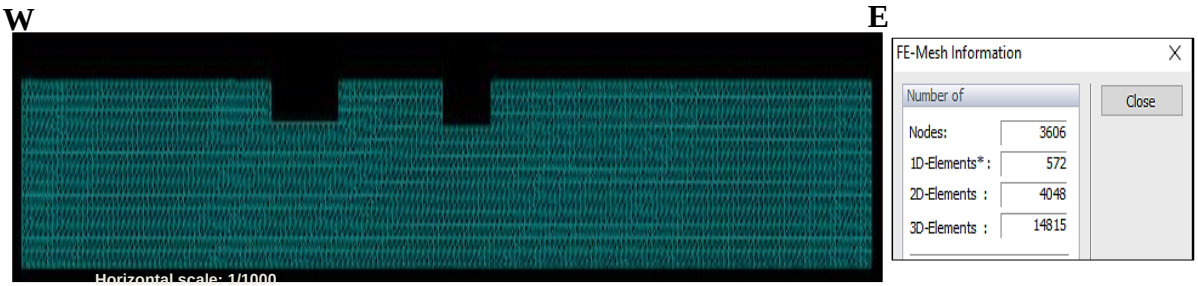

Figure 25. Distribution of finite element mesh along the (W-E) domain

5.2.2. Boundary Conditions

One of the important parts of numerical modeling is assigning boundary conditions. It is not an easy task to convert real processes that take place on the boundary into mathematical relations. In order to obtain realistic results, boundary conditions should be assigned carefully.

The model boundaries were determined from both the geological and hydrogeological characteristics of the study area. Based on the data obtained from geological and hydrogeological investigations and cross-sections, the model domain can be defined by the schist and gneiss at the bottom while the alluvial fan materials are in the other directions. Since the flow of recharge water is modeled in 3D by the constant head boundary condition method, the upper part of the domain is represented by the ground surface (atmospheric boundary). Basically, the schist and gneiss are represented by no-flow boundary (denoted by 1), thus they were not included in the solution of the flow equation. The ground surface is exposed to meteorological events, and atmospheric boundary condition (denoted by 3) was chosen to represent Ödemiş Meteorological Station data. The northern, southern, eastern and western part of the study area is expressed with free flow-flux type boundary condition (denoted by 4), which represents the flow of water out of the system. During the simulation period (180 days) on Eğri Creek, daily flow rates showed that the flow rates were low (Table 5). Eğri Creek's bed is very wide (60m). The artificial recharge pool base elevation (125 msl) is 1 m below Eğri Creek base elevation (126 msl). According to daily flow rates, Eğri Creek represents constant flux (specified head (denoted by 5)) boundary conditions (Figures 26 & 27). Eğri Creek natural flows decreased because of upstream projects. Also, the artificial recharge pool represents a constant head boundary condition (denoted by 2) (3 m) during the simulation period (180 days).

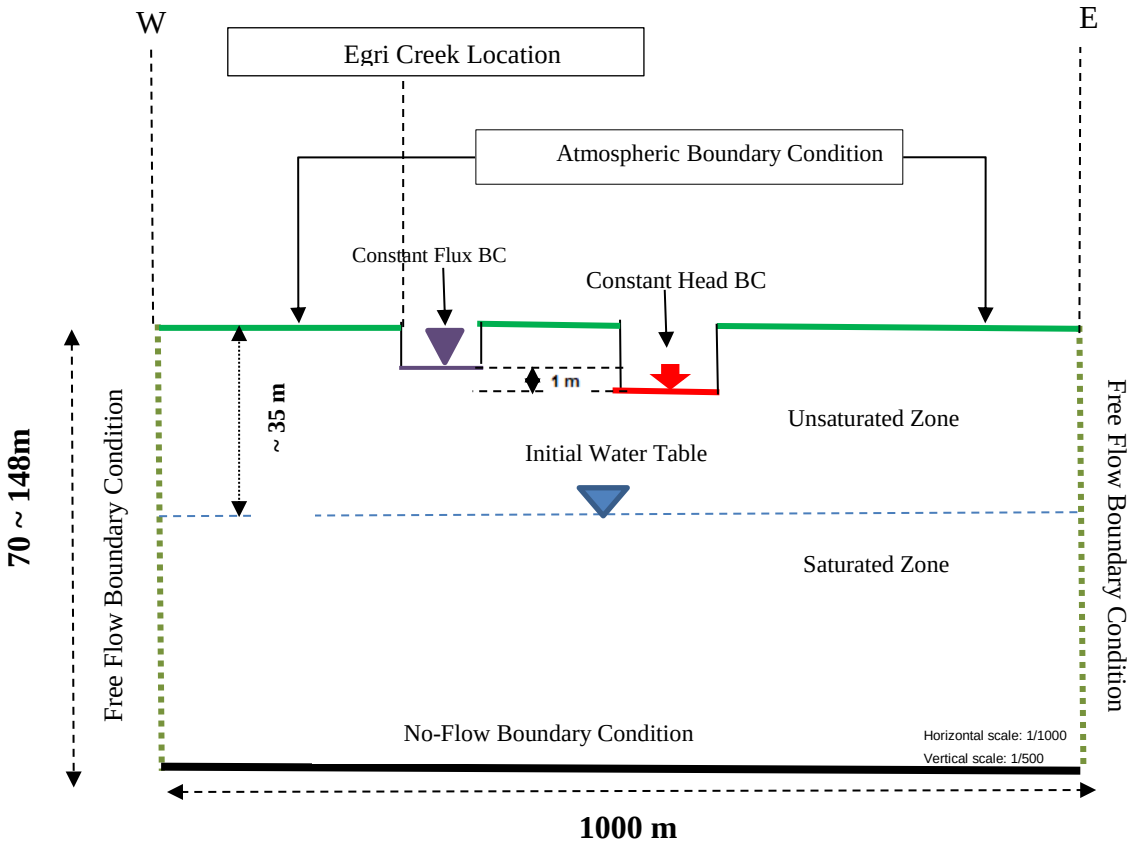

Figure 26. Cross-section W-E location and 2D view with boundary conditions.

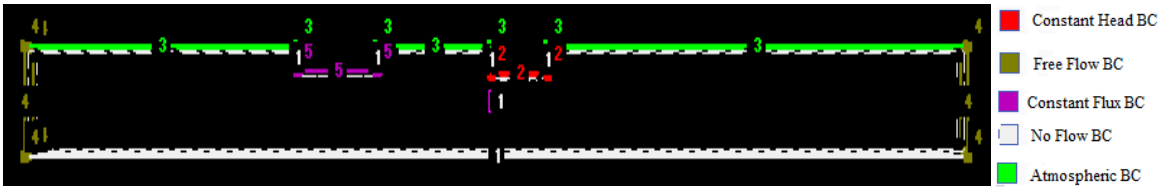

Figure 27. Boundary conditions used in the model.

Table 5. Daily discharge of Eğri Creek in simulation period (m^3/sec.).

Days	Oct.	Nov.	Dec.	Jan.	Feb.	March	April
1	0.000	0.003	0.031	0.000	0.071	0.001	0.244
2	0.000	0.003	0.034	0.146	0.055	0.011	0.390
3	0.000	0.000	0.006	0.000	0.474	0.011	0.050
4	0.000	0.000	0.037	0.004	0.342	0.018	0.154
5	0.000	0.000	0.046	0.030	0.224	0.023	0.407
6	0.000	0.000	0.044	0.030	0.106	0.028	0.315
7	0.000	0.000	0.041	0.250	0.012	0.033	0.007
8	0.000	0.000	0.033	0.250	0.130	0.038	0.509
9	0.000	0.003	0.031	0.061	0.248	0.043	0.406
10	0.000	0.002	0.029	0.056	0.037	0.048	0.354
11	0.000	0.018	0.027	0.046	0.098	0.053	0.007
12	0.000	0.018	0.026	0.121	0.060	0.058	0.012
13	0.000	0.036	0.024	0.128	0.072	0.063	0.017
14	0.000	0.025	0.022	0.135	0.238	0.068	0.022
15	0.000	0.198	0.020	0.142	0.356	0.073	0.110
16	0.000	0.198	0.019	0.149	0.074	0.078	0.223
17	0.000	0.025	0.016	0.156	0.192	0.083	0.337
18	0.000	0.000	0.015	0.163	0.210	0.088	0.450
19	0.000	0.250	0.133	0.170	0.328	0.093	0.563
20	0.000	0.198	0.115	0.177	0.346	0.098	0.577
21	0.000	0.020	0.097	0.184	0.464	0.103	0.490
22	0.000	0.015	0.080	0.191	0.382	0.108	0.603
23	0.000	0.000	0.062	0.198	0.502	0.113	0.017
24	0.005	0.002	0.044	0.002	0.018	0.118	0.130
25	0.043	0.015	0.026	0.001	0.136	0.123	0.243
26	0.026	0.010	0.009	0.020	0.254	0.128	0.357
27	0.028	0.010	0.009	0.041	0.372	0.133	0.470
28	0.028	0.014	0.027	0.036	0.490	0.103	0.583
29	0.028	0.016	0.044	0.026	//	0.143	0.497
30	0.028	0.018	0.062	0.065	//	0.148	0.510
31	0.028	//	0.080	0.153	//	0.152	//
Σ(m^3/s)	**0.214**	**1.096**	**1.288**	**3.130**	**6.291**	**2.372**	**9.055**
Σ(hm^3)	**0.0185**	**0.0947**	**0.1113**	**0.2705**	**0.5436**	**0.2050**	**0.7824**

5.2.3. Initial Conditions

The HYDRUS 3D is a windows-based software program that can solve the groundwater flow equations numerically. The solving of groundwater flow equations depends primarily on the formation of appropriate initial & boundary conditions. As can

be seen from Equation (2.1). HYDRUS-3D allows the use of the two different initial conditions such as water content and pressure head. The initial conditions of the model can be expressed in terms of water content and pressure head as follows;

$$\theta(z,t) = \theta_i(z,0) \quad (5.1)$$

$$h(z,t) = h_i(z,0) \quad (5.2)$$

Where; Θ_i [-] and h_i [L] represent water content and pressure head, respectively. Accordingly, water content values of the vadose zone determined in the laboratory were used in the study as initial condition Equation 5.2. According to research well and laboratory results are represented from the lowest located nodal point of unsaturated zone is (z) 35 m. HYDRUS sets the pressure at the bottom of the domain equal to 35m. So, calculates the hydrostatic equilibrium (i.e., H=h+z=constant) where H is the total head, h is the pressure head and z is the gravitational head for all other nodes. The pressure head at the top of the domain will thus be equal to -35 m (=35-70m) since the domain has a height of 70m.

5.2.4. Model Calibration and Validation

Calibration of the model is used to check whether the system inputs reflect the actual field conditions. In the calibration analysis, the trial and error method was used to modify input parameters, such as hydraulic conductivity, initial or boundary conditions etc. These parameters were then adjusted within reasonable limits, until a good match between calculated and observed groundwater levels was obtained. This is expected because modeling is just a simplification of reality, and approximations and computational errors are inevitable. The process of model calibration is aimed at fine-tuning the model results to match the measurements in the field. In a groundwater flow model, the resulting groundwater head is forced to match the head at measured points. This process requires changing model parameters (i. e. hydraulic conductivity or groundwater recharge) to achieve the best match. Calibration can be manually done or automatically.

In this study, the groundwater table profiles obtained from the field measurements of water levels in October 2018 and April 2019 were used in the calibration process.

The simulation covered a period of 180 days. This period corresponds to a wet season during which no pumpage took place for irrigation purposes. Thus, one of the parameters belonging to the real system, i.e., groundwater pumpage through wells was eliminated in the calibration process. Starting with the end of the dry season water table (October 2018), the aim was to match the observed water table profile at the end of the wet-season (i.e., April 2019).

Initial conditions should be determined, where the system gets the soil pressures at the start of the period. In the model, the initial conditions were specified by drawing the initial water table, i.e., water table elevations of October 2018. Then, the system computed the necessary initial pore water pressures or head conditions from the assigned water table. The groundwater recharge for the corresponding period was assigned as a constant head boundary condition & atmospheric boundary condition, which are represented by a constant recharge pool depth (3 m) and daily Ödemiş Observation Station data (Figure 28) from October 2018 to April 2019.

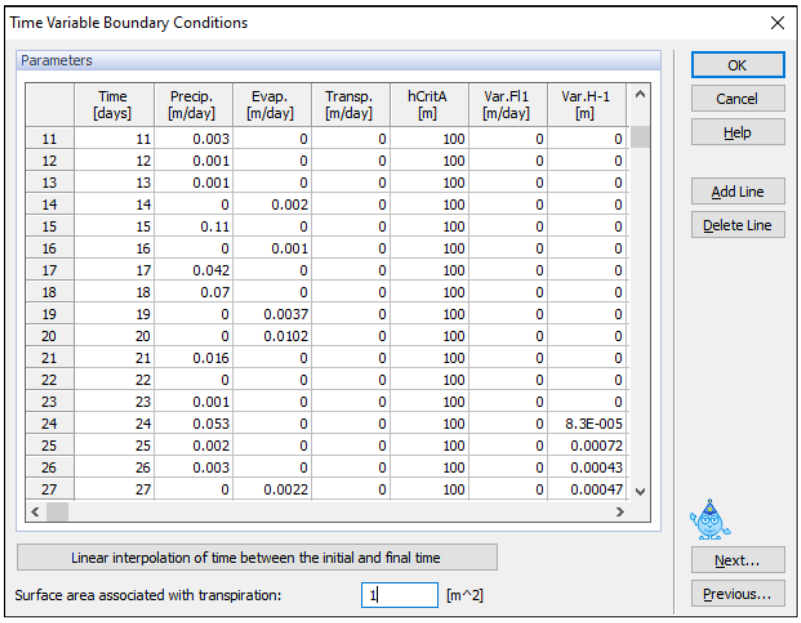

	Time [days]	Precip. [m/day]	Evap. [m/day]	Transp. [m/day]	hCritA [m]	Var.Fl1 [m/day]	Var.H-1 [m]
11	11	0.003	0	0	100	0	0
12	12	0.001	0	0	100	0	0
13	13	0.001	0	0	100	0	0
14	14	0	0.002	0	100	0	0
15	15	0.11	0	0	100	0	0
16	16	0	0.001	0	100	0	0
17	17	0.042	0	0	100	0	0
18	18	0.07	0	0	100	0	0
19	19	0	0.0037	0	100	0	0
20	20	0	0.0102	0	100	0	0
21	21	0.016	0	0	100	0	0
22	22	0	0	0	100	0	0
23	23	0.001	0	0	100	0	0
24	24	0.053	0	0	100	0	8.3E-005
25	25	0.002	0	0	100	0	0.00072
26	26	0.003	0	0	100	0	0.00043
27	27	0	0.0022	0	100	0	0.00047

Figure 28. Time variable boundary conditions data from the Ödemiş Station.

At first, the system was thought to be composed of a single material, which was determined as sandy loam. The HYDRUS models have a soil texture modeling capability.

The saturated hydraulic conductivity (Ksat (m/day)) was calibrated duration the wet season (Figure 29).

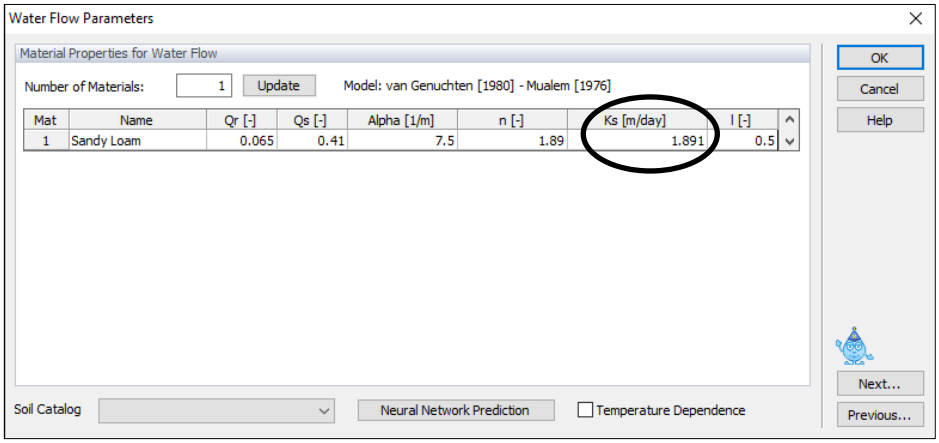

Figure 29. Material properties for water flow in the model domain.

For the initial model runs, material properties were assumed to be uniform and were represented by sandy loam (SP-SM) soil type throughout the model domain. The corresponding parameters of sandy loam were assigned in the model (Figure 30).

In this study, daily mean observed groundwater level from the groundwater observation well located near the recharge pool and SK_K27 well were used to calibrate the HYDRUS-3D model for a simulation period -180 days- (Figure 31).

Calibration of the model was carried out and goodness of fit was determined by comparing the simulated groundwater levels (h_s) with the measured groundwater levels (h_m).

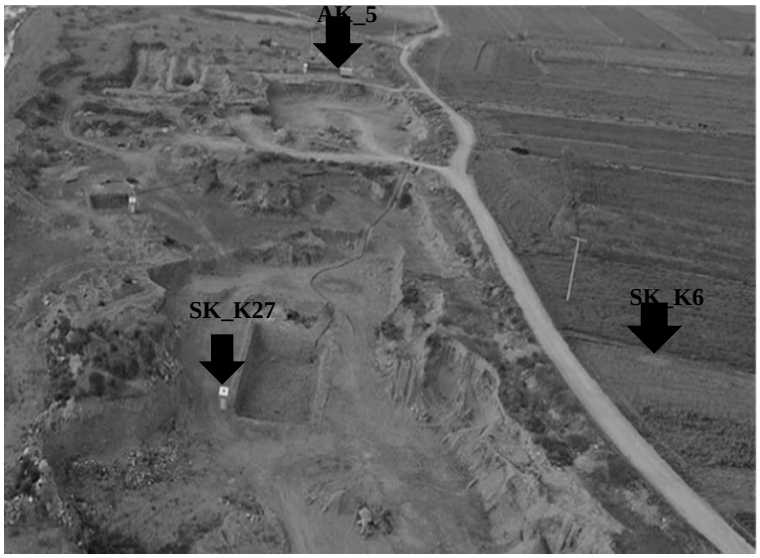

Figure 30. Location of observation wells.

For the calibration step, saturated hydraulic conductivity (K_s) was manipulated within reasonable ranges until the simulated model results closely matched the observed variables. The final model simulation was a good fit for the observed groundwater level and simulated groundwater level (SK_K27) (Figure 32 – 33).

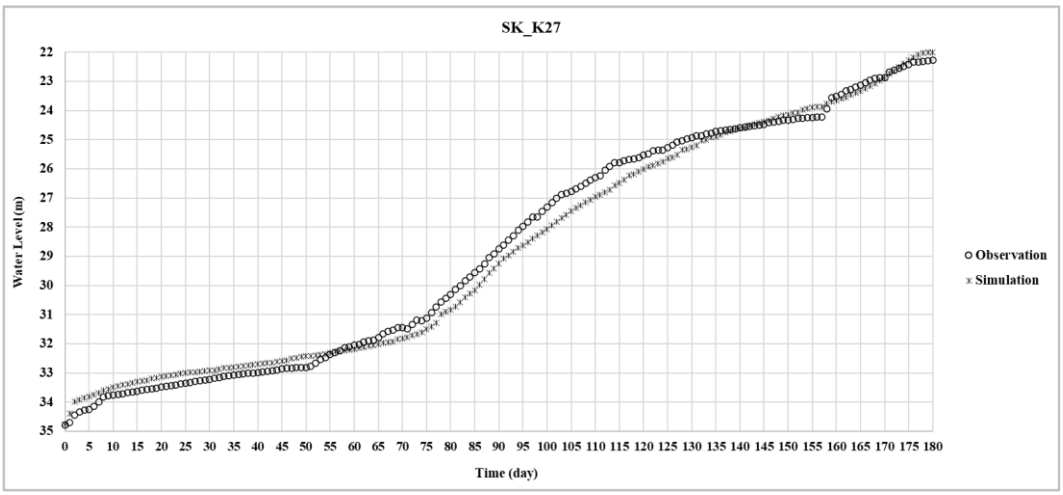

Figure 31. SK_K27 simulated and observed GWL.

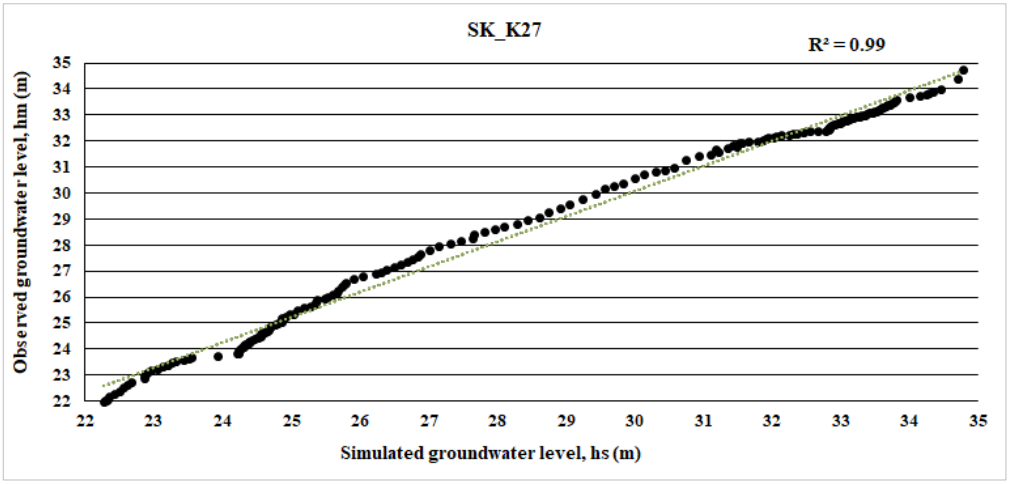

Figure 32. Relationship between the observed and simulated groundwater levels.

The agreement between predicted and observed groundwater level data was evaluated by the coefficient of determination (R^2). In this study, R^2 was used for model calibration. R^2 correlation is an important statistical measure that in a regression model represents the proportion of the difference or variance in statistical terms for a dependent variable which can be explained by an independent variable or variables. In short, R-squared correlation determines how well data is fit the regression model or how well the modeled data is fit to observation data. R^2 ranges from 0 to 1, with values greater than 0.5 considered to be acceptable (Moriasi et al., 2007).

As illustrated in Figure 34, a good agreement between modeled and observed groundwater levels as indicated by high R^2, which was found 0.99.

5.2.4.1. Model Validation

The term "validation" is not completely true when used in groundwater modelling. Oreskes (1994) asserted it is impossible to validate a numerical model because modeling is only an approximation of reality. Model verification and validation is the next step after calibration. The objective of model validation is to check if the calibrated model works well on any dataset. Because the calibration process involves changing different parameters (i. e., hydraulic conductivity, recharge, pumping rate, etc.) different sets of values for these parameters may produce the same solution.

After the calibration process, the artificial groundwater recharge effect was discussed for the other two wells (SK_K6 and AK_5). The comparison between observation and model data is given in Figures 35 and 36.

The location of SK_K6 is the east side of the artificial recharge pool. The distance of the well to the recharge pool is approximately 63m. Also, the location of AK_5 is the north side of the artificial recharge pool. The distance of the well to the recharge pool is approximately 165m. Figures 35 and 5.36 show the results of the simulation for 180 days. Measured and simulated groundwater levels at a distance from the recharge pool, the groundwater levels in the recharge pool are presented. Notice that the modeling results correspond equally well with the measured data during the calibration and validation parts of the experiment.

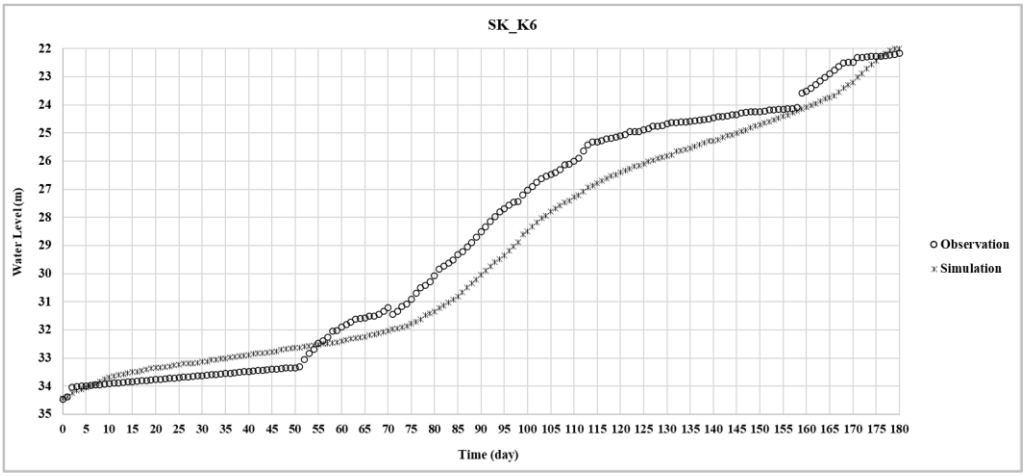

Figure 33. SK_K6 simulated and observed GWL.

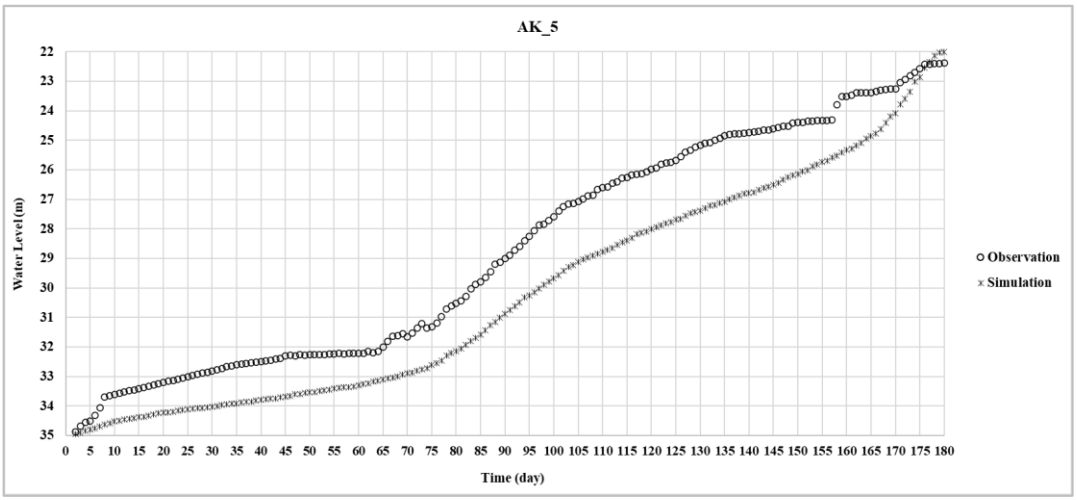

Figure 34. AK_5 simulated and observed GWL.

The graphs below show the relationship between observation and simulated data of SK_K6 and AK_5 wells. The coefficient of determination is a measurement used to explain how much variability of one factor can be caused by its relationship to another related factor. When the data of the SK_K6 observation well examined, which located to the east of the artificial recharge pool. It observed that the groundwater level has risen. In the period of locally heavy precipitation transitions in the region, the data between the model and the observation changes without large deviations. As illustrated in Figure 37, a good agreement between simulated and observed groundwater levels as indicated by high R^2, which was found 0.96.

When the data of the AK_5 observation well examined, which is located to the north of the artificial recharge pool. It observed that the groundwater level has risen. In the period of locally heavy precipitation transitions in the region, the data between the model and the observation changes without large deviations. As illustrated in Figure 38, a good agreement between simulated and observed groundwater levels as indicated by high R^2, which was found 0.90. It is indicated that the differences between the observation and the simulation data have low goodness than the other two wells. The reason is thought to be the distance of the AK_5 well to the recharge pool. Also, this soil formation sometimes includes small amount of clay content but not in the form of thick bands or lenses. One of the reasons for the low correlation may be that the presence of clay lenses causes a delay in the groundwater motion. Also, in Chapter 3, groundwater contours tend to move towards the northwest. So, AK_5 and SK_K6's locations are not corresponding to that direction. The reasons listed above are for the relatively low correlation for SK_K6 and AK_5.

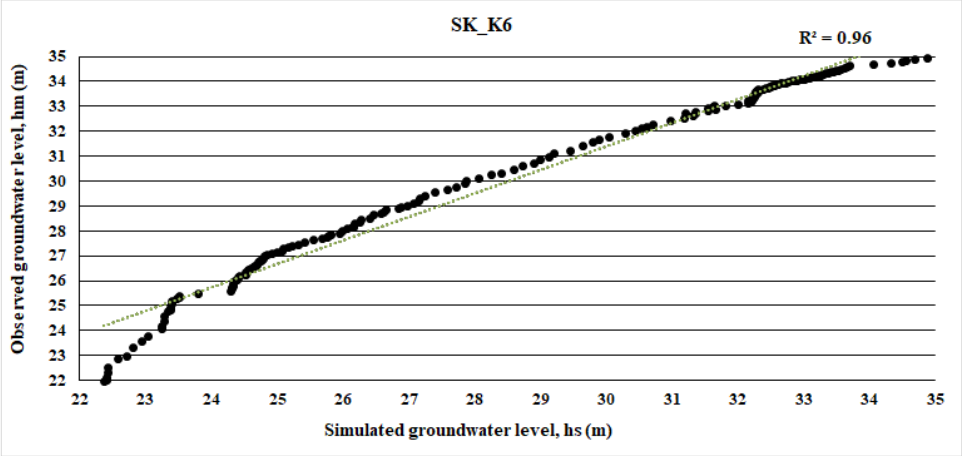

Figure 35. Relationship between observed and simulated groundwater levels.

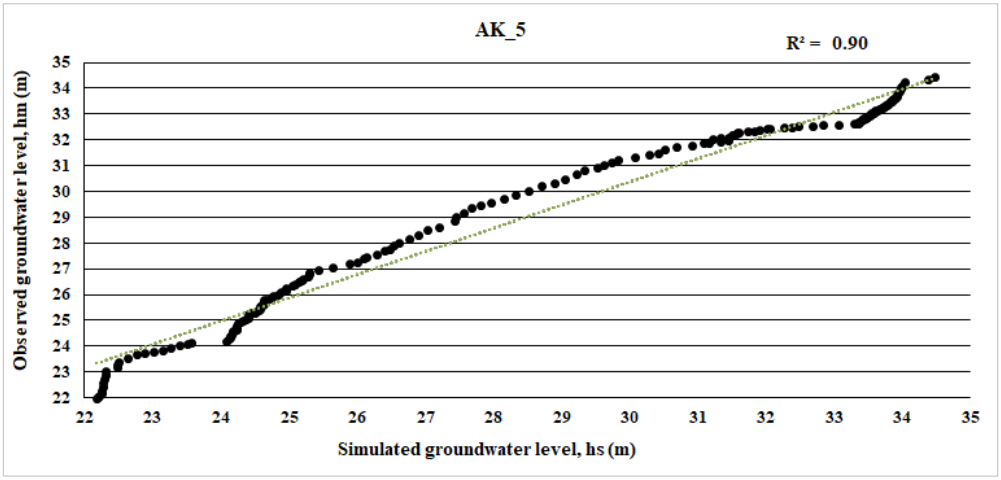

Figure 36. Relationship between observed and simulated groundwater levels.

The calibration and validation of the model was carried out and goodness of fit was determined by comparing the simulated groundwater levels (h_s) with the observed groundwater level (h_m). Moreover, two error statistics were also used as the goodness of the fit between the simulated and observed water levels.

- RMSE (Root Mean Square Error) is a frequently used measure of the difference between values predicted by a model and the values actually observed from the environment that is being modeled. These individual differences are also called residuals, and Root Mean Square Error serves to aggregate them into a single measure of predictive power. In study, the RMSE is the average of the squared differences in measured and simulated heads (Equation 5.3).

$$\mathrm{RMSE} = [\frac{1}{n}\sum_{i=1}^{n}(h_m - h_s)_i^2]^{0,5} \qquad (5.3)$$

Where n is number of observations.

- The Mean Absolute Error (MAE), the simplest measure of forecast accuracy is called MAE. Mean Absolute Error is simply, as the name suggests, the mean of the absolute errors. The absolute error is the absolute

value of the difference between the simulated value and the actual value. The mean absolute tells us how big of an error we can expect from the forecast on average. The mean absolute error can range from 0 to ∞ (Equation 5.4).

$$\mathrm{MAE} = \frac{1}{n}\sum_{i=1}^{n}|(h_m - h_s)_i| \quad (5.4)$$

The simulated and the observed (measured) groundwater levels for April 2019 conditions were plotted for comparison above the figures. The overall root mean square error (RMSE) equals to the 0.86 m and the mean absolute error (MAE) equals to 0.49.

The precision of the mean error value, depending on the thickness of the aquifer, corresponds to 0.012. Values of both stages (calibration & validation) are summarized in Table 6.

Table 6. Values of R^2, root mean square error and mean absolute error

Type of Stats.	**Calibration**	**Validation**	
	SK_K27	**SK_K6**	**AK_5**
R^2	0.99	0.96	0.90
RMSE (m)	0.39	0.89	1.31
MAE (m)	0.08	0.43	0.98

CHAPTER 6

ARTIFICIAL RECHARGE SCENARIOS

6.1. Introduction

Once the model calibration is completed, the model is ready for further investigations, planning, and operations. In the case of the present study, the effect of recharged water on the water table elevation was simulated for various recharge pool dimensions determined from the aim is to utilize excess water (that is rest of the water budget with other projects) as a source to recharge the aquifer. In addition to recharge basins, an underground dam was simulated to test if the groundwater levels could be increased further. Due to the limitation in the surface water resources (1 hm^3), the scenario that recharged water to the ground in total (1 hm^3) was taken as a reference to compare various scenarios.

The simulations were conducted for a period of 180 days between October 2018 and April 2019, where the initial and boundary conditions are known. Furthermore, this period corresponds to a wet season during which well discharge for irrigated agriculture did not take place. Hence, a maximum response from groundwater storage via artificial recharge was obtained.

6.2. Recharge Basin Design

The recharge basin design involves the construction of the basins along the Eğri Creek to collect the water which diverted from the Eğri Creek regulator. The dimensions of the basin were determined by site test results to check the available space for construction, with a limiting factor that the depth of the recharge basin should not exceed 6 m to provide stability (Figure 39).

Figure 37. Location of the recharge basin.

6.3. Artificial Recharge Scenarios

Alternative scenarios for the artificial recharge of groundwater via recharge basins involve repeating the simulations for different recharge pool dimensions and so recharge water amounts. The simulation period starts from October 2018 to April 2019, where the calibrated model is closely compatible with actual field conditions.

Below, Table 7. shows the effect of different sizes of recharge pools on the groundwater level. It desired to obtain the most suitable groundwater recharge project in these seven scenarios. It is observed that the average groundwater level increases due to increasing pool sizes. Due to the projects developed upstream of the project site, the water budget is limited $1*10^6$ m^3/year.

In the model, the operation of recharge basins starts when the simulation time period starts, i.e., October 2018. The operation of the recharge basin at the beginning of the simulation was performed to allow time for the recharged water to infiltrate into the ground, to reach the water table, and hence to increase the water table elevation during the simulation period of 6 months.

A number of scenarios were developed to find optimal recharge basin dimensions. After the correlation between 06-11 and 06-42 stream gauge station (Equ. 3.1). It indicates the amount of water that can be artificially recharged. According to the scenarios, the depth of the recharge basins varies between 3m – 6m.

The overall effect of artificial recharge was revealed as an average increase in the phreatic surface from 12.5m to 34.14m. The increase in the groundwater level in this process, which is done in the rainy period and which is the period when evaporation is low, also means an increase in underground storage. This amount of storage is approximately equal to the volume in artificial recharge. The volume ranges from 212270 m^3 to 1400000m^3 (Table 7).

Due to the upstream project of Eğri Creek, approximately $1*10^6$ m^3 of water will be sufficient from Eğri Creek to the recharge basin.

Table 7. Depth of recharge water & corresponding hydraulic level in recharge basin for different recharge basins & dimensions.

Scenario	Number of Basin	Dimensions (m)	Depth (m)	Cum.Recharge (m^3)	Daily Ave. Recharge (m^3)	Ave. Increase of Groundwater Level (m)
1	1	6x6	3	212,270	1207	12.5
			4	256,150	1,423.05	13.08
			5	275,880	1,532.67	13.73
			6	344,320	1,912.88	14.22
2	1	10x10	3	352,300	1,957.22	13.8
			4	432,550	2,403.06	14.6
			5	488,250	2,712.50	16.1
			6	506,990	2,816.61	16.82
3	1	20x20	3	671,220	3,729	17.77
			4	716,980	3,983.22	18.34
			5	815,710	4,531.72	21.67
			6	963,140	5,517.40	22.83
4	1	30x30	3	964,770	5,350.39	25.1
			4	965,380	5,363.22	26.5
			5	967,480	5,374.88	27.64
			6	980,440	5,446.73	29.3
5	1	50x50	3	1,181,100	6,561.67	30.61
			4	1,245,300	6,918.33	31.46
			5	1,379,000	7,661	33.88
			6	1,400,000	7,777.78	34.14
6	2	6x6	3	406,400	2,257.78	14.42
			4	498,130	2,767.40	16.22
			5	589,620	3,275.67	17.3
			6	694,650	3,859.167	18.04
7	2	10x10	3	1,062,400	5,902.22	19.87
			4	1,104,600	6,136.367	22.03
			5	1,201,300	6,673.88	22.82
			6	1,273,600	7,075.56	23.1

The average increase in groundwater levels was obtained from observation points in HYDRUS-3D modeling set-up. These observation points were appointed randomly in the modeling domain in HYDRUS-3D (Figure 40). The location of the observation points is such that it corresponds to the increase in groundwater levels to represent the whole system. The HYDRUS-3D domain observation points show changes in groundwater levels.

The model runs for approximately six months through two stress periods. The first stress period is as short as one day. This stress period is added to everything in the model

works fine. The second stress period is 180 days and represents the artificial recharge period with meteorological events.

Figure 41 shows the cumulative water (m^3) recharge for various artificial recharge scenarios (October 2018 – April 2019). The volume ranges from 212,270 m^3 to 1,400,000 m^3.

Figure 42 shows the change in water table elevations with respect to the initial (October 2018) and groundwater level with artificial recharge for various scenarios. The average increase in groundwater levels ranges from 12.5m to 34.14m.

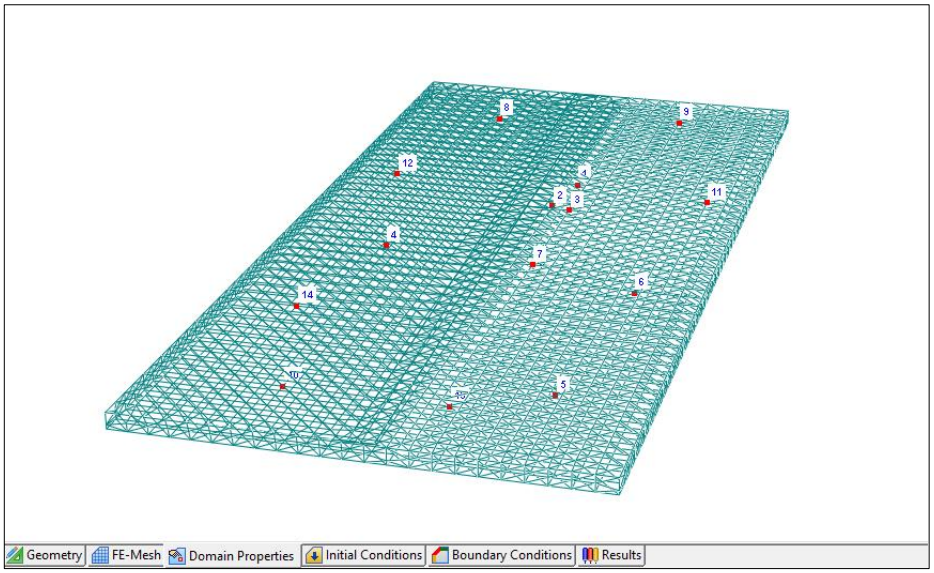

Figure 38. Location of the observation points in the HYDRUS-3D.

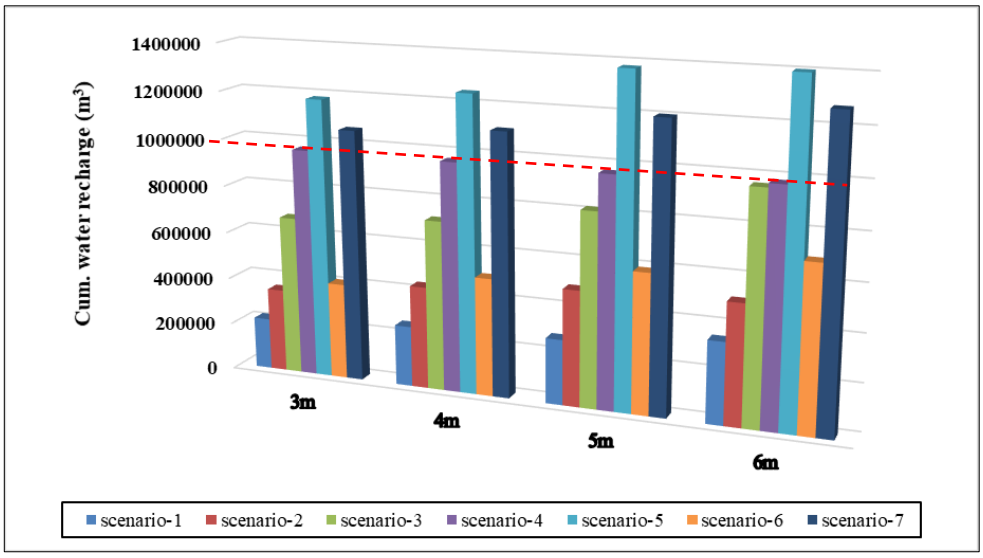

Figure 39. Cumulative water recharge (m^3) for various artificial recharge scenarios.

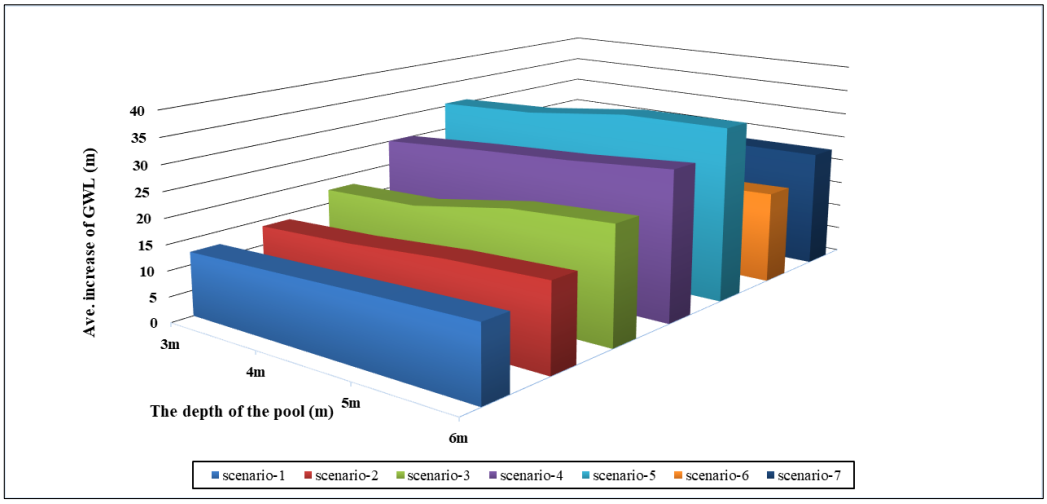

Figure 40. Average increase in GWL (m) for various artificial recharge scenarios.

6.4. Underground Dam

Underground dams are also considered as an artificial recharge method, which prevents groundwater flow and store water beneath the ground (Nilsson, 1988). They are used where surface storage becomes impractical owing to high evaporation rates, reservoir siltation, and pollution risks. Although this technology is not new, its efficiency and simplicity have revived interest. Underground dams are constructed in well-defined and narrow valleys, natural dikes are preferred for locating underground dams. The model domain was selected based on these conditions and with the help of Google earth maps (Figure 43). Also, the model domain is illustrated in ArcGIS (Figure 44).

Figure 41. Underground dam location (the map from Google Earth)

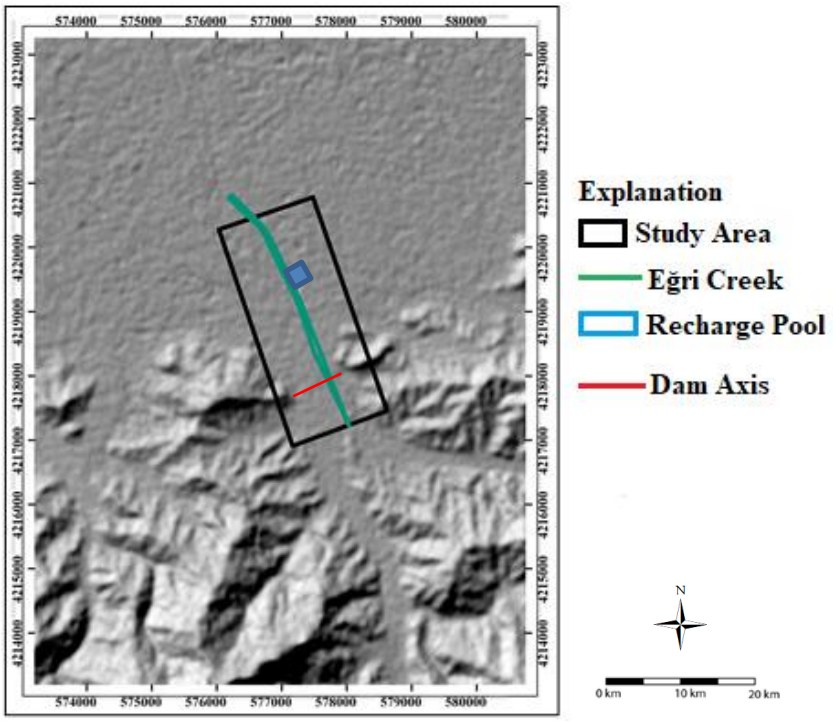

Figure 42. Location of underground dam.

Underground dam can enhance the storage of recharged water in the system by reducing or eliminating outflow from the system. In this study, an underground dam was simulated with recharge originating from artificial recharge basins to determine the contribution of dam construction on groundwater levels and storage. In the model, the dam construction was simulated at the downstream edge (i. e., along the northern boundary), where flow of water out of the system is prohibited. The suitable region is in the southern part of the system in the direction of underground flow where alluvial thickness is low and where water is not allowed to escape by design requires, therefore, creating a significant increase in groundwater storage. The dam construction was represented by assigning a no-flow boundary at the downstream edge. Since the main interest in the model is the flow of water in the subsurface and the impervious layers are not included in the domain, the actual dimensions of the underground dam were considered and modeled.

6.4.1. Modeling of Underground Dam

Hydrogeological and topographic investigations reveal that the Eğri Creek subbasin is suitable for underground dam applications. The material parameters used in the model for saturated and unsaturated conditions are taken from previous studies (i.e., Zeytinova, Aktaş regulator project). A schematic view of the subsurface material based on the previous projection of well logs is given in Figure 45. Alluvium lies in a 175 m wide strip at the axis. The impermeability curtain will be constructed as 109 pieces of interlocking plaster strip. The height between the talweg and the crest level is 23m. The total crest length is 196m. by being socketed into the bedrock on the slopes.

The simulation period begins in October 2018 and ends in April 2019. The initial conditions were determined from the water table elevation drawn for October 2018. The simulations were repeated without the presence of a recharge basin. During the simulation period (180 days) on Eğri Creek, daily flow rates showed that the flow rates were low (see also Table 5).

The underground dam modeling only allows for the groundwater levels to be mainly raised in the upstream part of the domain because the axis of the dam prevents the seepage of water with its impermeability (bentonite) wall, thus water accumulates in that (upstream part) location. The distance between the study area edge and the dam axis (upstream) is 680m. Table 8 shows the accumulated (stored) water volume (m^3) of the underground dam depending on the level. Figure 46 shows the storage volume (m^3) corresponding to the reservoir elevation (m).

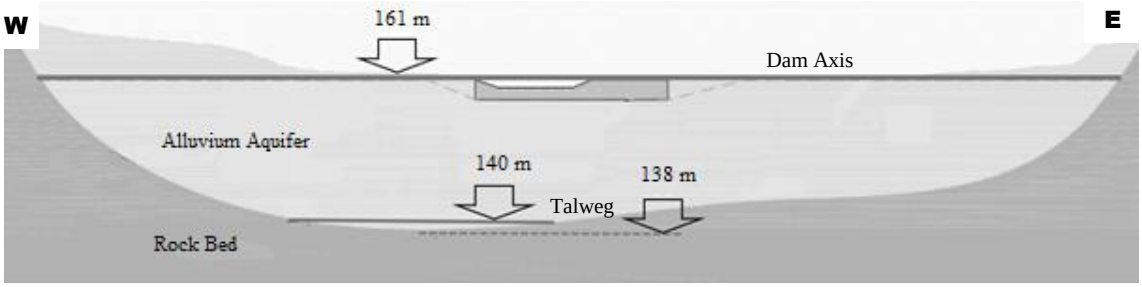

Figure 43. A schematic view of subsurface material types in the model domain

Table 8. Underground dam volume (m^3) – elevation (m) values

Volume (m^3)	Eleva. (m)
0	138
9	139
154	140
88,501	141
109,016	142
151,880	143
193,078	144
204,574	145
236,295	146
268,256	147
300,365	148
312,783	149
355,443	150
388,308	151
421,365	152
424,580	153
427,936	154
430,885	155
453,047	156
498,809	157
542,678	158
546,720	159
651,053	160
720,450	161

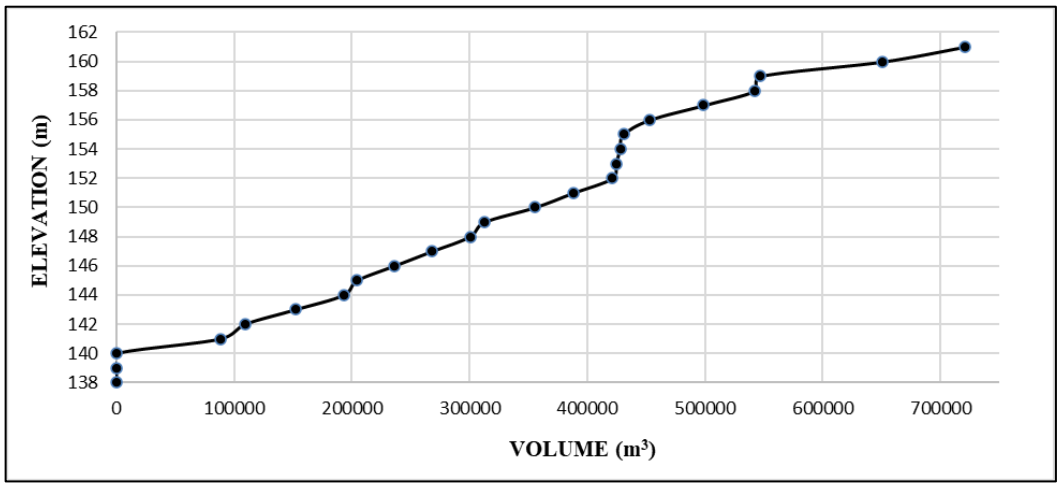

Figure 44. Underground dam reservoir elevation (m) – volume (m^3) graph

6.4.2. Finite Element Grid

Discretization or meshing is a critical step in numerical modeling. Discretization involves the division of the system that is being modeled into small pieces where the governing equations are solved to obtain the overall solution. Determination of the size and shape of elements depends on the model geometry and aim of the study. In order to obtain the most suitable mesh size and shape, the trial and error method was used, where the effect of each mesh type on the solution was investigated. As a result, the mixed type gave the best results, and hence was selected. The element size in the model was assigned as 3 m with a width of 1 m, which resulted in 150 nodes and 388 elements (Figure 45).

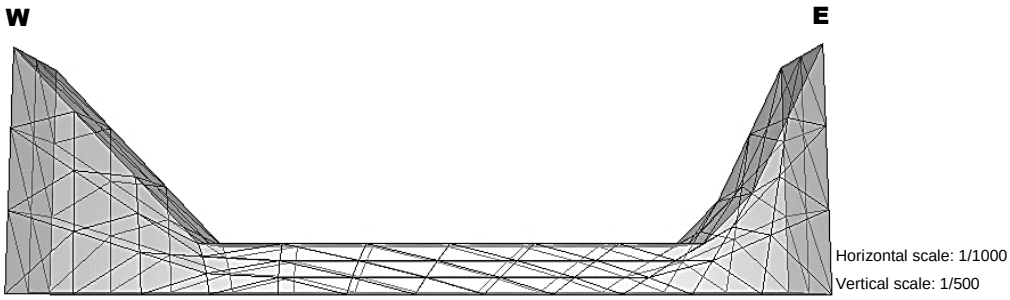

Figure 45. Distribution of finite element mesh along the dam axis

6.4.3. Boundary Conditions

The model boundaries were determined from both the geological and hydrogeological characteristics of the study area. Based on the data obtained from geological and previous hydrogeological investigations, and cross-sections; the model domain can be defined by the schist and gneiss in the western, easthern and at the bottom, while alluvial fan materials overlain on the bedrock (schist).

The ground surface is exposed to meteorological events, atmospheric boundary condition was chosen to represent Ödemiş Meteorological Station data. The Northern, Eastern and Western part of the study area is expressed with no-flow boundary condition because of Eastern and Western part corresponds to mountain. Eğri Creek flows from the southern part of the study area to the northern. It is defined as the constant flux boundary

conditions. The model basement is defined as the no-flow boundary condition due to the presence of a schist layer.

6.4.4. Underground Dam Model Results

HYDRUS-3D allows the modeling of underground dam. The hydraulic features of Van Genuchten (1980) were chosen in this study. The method is explained in Chapter 4. Eğri Creek stream flow data were obtained from Ödemiş Station. The simulation begins in October 2018 and ends in April 2019.

The rise in groundwater storage equals the amount of percolation (due to precipitation) and Eğri Creek daily stream calculation. The observation points (1 to 11) were assigned to the model area randomly (Figure 46). The groundwater levels in the upstream direction of the underground dam show a significant increase (Figure 47). The water budget consists of the percolation of the Eğri Creek and atmospheric conditions (e.g., precipitation) giving the budget of the total water stored HYDRUS-3D modeling (Figure 48).

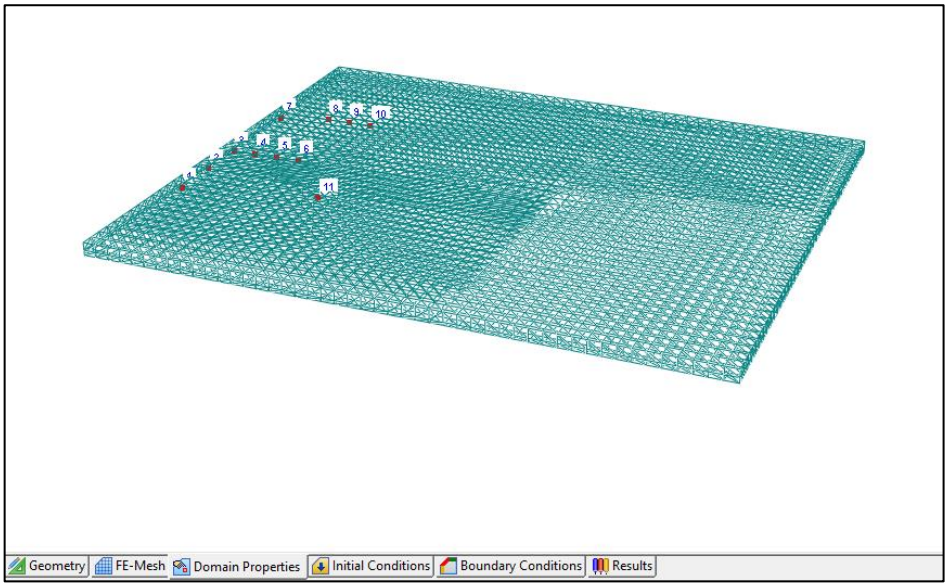

Figure 46. The observation points in the model domain

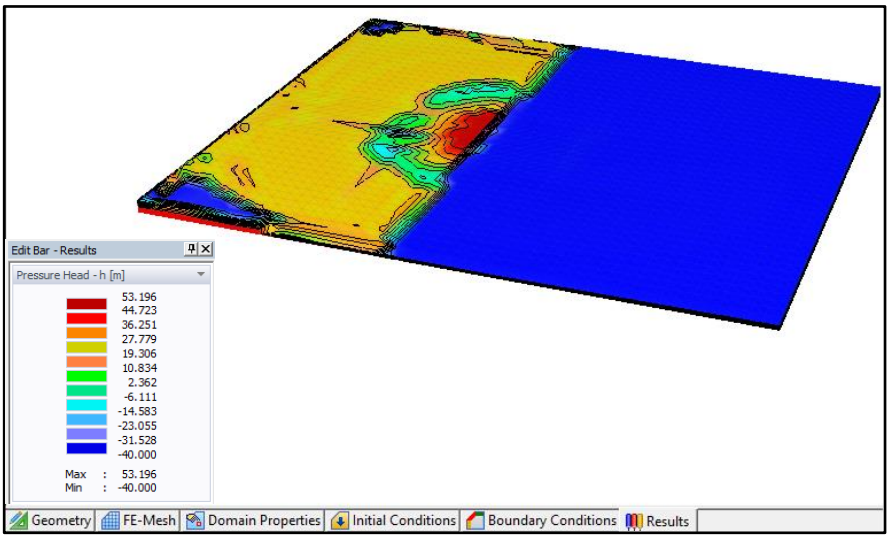

Figure 47. Modeling of the underground dam with HYDRUS-3D

When the underground dam is modeled alone, the groundwater levels are mainly increased in the downstream part of the domain, because the dam prevents subsurface outflow and groundwater accumulates in that region. The change in the water table elevation is shown in Figure 49.

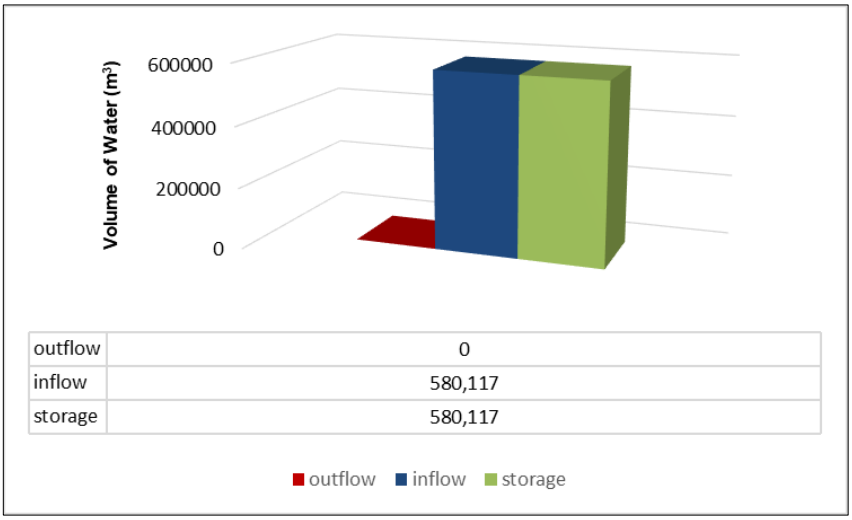

Figure 48. Calculated water budget of underground dam simulation

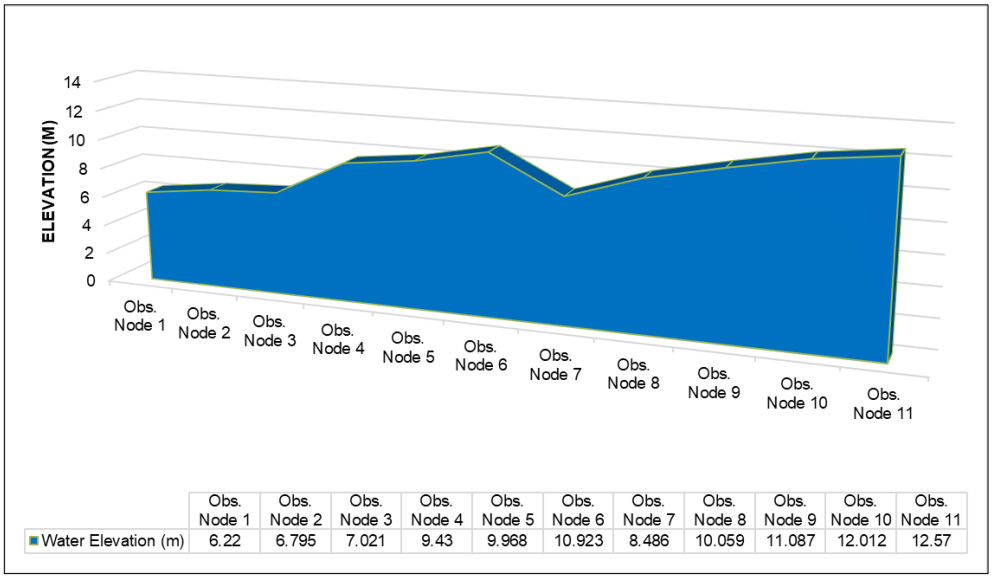

	Obs. Node 1	Obs. Node 2	Obs. Node 3	Obs. Node 4	Obs. Node 5	Obs. Node 6	Obs. Node 7	Obs. Node 8	Obs. Node 9	Obs. Node 10	Obs. Node 11
Water Elevation (m)	6.22	6.795	7.021	9.43	9.968	10.923	8.486	10.059	11.087	12.012	12.57

Figure 49. Water table elevation corresponds to observation points

6.5. Discussion of the Results

The aim of the study is to investigate the potential for artificial recharge of groundwater in the Küçük Menderes River Basin, especially in the Eğri Creek subbasin. The most suitable artificial recharge areas include highly porous media with thick unsaturated zone and the absence of any impending layers. In the study, the modeling is achieved in a representative area characterized by these conditions.

Due to the upstream development of the study area, which is Zeytinova and Aktaş water supply projects utilize Eğri Creek flows. Because of that, the water potential used for the artificial recharge project is limited. The design flow rate is 70 l/sec. and the amount of water to divert to the total study area is 1 hm^3/year.

The results of the case studies point out that the proposed recharge pool design procedure is effective at augmenting the groundwater level. The simulation results show that groundwater table elevations rise in different amounts depending upon the dimension of the recharge pool. The average increase in groundwater levels was obtained from observation points in HYDRUS-3D, which is illustrated in Figure 46. These observation points were appointed randomly in the modeling domain. The location of the observation points in HYDRUS-3D is such that it corresponds to the increase in groundwater levels to represent the whole domain.

Because of the limitation of water resources, and stability issues of recharge pool design every scenario is divided into four subgroups. Among the scenarios, the most suitable one is scenario 4, which has a depth of 6 meters and dimensions of 30m (length) x 30m (width). The scenario raises the groundwater level by an average of 29.3 m.

Increasing the number of artificial recharge pools have the desired effect on the groundwater level. However, a single recharge pool was determined to be more economical.

The underground dam construction in the model domain results in approximately 580,117 m^3 increase in groundwater storage, however this increase in groundwater levels is not significant to warrant the construction of the underground dam. On the other hand, they are used where surface storage becomes impractical owing to high evaporation rates, reservoir siltation, pollution risks, etc. It may be beneficial to build in the study area according to the temperature values in recent years.

The rise in groundwater storage equals the amount of percolation (due to precipitation) and Eğri Creek daily stream calculation. The groundwater level increases more rapidly at points close to the dam axis.

The underground dam raises the groundwater level by an average of 9.5 m. The rising of underground water levels can be categorized into two terms. Precipitation (rainfall) and seepage of Eğri Creek. Precipitation intensity and infiltration rate of the soil characteristics are the main factors for underground dam applications.

CHAPTER 7

GROUNDWATER TABLE HYDRAULIC IMPACT ASSESSMENTS FOR INFILTRATION BASIN

7.1. Introduction

In the previous chapter, we discussed the effectiveness of two artificial recharge methods in the Eğri Creek Sub-basin. The results indicate that the rising of groundwater below the recharge pool is higher than in vicinity locations. The design engineer should assess the hydraulic impact on the groundwater table to avoid adverse hydraulic impacts. In order to determine the height and range of groundwater mounding, U.S. Geological Survey (USGS), in cooperation with Department, developed a Microsoft Excel Workbook of Spreadsheets to simulate groundwater mounding beneath artificial recharge pools.

7.2. Analytical Modeling

Analytical expressions for the formation of groundwater ridges and mounds beneath spreading basins are available for several cases of this flow phenomenon. Among these are those presented by Baumann (1952), Bittinger and Trelease (1960) and Glover (1961). Experimental studies have verified the usefulness of these solutions. Artificial recharge by spreading and application of irrigation water on more or less rectangular or circular areas is not rare in practice. In this study, we will examine a rectangular shape artificial recharge pool.

To determine the height and range of groundwater mounding, the U.S. Geological Survey (USGS), in cooperation with the department and developed a report and a Microsoft Excel workbook of spreadsheets to simulate groundwater mounding beneath infiltration basins. The model developed by USGS, hereafter referred to as the Hantush Spreadsheet, calculates the maximum height of the transient mounding formed and assumes all groundwater flow is horizontal above an infinite aquifer. The maximum height of the mounding occurs when the entire volume of runoff has been infiltrated into

the subsoil through the bottom of a recharge pool. It is assumed that if the calculated steady-state mounding reaches the bottom of the recharge pool, then infiltration will not occur as expected.

7.2.1. An Overview of The Hantush Spreadsheet

At first glance of the spreadsheet that is found on the 'Results' tab of the workbook file, the user will see an 'Input Values' section with cells filled in a gold or orange-yellow color, followed by two sets of output data represented by cells filled in red, a blue rectangular button labeled 'Re-Calculate Now'.

Once the parameter values are input, the user will click on the blue button to enable the macro to simultaneously solve the embedded equations. As for the graph depicted, the Hantush Spreadsheet sets the water table at zero elevation, with the coordinate origin (0, 0, 0) situated under the center of the recharge pool. The x-axis depicts a representative slice of the right-hand half of the groundwater mounding in the direction of the basin length being analyzed, showing the extent of the groundwater mounding in that direction only. The left half of the mounding is assumed to be symmetrical (Figure 50).

Variables in the spreadsheet include recharge rate (m/day), specific yield, hydraulic conductivity, the length and width of the recharge pool, the duration of infiltration and initial thickness of the aquifer.

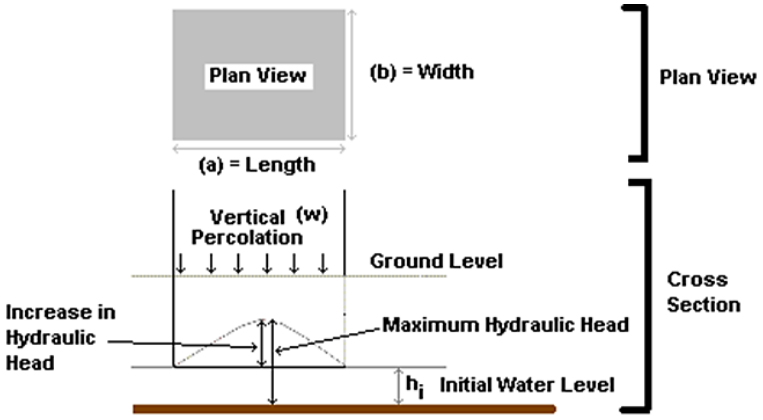

Figure 50. Representation of groundwater mound beneath the rectangular recharging area

7.3. Mounding Scenarios

After the recharge pool dimension is decided, the Hantush and calibrated model relationship is revealed. The length and width are 30m and the depth of the pool is 6m. Figure 51 shows the results of groundwater mounding and water level depending on the recharge pool distance.

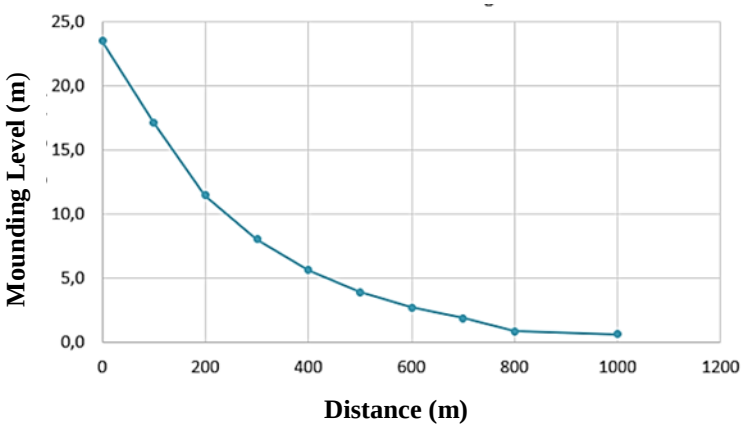

0	23.54
100	17.15
200	11.52
300	8.06
400	5.67
500	3.97
600	2.75
700	1.90
800	0.92
1000	0.66

Figure 51. The Hantush results of groundwater level

Mounding results in the x-axis after modeling with HYDRUS-3D are given in Figure 52. Also, groundwater mounding results based on the distance from the recharge pool with the Hantush and HYDRUS-3D are shown in Figure 53.

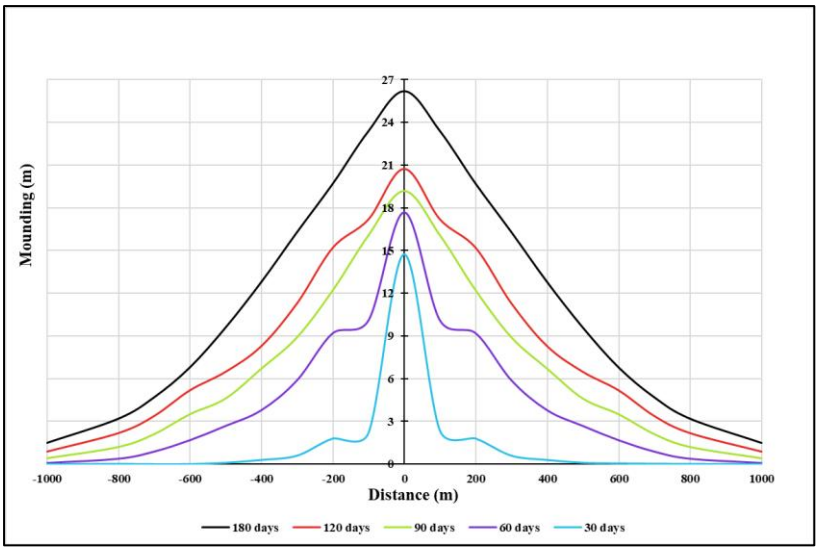

Distance (m)	180.day	120.day	90.day	60.day	30.day
1000	1.5	0.9	0.4	0.1	0.002
800	3.2	2.2	1.2	0.4	0.017
700	4.7	3.4	2.1	0.9	0.032
600	6.8	5.2	3.5	1.7	0.057
500	9.6	6.5	4.6	2.7	0.1
400	12.8	8.3	6.7	3.8	0.3
300	16.3	11.3	8.9	5.9	0.6
200	19.7	15.2	12.2	9.2	1.8
100	23.4	17.2	16.07	10.1	2.35
0	26.2	20.74	19.18	17.67	14.72
-100	23.4	17.2	16.07	10.1	2.19
-200	19.7	15.2	12.2	9.2	1.8
-300	16.3	11.3	8.9	5.9	0.6
-400	12.8	8.3	6.7	3.8	0.3
-500	9.6	6.5	4.6	2.7	0.1
-600	6.8	5.2	3.5	1.7	0.0057
-700	4.7	3.4	2.1	0.9	0.032
-800	3.2	2.2	1.2	0.4	0.017
-1000	1.5	0.9	0.4	0.1	0.002

Figure 52. Modeling results of groundwater mounding with HYDRUS-3D

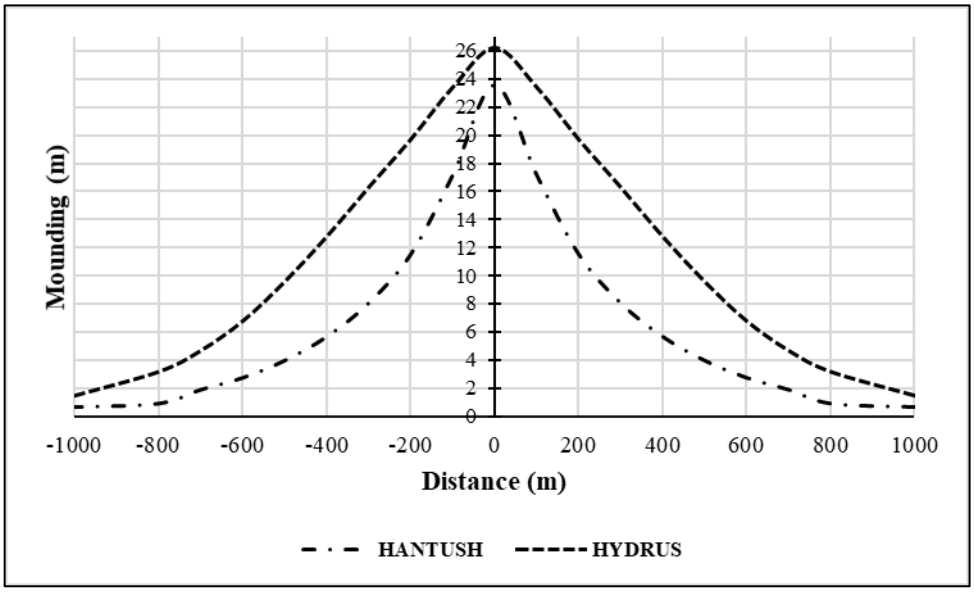

Figure 53. The Hantush and HYDRUS-3D mounding results

The relationship between HYDRUS-3D and Hantush gives important information about the mechanism of the groundwater mounding system. A linear relationship was observed between HYDRUS-3D and Hantush for the simulation period correlations and the correlation coefficient was 0.93 (Figure 54). The high correlation coefficient obtained in Figure 55 between HYDRUS–3D and Hantush indicate that the alluvium aquifer is affected by the artificial groundwater recharge system in the study area.

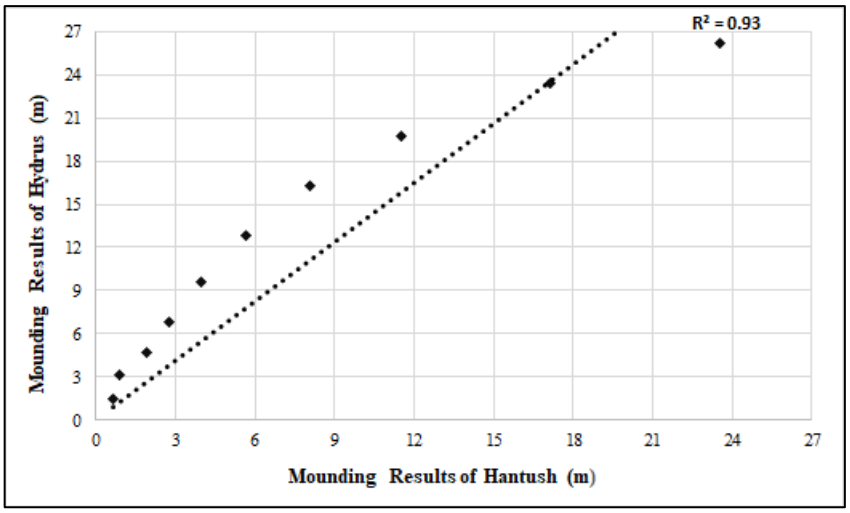

Figure 54. The relationship between HYDRUS-3D&Hantush mounding results

7.3.1. Adjustment of Basin Size, Hydraulic Properties and Recharge Rate

In this chapter, we ran several mounding scenarios using a USGS Excel Spreadsheet. The Spreadsheet utilized the Hantush (1967). Some adjustments to the recharge and hydraulic properties should be taken to consideration the distance used by the spreadsheet for graphing is appropriate for the new size of the artificial recharge pool.

The graphs produced by the Hantush spreadsheet are also a curve providing the height of groundwater mounding extending radially from the center of the artificial basin at the end of the duration of the infiltration period. The actual groundwater may expand farther horizontally after the infiltration period ends.

Table 9. shows scenarios of groundwater mounding depending on variable parameters.

Table 9. The scenarios of groundwater mounding depend on different parameter

K_{sat} (m/day)	Sy	Aquifer Thickness (m)	Recharge Rate (m/day)	Length (m)	Width (m)	Value (m)	Distance to Trigger (m)
0.1	0.08	5	1	6	6	22.9	29.9
0.1	0.08	10	1	6	6	26.1	33.1
0.1	0.08	15	1	6	6	28.5	35.5
0.1	0.08	20	1	6	6	30.6	37.6
0.1	0.08	30	1	6	6	34	41
0.1	0.08	40	1	6	6	35.8	43.8
0.1	0.08	50	1	6	6	39.2	46.2
1.891	0.15	5	3	10	10	26.5	33.5
1.891	0.15	10	3	10	10	31	38
1.891	0.15	15	3	10	10	34	41
1.891	0.15	20	3	10	10	36.5	43.5
1.891	0.15	30	3	10	10	40	47
1.891	0.15	40	3	10	10	43	50
1.891	0.15	50	3	10	10	45.5	52.5
3.25	0.21	5	1.5	20	20	31	38
3.25	0.21	10	1.5	20	20	36.7	43.7
3.25	0.21	15	1.5	20	20	40.6	47.6
3.25	0.21	20	1.5	20	20	43.2	50.2
3.25	0.21	30	1.5	20	20	47.6	54.6
3.25	0.21	40	1.5	20	20	48.2	57
3.25	0.21	50	1.5	20	20	50.1	59
4.72	0.26	5	3	30	30	45	47.9
4.72	0.26	10	3	30	30	40.9	53.5
4.72	0,26	15	3	30	30	46.5	56
4.72	0.26	20	3	30	30	49	57
4.72	0.26	30	3	30	30	50	56.8
4.72	0.26	40	3	30	30	49.8	54.9
4.72	0.26	50	3	30	30	47.9	52
7.17	0.30	5	3	50	50	45	55.2
7.17	0.30	10	3	50	50	48.2	57.2
7.17	0.30	15	3	50	50	40.2	55.4
7.17	0.30	20	3	50	50	48.4	52
7.17	0.30	30	3	50	50	45	55.2
7.17	0.30	40	3	50	50	28.2	57.2
7.17	0.30	50	3	50	50	20	55.4

The USGS Hantush Excel Spreadsheet was repeated with the different parameters (Table 7). The correlation of parameter changes with groundwater mounding and distance is shown in Appendix B. The graphs provide the possibility for making a comparison based on the recharge parameters with distance to trigger. The increase in recharge

capacity is significant to the increased phreatic surface beneath the artificial recharge basin pool in the study area. The recharge rate (m/day) and saturated hydraulic conductivity (K (m/day)) are the two parameters that most affect the groundwater mounding.

7.4. Discussion of the Results

Groundwater mounding occurs beneath stormwater management structures designed to infiltrate stormwater runoff. In this study, the effect of Eğri Creek on groundwater was investigated in the project of diverting the flows to the artificial recharge pool.

After the recharge pool dimension is decided, the Hantush and calibrated model relationship is revealed. The length and width are 30m and the depth of the pool is 6m. The groundwater mounding beneath the artificial recharge pool was calculated as 23.54m with the Hantush Excel Spreadsheet. The observations show that the height and effecting radius of the groundwater mounding decreased as the distance to the pool center.

The groundwater mounding and effecting radius were examined with the HYDRUS-3D, with a like dimension. The groundwater mounding beneath the artificial recharge pool was calculated as 26.2m with the HYDRUS-3D. The HYDRUS-3D model results are higher than Hantush spreadsheet results. Nonetheless, A linear relationship was observed between HYDRUS-3D and Hantush for the simulation period correlations, and the correlation coefficient was high (0.93). The fact that HYDRUS-3D results are higher than the Hantush analytical results is thought to be due to the numerical modeling algorithm. Also, the Hantush Excel spreadsheet is an analytical solution method. The Hantush analytical solution contains some assumptions. So, these assumptions can affect the results.

Moreover, The USGS Hantush Excel Spreadsheet was repeated with the different parameters. The correlation of parameter changes with groundwater mounding and distance is examined.

The increase in recharge capacity is significant to the increased phreatic surface beneath the artificial recharge basin pool in the study area. The recharge rate (m/day) and saturated hydraulic conductivity (K (m/day)) are the two parameters that most affect the groundwater mounding.

CHAPTER 8

EXPENDITURE & ECONOMICAL FEASIBILITY OF ARTIFICIAL RECHARGE PROJECT OF EĞRİ CREEK

8.1. Introduction

After determining the ideal dimensions of the project in Chapter 6, we will discuss the economic feasibility of the project in this chapter. The facilities will be built within the scope of 'Eğri Creek Artificial Recharge Project' published by the "DSİ Dams and HEPP Department" in the cost calculation for the year 2021. Unit price tables, construction and installation unit prices were obtained from the Minister of Environment and Urbanization for 2021. Other prices are obtained from the markets. All costs are defined in dollars ($).

The project comprises the regulator body, body intake structure, sedimentation pool, the lengths of the transmission line, the construction site and other facilities costs calculated.

1/1000 map was used in the calculations. The costs of estimation are increased by 15% against the unknown expenses and the facility price is obtained. The project costs were obtained by adding 10% survey, project and inspection expenses. The investment costs were obtained by adding interest during the construction period.

The distance that forms the basis of the transport items are calculated by taking into account the manufacturing distance of the material borrow pits for excavation and fillings over the road for cement and steel.

In chapter 6, artificial recharge scenario four (4) was selected. The considering dimension of the pool is 30x30 m, and the depth is 6m. The excavation costs were calculated.

Clogging is considered as the most limiting factor affecting the artificial recharge of aquifers, because it may condition the feasibility of the plants. The siltation pool is considered and designed to prevent siltation. The height of the siltation pool is 2.5m and floor covering approximately is 2500 m^2. It is considered clay covered base. Table 10 shows the bill of quantities for each workflow unit. The table describes the definition of work the work, unit, unit price and costs.

Table 10. Bill of quantity Eğri Creek artificial recharge pool project (**1$=14.65**)

EGRI CREEK ARTIFICIAL RECHARGE PROJECT								
REGULATOR								
BILL of QUANTITY								
NO	**Quantity No**	**Types**				**Unit of Measure**	**Quantity**	**Unit Costs ($)**	**Sum ($)**
1	B-15.301	Dam in all types and classes except rock and swamp ground excavating floors and putting them in storage				m^2	8,860	3.83	33,934
2	B-15.342	Putting filter material in dams (all-in)				m^3	600	6.15	3,690
3	B-15.308	Dams, quarries and / or material borrow areas soft rock excavation and fill, embankment and / or dam put into filling				m^3	3,544	15.59	55,251
4	Market	Concrete made with C20 Sand and Gravel or B.A. Concrete				m^3	4,200	12.30	51,604
5	Market	Concrete made with 150 doses of sand and gravel				m^3	300	10.24	3.071
6	B-18.501	The supply of PVC water and injection traps and under ground and replacement in above ground structures				kg	1,065	23.25	24,761
7	B-21.015	All kinds of flat surface concrete or reinforced concrete formwork				m^2	2,360	4.72	11,145
8	B-21.024/2	Curved formwork giving F3 type concrete or reinforced concrete surface				m^2	390	13.11	5.111
9	B-23.002	Reinforced concrete in dams (domestic goods Ø14 and larger diameter)				ton	126	21.82	2,748
10	23.D/2.B1	Production of steel İhzar Private Parts (Reduction)				kg	1,235	20.72	25,587
11	B-23.255	Inlet Grille, all kinds of Iron Covers				kg	520	38.18	19,854
12	B-23.176	Simple Iron Works				kg	1,250	15.61	19,513
13	B-15.348	Riprap with rock obtained from quarry or borrow in dams.				m^3	155	39.21	6,078
EGRI CREEK CONDUIT LINE								
Excavation Works								
1	15.001/1	All types of machinery other than swamp, grudge and rock soils Excavating the Ground, Laying It Into Depot or Fill				m^3	950	3.70	3,515.00

8.2. Annual Interest and Amortization Expenses

It is the sum of the annual interest amortization expenses, investment costs of the proposed facilities, the project costs, and the interest to be applied to expensed according to the years to be made during the construction period.

Interest expenses are to be applied every year during the construction period and 5% is taken. Accordingly, the interest rates are applied each year are calculated according to the compound interest. The interest expenses of each facility during the one-year construction period were found by adding up the interest for each year.

The amortization expense is calculated by multiplying the amortization factor with the investment value (Equation 8.1).

$$\text{Amortization Factor} = \frac{i+(i+1)^n}{(i+1)^n-1} \tag{8.1}$$

i: rate of interest to charging on investment (0.05)

n: the economic life of the facility

In this project, the amortization factor was selected as **0.05478.**

8.3. Annual Operating and Maintenance Expenses

The annual operating and maintenance expenses are calculated by multiplying the cost of each facility by the operating and maintenance coefficient. These coefficients are obtained from DSİ Workbook 2016. The operation and maintenance coefficients of the facilities are given below.

Regulator: 0.010

Conduit Line: 0.020

Artificial Recharge Pool: 0.010

8.3.1. Renovation Factor

The renovation factor is the factor that calculates the cost to be paid each year for the renovation of some parts or all of units as a percentage (%) within the economic period, depending on the facility price (Equation 8.2).

$$\text{Renovation Factor} = \frac{i}{(i+1)^n - 1} * C \tag{8.2}$$

i: rate of interest (0.05)

n: the economic life of the facility

c: renovation rate

The maintenance costs are obtained by multiplying the facility cost of each part by the renovation factor.

Accordingly, the calculated value for each facility is given in Table 11.

Table 11. Renovation period and renovation factors

No	Facility Name	Renewal Period (years)	Renewal Rate (%)	Renewal Factor (i=0.05)
1	Regulator	45	2	0.000125
2	Conduit Line	45	2	0.000125
3	Recharge Pool	45	2	0.000125

The renovation and operating maintenance expenses of the recharge pools are given in Table 12.

Table 12. The renovation, operating and maintenance expenses

No	Facility Name	Estimated Costs ($)	Facility Costs ($)	Renewal		Operating& Maintenance
				Time (Year)	Rate (%)	Factors
1	Regulator	131,853.11	145,038.42	45	2	0.010
2	Conduit Line	40,753.58	44,828.94	45	2	0.020
3	Recharge Pool	144,383.48	158,821.83	45	2	0.010
Total		**316,990.17**	**348,689.19**	-	-	-

After all, the annual operating, maintenance, renovation and amortization expenses were calculated as 26,504.57$. This value is also the annual expense of the facility.

8.4. Revenue of The Project

The groundwater supply project to be built in Tire Gökçen will play a crucial role in the storage. The study shows that with artificial recharge, the groundwater level in the region rises by 12.5m on average. It means an energy-saving worth 27,303.75$ in total. Details of energy-saving are given in Appendix B. Considering the groundwater level rise approximately 819.112$ will be saved in energy consumption. Equation 8.3 shows the amount of energy consumption. Also, Equation 8.4 shows the energy cost due to consumption.

$$\text{Energy Consumption (EC) (kWh)} = 13 \times H_m \times Q \tag{8.3}$$

H_m: Head (meter)
Q: Flow rate (m^3/sec.)

$$\text{Energy Cost (₺)} = 0.79 \times (\text{EC}) \tag{8.4}$$

8.5. Rantability

The ratio of the profit obtained in a period to the capital used in the business in that period is called rantability. For an investment to be profitable, its profitability must be 1 (one) or greater than 1. In this study, as mentioned before the annual electrical energy benefit of the project is 27,303.75$. The total expenses are 26,504.57$. Table 13 shows rantability of the artificial recharge pool (scenario 4).

Table 13. The annual income and expense ratio (R)

Income ($)	Expense ($)	Income-Expense ($)	R
27,303.75	26,504.57	799,18	**1.03**

8.6. Construction Work Schedule and Interest Application Periods

Investment costs were found by adding the interest during the construction period to the project costs. A 5% social discount rate was accepted in the investment period interest. The construction time interest factor was calculated for each facility. This factor brings the money spent during the construction of each facility proposed in the project to the contemporizing in the economic analysis. Equation 8.5 shows how to calculate the construction time interest factor in a period.

$$\text{Construction time interest factor} = (i + 1)^n - 1 \quad (8.5)$$

i: social discount rate = 0.05

n: construction interest application period

The work schedule of construction interest application periods are calculated for each facility is given in Table 14.

Table 14. The work schedule and construction interest application period

NO	Name of Process	Between the middle of construction and end of the project (month)	Construction interest application period	Starting Month	Construction Period	Month
						1 3 5 8 10 12
1	Regulator/Water intake/sedimentation basin	7	0,58	1	8	
2	Conduit Line	5	0,42	5	6	
3	Artificial Recharge Area	1	0,08	11	2	
4	Construction Site Facilities	11,5	0,96	1	1	

8.7. Economic Feasibility of Underground Dam

After investigating the underground dam dimensions of the project in Chapter 6, we will discuss the economic feasibility of the project. The facilities will be built within the scope of 'Eğri Creek Underground Dam' published by the "DSİ Dams and HEPP Department" in the cost calculation for the year 2021. Unit price tables, construction and installation unit price were obtained from the Minister of Environment and Urbanization for 2021. Other prices are obtained from the markets.

Also, we will discuss the comparison with the economic feasibility of the artificial recharge pool. The general account principles were performed in previous headlines detailed for the artificial recharge pool.

8.7.1. The Cost of an Underground Dam

An underground dam consists of an impermeable curtain, floodwall, regulation pool, pumping wells, pumping pool and transmission pipe. These facilities' estimated costs were calculated. Table 15 shows the estimated costs of the underground dam. The estimated cost of the underground dam was calculated as 523,192.15$.

Table 15. The estimated costs of the underground dam

Name	**Estimated Costs ($)**
Slurry Trench Curtain	487,125.46
Grout Works	22,730.51
Regulation Storage	4,778.02
Deep Water Well Drilling	4,150.17
Pumping Costs	327.65
Construction Facilities	4,080.27
Total	**523,192.15**

8.7.2. The Facility Costs

The facility costs were obtained by adding 10% unknown costs to the estimated costs. Accordingly, the total cost of the underground dam was calculated as 577,784.37$ (Table 16).

Table 16. The facility costs of the underground dam

Name	**Estimated Costs ($)**	**Facility Costs ($)**
Slurry Trench Curtain	487,125.46	535,838.01
Grout Works	22,730.51	25,003.56
Regulation Storage	4,778.02	5,255.82
Deep Water Well Drilling	4,150.17	4,565.18
Pumping Costs	327.65	360.415
Construction Facilities	4,080.27	4,488.30
Total	**523,192.15**	**575,511.37**

8.7.3. Annual Operating and Maintenance Expenses

The annual operating and maintenance expenses are calculated by multiplying the cost of each facility by the operating and maintenance coefficient. These coefficients are obtained from DSİ Workbook 2016. The operation and maintenance coefficients of the facilities are given below.

Slurry Trench: 0.005

Regulation Pool: 0.010

Pumps: 0.015

8.7.4. Renovation Factor

The renovation factor is the factor that calculates the cost to be paid each year for the renovation of some parts or all of units as a percentage (%) within the economic period, depending on the facility price (Equation 8.6). Also, Table 17 summarizes the renovation factor for each facility.

$$\text{Renovation factor} = \frac{i}{(i+1)^n - 1} * C \quad (8.6)$$

i: rate of interest (0.05)

n: the economic life of the facility (50 years)

c: renovation rate

Table 17. The renovation factors for each facility

Name	**Renewal (year)**	**Renewal Rate (%)**	**Renewal Factor (i=0,05)**
Slurry Trench Curtain	45	2	0,000125
Regulation Storage	45	2	0,000125
Pumps	35	100	0,011072

8.8. Revenue of the Underground Dam

The project revenues are agricultural incomes provided by Eğri Creek underground dam. The irrigation area is 41.1 hec. The mentioned agricultural revenue is the income of 41 hec. The following Table 18 shows the agricultural benefit of the area.

Table 18. The revenue of the underground dam

National agricultural income ($/decare)	22.32
Gross project area (decare)	411
National agricultural income at the gross area ($)	9,173.52
National agricultural income with project ($/dec)	157.95
Net project area (decare)	372
National agricultural income in the net area with the project ($)	58,745.53
Development period coefficient	0.879
Annual national agricultural income increase achieved by the project ($)	**59,657.68**

The annual national agricultural income increase achieved by the underground dam project is 59,657.58$. This value is used in the profitability (rantability) calculation. The profitability (rantability) is 1.01 (Table 19).

Table 19. Annual income and outcome ratio (rantability)

Income ($)	Outcome ($)	Income – Outcome ($)	Rantability (R)
59,657.58	59,061.10	596.48	**1.01**

8.9. Discussion of the Results

The most crucial issue in the model is an increase in groundwater levels in other parts of the basin, apart from the rise of groundwater levels beneath the artificial groundwater recharge pools.

In the underground dam method, on the other hand, the volume change of the water in the aquifer formation is equal to the total volume of the water inflow with artificial recharge and the outflow because of the water demand activities. The reason is that the bottom of the underground dam is defined no-flow boundary condition.

According to the studies, the artificial recharge project method (R=1.03) and the underground dam method (R=1.01) are profitable projects.

The construction time of the underground dam is longer than the artificial groundwater recharge project.

In terms of the application technique, the underground dam requires a good design.

The artificial groundwater recharge project is a cheaper and easily applicable method.

Although both applications are economical initial investment cost of the underground dam is more expensive than the artificial groundwater recharge project.

The operating and maintenance cost of the underground dam is more expensive than the artificial groundwater recharge project.

The underground dam is not a method that can be applied in every region.

CHAPTER 9

SUMMARY, CONCLUSIONS AND FUTURE STUDIES

The aim of the study is to investigate the potential for artificial recharge of groundwater in the K. Menderes River Basin, especially in the Eğri Creek subbasin. The most suitable artificial recharge areas include highly porous media with thick unsaturated zone and the absence of any impending layers. In the study, the modeling is achieved in a representative area characterized by these conditions (i.e. the Eğri Creek Basin).

Due to the absence of site-specific data, the material properties used in this study were obtained from site tests and DSİ literature and laboratory tests.

Meteorological data such as the amount of precipitation, wind direction and speed, humidity, air temperature were measured from these stations. In K. Menderes River Basin, there are 10 meteorological stations, however only three of them are located adjacent to the study area, namely Tire, Ödemiş and Ovakent. Ödemiş Station is the closest station to the model area (about 12 km) and topographically at the same elevation as the model domain. Therefore, the meteorological data used in this study have been obtained from Ödemiş Station, which is still operated and best represents the model area.

The study area is located near the Gökçen region, which lies between Tire in the west and Adagüme in the east. There are two main lithologic units: alluvial fan deposits and Menderes Massif metamorphic.

The Küçük Menderes River Basin is drained by the Küçük Menderes River and its tributaries. One of these tributaries, the Eğri Creek drains the study area. Eğri Creek flows in northerly direction and joins the Küçük Menderes River at the north. In artificial recharge projects, the aim is to utilize excess water (that is the rest of the water budget with other projects) as a source to recharge the aquifer. Hence, the potential volume of water that can be collected should be first determined from flow measurements.

The two DSİ stream gauging stations operating adjacent to Eğri Creek, namely the Kızılkaya-Eğri Creek and Rahmanlar stations, were used to determine the discharge pattern in the study area. Correlation analysis is started to calculate missing data of the years (1980-1989 and 1991-2010). Then to obtain a relation between the flow data for the period between 1986-2019. 2011-2019 period flows are observed flow values of stream

gauge station no. 06-42 (Kızılkaya AGİ). The underline 1980-1989 and 1991-2010 period flows were completed with daily correlation with stream gauge station no. 06-11 (Rahmanlar AGİ).

The discharge rates of the Eğri Creek were calculated to determine the maximum and minimum flow rates obtained for each year. The minimum flow rate is necessary to design a regulatory project system.

Eğri Creek discharge showed that 1 (one) hm3 volume of water could utilize for groundwater recharge in six months (rainy period).

When the Eğri Creek upstream flows are examined. The results showed that Eğri Creek artificial recharge project could be operated for six months. The design discharge value is 70 l/sec.

Estimation of hydraulic parameters is a critical issue and directly affects the characterization of the system. Since hydrogeological models usually deal with aquifer simulations, estimation of saturated zone parameters is generally sufficient. However, in artificial recharge models, both saturated and unsaturated parameters should be taken into consideration.

Saturated hydraulic conductivity values derived from 13 pumping test results performed in the study area vary from 1.3 to 7.2 m/day (via Aquifer Test Pro.). The average hydraulic conductivity and storage coefficients of 13 tests with observation wells within the study area and its vicinity were calculated by the Aquifer Test Pro program.

The depth of the unsaturated zone is observed to decrease from north to south. The depth ranges from 60m to 20m throughout the Eğri Creek subbasin, with an average depth of 35m in the study area. Hydraulic parameters for the unsaturated zone are available in the site tests. The Van Genuchten's (1980) Soil-Water Retention Curve numerical solution helped determine hydraulic conductivity relationship with water content in HYDRUS 3D.

1020 m total depth research wells were drilled at 16 points to define the alluvium aquifer lithology of the study area (SK-1 to SK-16). The depth of the research wells ranges from 26 m to 148 m. Research wells correctly reflect the properties of the alluvium aquifer in the study area.

The laboratory test results were determined soil type is poor-sand/silty-sand (SP-SM).

Water content experiments are one of the first experiments in the laboratory in core samples taken from research wells. The range of results is between 1.5% to 14.9%.

where, n is the porosity [-] and V is the volume [L3]. In the study, porosity values could be obtained from soil core samples from research wells. The range of results is between 0.34 to 0.42.

Permeability is a measure of the water transmission capacity of soils. Permeability is a parameter that can be determined in the laboratory and in the field. Permeability tests in laboratory are carried out with constant head permeability tests on coarse-grained soils, while falling head permeability tests are applied on fine-grained units such as sand and clay. In the field, permeability can be calculated borehole tests (sending water to soil). In this study, permeability values were obtained by constant head tests in the DSİ laboratory. The range of results is between 2.55x10-5 to 5.30x10-4 m/sec.

Since HYDRUS-3D uses a 3D representation of the subsurface, in this study a length of about 1 km along the recharge pool center in north-south and east direction. Eğri Creek is defined natural boundary on the west side. The distance of Eğri Creek to the center of the recharge pool is accepted 90m. The thickness of the domain ranges from 26m to 148m.

Determination of the size and shape of elements depends on the model geometry and aim of the study. In order to obtain the most suitable mesh size and shape, trial and error method was used, where the effect of each mesh type on the solution was investigated. As a result, the mixed type gave the best results, and hence was selected. The element size in the model was assigned as 5m with a width of 0.5 m, which resulted in 3606 nodes and 14815 3D-elements.

One of the important parts of numerical modeling is assigning boundary conditions. It is not an easy task to convert real processes that take place on the boundary into mathematical relations. In order to obtain realistic results, boundary conditions should be assigned carefully. Since the flow of recharge water is modeled in 3D by constant head boundary condition method, the upper part of the domain is represented by ground surface (atmospheric boundary). Basically, the schist and gneiss are represented by no flow boundary (denoted by 1), thus they were not included in the solution of the flow equation. The ground surface is exposed to meteorological events, atmospheric boundary condition (denoted by 3) was chosen to represent Ödemiş Meteorological Station data. Northern, southern, eastern and western part of the study area is expressed with free flow-flux type boundary condition (denoted by 4), which represents flow of water out of the system. During the simulation period (180 days) on Eğri Creek, daily flow rates showed that the flow rates were low (Table 5). Eğri Creek's bed is very wide

(60m). The artificial recharge pool base elevation (125 msl) is 1 m below than Eğri Creek base elevation (126 msl). According to daily flow rates, Eğri Creek represents constant flux (specified head (denoted by 5)) boundary conditions. Also, the artificial recharge pool represents a constant head boundary condition (denoted by 2) (3 m) during the simulation period (180 days).

Calibration of the model is used to check whether the system inputs reflect the actual field conditions. In the calibration analysis, trial and error method was used to modify input parameters, such as hydraulic conductivity, initial or boundary conditions etc. These parameters were then adjusted within reasonable limits, until a good match between calculated and observed groundwater levels was obtained.

In this study, the groundwater table profiles obtained from the field measurements of water levels in October 2018 and April 2019 were used in the calibration process. The simulation covered a period of 180 days. This period corresponds to a wet season during which no pumpage took place for irrigation purposes. Thus, one of the parameters belonging to the real system, i.e., groundwater pumpage through wells was eliminated in the calibration process. Starting with the end of the dry season water table (October 2018), the aim was to match the observed water table profile at the end of the wet-season (i.e., April 2019).

At first, the system was thought to be composed of a single material, which was determined as sandy loam. The HYDRUS models have a soil texture modeling capability. The saturated hydraulic conductivity (Ksat (m/day)) was calibrated duration the wet season. a good agreement between modeled and observed groundwater level as indicated by high R^2 which was found 0.99.

. Model verification and validation is the next step after calibration. The objective of model validation is to check if the calibrated model works well on any dataset. After calibration process, the artificial groundwater recharge effect was discussed for the other two wells (SK_K6 and AK_5). When the data of the SK_K6 observation well examined, a good agreement between simulated and observed groundwater level as indicated by high R^2 which was found 0.96. When the data of the AK_5 observation well examined, which located to the north of the artificial recharge pool. a good agreement between simulated and observed groundwater level as indicated by high R^2 which was found 0.90. The precision of the mean error value, depending on the thickness of the aquifer, corresponds to 0.0008.

The recharge basin design involves the construction of the basins along the Eğri Creek to collect the water which diverted from the Eğri Creek regulator. The dimensions of the basin were determined by site test results to check the available space for construction, with a limiting factor that the depth of the recharge basin should not exceed 6 m to provide stability. Alternative scenarios for the artificial recharge of groundwater via recharge basins involve repeating the simulations for different recharge pool dimensions and so recharge water amounts. The simulation period starts in October 2018 and ends in April 2019, where the calibrated model is closely compatible with actual field conditions. The overall effect of artificial recharge was revealed as an average increase in the phreatic surface from 12.5m to 34.14m. The increase in the groundwater level in this process, which is done in the rainy period and which is the period when evaporation is low, also means an increase in underground storage. This amount of storage is approximately equal to the volume in artificial recharge. The volume ranges from 212270 m^3 to 1400000m^3. The average increase in groundwater levels ranges from 12.5m to 34.14m.

Hydrogeological and topographic investigations reveal that the Egri Creek subbasin is suitable for underground dam applications. The material parameters used in the model for saturated and unsaturated conditions are taken from previous studies (i.e. Zeytinova, Aktaş regulator project). Alluvium lies in a 175 m wide strip at the axis. The impermeability curtain will be constructed as 109 pieces of interlocking plaster strip. The height between the talweg and the crest level is 23m. The total crest length is 196m. by being socketed into the bedrock on the slopes.

The simulation period begins in October 2018 and ends in April 2019. The initial conditions were determined from the water table elevation drawn for October 2018. The simulations were repeated the without the presence of a recharge basin. The ground surface is exposed to meteorological events, and atmospheric boundary condition (denoted by 3) was chosen to represent Ödemiş Meteorological Station data. Northern, Eastern and Western part of the study area is expressed with no flow boundary condition (denoted by 1). Eğri Creek flows from the southern part of the study area to the northern. It is defined as the constant flux boundary conditions (denoted by 5). The model basement is defined as the no-flow boundary condition due to the presence of a schist layer.

The underground dam construction in the model domain results in approximately 580,117 m^3 increase in groundwater storage, however, this increase in groundwater levels is not significant to warrant the construction of the underground dam. On the other hand,

they are used where surface storage becomes impractical owing to high evaporation rates, reservoir siltation, pollution risks, etc.

The rise in groundwater storage equals the amount of percolation (due to precipitation) and Eğri Creek daily stream calculation. The groundwater level increases more rapidly at points close to the dam axis.

The underground dam raises the groundwater level by an average of 9.3 m. The inadequate rising of underground water levels can be categorized into two terms. Rainfall and seepage of Eğri Creek. Infiltration rate is the main factor for underground dam applications.

Also, the cost of application and maintenance of the underground dam is higher than the surface spreading method.

After the recharge pool dimension is decided, the Hantush and calibrated model relationship is revealed. The length and width are 30m and the depth of the pool is 6m. The groundwater mounding beneath the artificial recharge pool was calculated at 23.54m with the Hantush Excel Spreadsheet. The observations show that the height and effecting radius of the groundwater mounding decreased as the distance to the pool center.

The groundwater mounding and effecting radius were examined with the HYDRUS-3D, with a like dimension. The groundwater mounding beneath the artificial recharge pool was calculated at 26.2m with the HYDRUS-3D. The HYDRUS-3D model results are higher than Hantush spreadsheet results.

A linear relationship was observed between HYDRUS-3D and Hantush for the simulation period correlations, and the correlation coefficient was high (0.93). The fact that HYDRUS-3D results are higher than the Hantush analytical results is thought to be due to the numerical modeling algorithm. The hydraulic conductivity is the parameter that most affects the groundwater mound.

The fact that the horizontal hydraulic conductivity (K_h) is higher than the vertical hydraulic conductivity (K_v) has led to results.

While, The Hantush is an analytical solution method, HYDRUS-3D gives the mounding of a numerical solution.

According to the studies, the artificial recharge project method (R=1.03) and the underground dam method (R=1.01) are profitable projects.

The construction time of the underground dam is longer than the artificial groundwater recharge project.

In terms of the application technique, the underground dam requires a good design.

The artificial groundwater recharge project is a cheaper and easily applicable method.

Although both applications are economical initial investment cost of the underground dam is more expensive than the artificial groundwater recharge project.

The operating and maintenance cost of the underground dam is more expensive than the artificial groundwater recharge project.

The underground dam is not a method that can be applied in every region.

The main problem in artificial recharge applications is the decline of infiltration rate as a result of clogging. In order to prevent clogging, recharge basins in the model were operated in a wet-dry cycle, where the clogged layer can be removed by draining and rinsing the infiltration basins during the dry period.

The quality of water is another important factor in artificial recharge projects. In water spreading methods, such as recharge basin applications, the quality of water is improved through physical, geochemical and bacteriological processes that take place in unsaturated zone during infiltration. Thus, additional treatment of water is not necessary. Besides, in the study area, the source of water considered for recharge is direct runoff from Eğri Creek with pipes from the regulator.

It is believed that artificial recharge of groundwater can help natural recharge and replenish groundwater in Eğri Creek sub-basin. While there are numerous benefits of an artificial recharge project, this study is focused on increasing groundwater storage in the area. This study suits as an insight for future researches on the artificial recharge of groundwater in Turkey in order to increase groundwater storage, groundwater level rise, water quality improvement and land subsidence prevention. The main goal of this study was to prove that an artificial recharge project in the study area is applicable and effective.

This research can lead to new studies on the applicability of artificial recharge of groundwater in different parts of Turkey using the surplus flow of rivers during the rainy season. The research can be extended to study various effects of artificial recharge of groundwater e.g., land subsidence prevention.

REFERENCES

Al-Muttair, F.F., and Al-Turbak, A.S., 1991. Modeling of infiltration from an artificial recharge basin with decreasing ponded depth. J. King Saud Univ. Eng. Sci., vol. 3, 89-100.

Al-Yahyai, R., Schaffer, B., Davies, F.S. and Munoz- Carpena, R., 2006. Characterization of soil-water retention of a very gravelly loam soil varied with determination method. Soil Science, vol. 171, 85-93.

Apaydın, A., 2009. Mali bogazi groundwater dam: an alternative model for semi-arid regions of Turkey to store and save groundwater. Environ. Earth Sci., vol. 59, 339-345.

Aubertin, M., Mbonimpa, M., Bussière, B. and Chapuis, R.P., 2003. A model to predict the water retention curve from basic geotechnical properties. Canadian Geotechnical Journal, vol. 40, no. 6. 1104-1122.

Banks, H. O., Richter, R. C., Coe, J. J., McPartland, J. W., and Kretsinger, R., 1954. Artificial recharge in California. California Div. Water Resources, 41 p.

Berend, J.E., 1967. An analytical approach to the clogging effect of suspended matter. Internat. Assoc. Sci. Hydrology Bull., vol. 12, no. 2, 42-55.

Blaney, H.F., 1936. General review- symposium on contribution to ground-water supplies. Am. Geophys. Union Trans., vol. 17, no. 2, 456-458.

Boochs, P. W., and Billib, M., 1994. Management of a small ground water reservoir by recharge water from a surface reservoir. In: Johnson, A.I. and Pyne, D.G., (eds.), Proceedings of the second international symposium on artificial recharge of ground water, 661-668.

Bouwer, H., 1994. Artificial recharge- issues and future. In: Johnson, A.I. and Pyne, D.G., (eds.), Proceedings of the second international symposium on artificial recharge of ground water, 2-10.

Bouwer, H., 2002. Artificial recharge of groundwater: hydrogeology and engineering. Hydrogeology Journal, vol. 10, 121-142.

Brashears, M.L., Jr., 1946. Artificial recharge of ground water on Long Island, New York. Econ. Geology, vol. 41, no. 5, 503-516.

Brashears, M.L., Jr., 1953. Recharging ground-water reservoirs with wells and basins. Minin Eng., vol. 5, 1029- 1932.

Brothers, K., Bernholtz, A., and Katzer, T., 1994. Artificial ground-water recharge in Las Vegas Valley, Clark County, Nevada: Model prediction- "No cone of depression here!". In: Johnson, A.I. and Pyne, D.G., (eds.), Proceedings of the second international symposium on artificial recharge of ground water, 669- 678.

Chapuis, R.P., Chenaf, D., Bussiere, B., Aubertin, M. and Crespo, R., 2001. A user's approach to assess numerical codes for saturated and unsaturated seepage conditions. Can. Geotech. J., vol. 38, 1113-1126.

Connorton, B.J. and McIntosh, P., 1994. EUREAU survey on artificial recharge. In: Johnson, A.I. and Pyne, D.G., (eds.), Proceedings of the second international symposium on artificial recharge of ground water, 11-19.

Dewey, H., 1933. The falling water level of the chalk under London. Water and Water Eng., vol. 35, no. 121. 440-447.

Engler, K., Thompson, D.G., and Kazmann, R.G., 1945. Ground water supplies for rice irrigation in the Grand Prairie Region, Arkansas. Arkansas Uni. Bull. 457, 56 p.

Flanigan, J.B., Sorensen, P.A., and Tucker, M.A., 1994. Use of hydrogeologic data in recharge pond design. In: Johnson, A.I. and Pyne, D.G., (eds.), Proceedings of the second international symposium on artificial recharge of ground water, 139-148.

Foster, S., and Tuinhof, A., 2004. Brazil, Kenya: Subsurface dams to augment groundwater storage in basement terrain for human subsistence. Sustainable Groundwater Management Lessons from Practice, Case profile collection no. 5, 1-8.

Fredlund, D.G., and Anqing Xing., 1994. Equations for the soil-water characteristic curve. Canadian Geotechnical Journal., vol. 31, 521- 532.

Geo-slope International, 2007. Seepage modeling with SEEP/W: an engineering methodology, Canada, 2nd edition, 290 p.

Green, R.E., and Corey, J.C., 1971. Calculation of hydraulic conductivity: a further evaluation of some predictive methods. Soil Science Society of America Proceedings, vol. 35, 3- 8.

Harrell, M.A., 1935. Artificial ground-water recharge- a review of investigations and experience. U. S. Geol. Survey open-file report, 34 p.

Hillel, D., 2008. Soil in the environment: crucible of terrestrial life. Elsevier/Academic Press, Amsterdam Boston, 289 p.

Houk, I.E., 1951. Irrigation engineering, vol. 1. New York: John Wiley and Sons, 545 p.

Imbertson, N.M., 1959. Replenishment of ground water with desilted storm water. In: Schiff, L. (ed.), Bienn. Conf. on ground-water recharge, 2d, Berkeley, Calif., Proc: Collins, Colo., Western Soil and Water Management Research Br., 66-70.

Ishaq, A.M., Al-Suwaiyan, M.S., and Al-Sinan, A.A., 1994. Suitability of wastewater effluents to recharge groundwater aquifers in Saudi Arabia. In: Johnson, A.I. and Pyne, D.G., (eds.), Proceedings of the second international symposium on artificial recharge of ground water, 376- 385.

Irwin, J.L., 1931. Report on water sinking experiment in the City of Arcadia well no. 2 Santa Anita Basin, open file report, Los Angeles County Flood Control Dist., 6 p.

Izbicki, J.A., Flint, A.L., and Stamos, C.L., 2007. Artificial recharge through a thick, heterogeneous unsaturated zone. Ground Water, vol. 46, no. 3, 475-488.

Jacobs, K.L. and Holway, J.M., 2004. Managing for sustainability in an arid climate: lessons learned from 20 years of groundwater management in Arizona, USA. Hydrogeology Journal, vol. 12, 52-65.

Jans, M., 1959. North Kern Water Storage District spreading activities. In: Schiff, L. (ed.), Bienn. Conf. on ground-water recharge, 2d, Berkeley, Calif., Proc: Collins, Colo., Western Soil and Water Management Research Br., 54-57.

Jansa, O.V.E., 1952. Artificial replenishment of underground water: Internat. Water Supply Assoc., 2d Cong., Paris, 105 p.

Kim, C.P., Stricker, J.N.M., and Torfs, P.J.J.F., 1996. An analytical framework for the water budget of the unsaturated zone. Water Resources Research, vol. 32, no. 12, 3475-3484.

Kimrey, J.O., 1989. Artificial recharge of groundwater and its role in water management. Desalination, 72, 135-147.

Lal, R., and Shukla, M.K., 2004. Principles of soil physics. Marcel Dekker, New York, 699 p.

Lane, D.A., 1934. Increasing storage by water spreading. Am. Water Works Assoc. Jour., vol. 26, no. 4, 421-429.

Laverty, F.B., 1952. Ground water recharge. Am. Water Works Assoc. Jour., vol. 44, no. 8, 677-681.

Laverty, F.B., Jordan, L.W., and van der Goot, H.A., 1951. Report on tests for the creation of fresh water barriers to prevent salinity intrusion performed in West Coastal Basin, Los Angeles County, California. Los Angeles, Los Angeles County Flood Control District, 70 p.

Lehr, J.H., 1982. Artificial ground-water recharge: a solution to many U.S. watersupply problems. Ground Water, vol. 20, no. 3, 262-266.

Light, M.E., 1994. Design, construction, and operation of a surface recharge facility for the purpose of reusing secondary effluent in an arid climate, Tucson, Arizona, USA. In: Johnson, A.I. and Pyne, D.G., (eds.), Proceedings of the second international symposium on artificial recharge of ground water, 342- 351.

Lytle, B.A., 1994. Deep bedrock well injection near Denver, Colorado. In: Johnson, A.I. and Pyne, D.G., (eds.), Proceedings of the second international symposium on artificial recharge of ground water, 81-90.

Markus, M.R., Thompson, C.A., and Ulukaya, M., 1994. Enhanced artificial recharge utilizing inflatable rubber dams. In: Johnson, A.I. and Pyne, D.G., (eds.), Proceedings of the second international symposium on artificial recharge of ground water, 120-128.

Mallants, D., Volckaert, G., and Marivoet, J., 1999. Sensitivity of protective barrier performance to changes in rainfall rate. Waste Management, vol. 19, 467- 475.

Muckel, D.C., 1945. Replenishing ground-water supplies by sinking water through wells or shafts. U. S. Soil Conserv. Service, 8 p.

Munévar, A., and Marino, M.A., 1999. Modeling analysis of ground water recharge potential on alluvial fans using limited data. Ground Water, vol. 37, no. 5, 649-659.

Mushtaq, H., and Mays, L.W., 1994. Operation of recharge basin systems: an optimal control approach. In: Johnson, A.I. and Pyne, D.G., (eds.), Proceedings of the second international symposium on artificial recharge of ground water, 352- 361.

Nielsen, D.R., van Genuchten, M.Th., and Biggar, J.W., 1986. Water flow and solute transport proceses in the unsaturated zone. Water resources research, vol. 22, no. 9, 89-108.

Nilsson, A., 1988. Groundwater dams for small-scale water supply. Intermediate Technology Publications, London, UK, 69 p.

Osman, Y.Z., and Bruen, M.P., 2002. Modelling stream-aquifer seepage in an alluvial aquifer: an improved loosing stream package for MODFLOW. Journal of Hydrology, vol. 264, 69-86.

Phillips, S.P., 2003. Aquifers, artificial recharge of. Encyclopedia of Water Science, vol. 1, no. 1, 33-36.

Peters, J.H., 1994. Artificial recharge and water supply in the Netherlands, state of art and future trends. In: Johnson, A.I. and Pyne, D.G., (eds.), Proceedings of the second international symposium on artificial recharge of ground water, 28-39.

Pyne, R.D.G., 1994. Seasonal storage of reclaimed waste water and surface water in brackish aquifers using aquifer storage and recovery (ASR) wells. In: Johnson, A.I. and Pyne, D.G., (eds.), Proceedings of the second international symposium on artificial recharge of ground water, 282- 298.

Reddy, K.R., 2008. Enhanced aquifer recharge. In: Darnault, C.J.G. (ed.), Overexploitation and Contamination of Shared Groundwater Resources, 275-287.

Richter, R.C., and Chun, R.Y.D., 1959. Geologic and hydrologic factors affecting infiltration rates at artificial recharge sites in California. In: Schiff, L. (ed.), Bienn. Conf. on ground-water recharge, 2d, Berkeley, Calif., Proc: Collins, Colo., Western Soil and Water Management Research Br., 48-52.

Schiff, L., and Dyer, K.L., 1964. Some physical and chemical considerations in artificial ground-water recharge. International Assoc. Sci. Hydrology Pub., vol. 64, 347-358.

Signor, D.C., Growitz D.J., and Kam, W., 1970. Annotated bibliography on artificial recharge of ground water, 1955-67. Geological Survey Water-Supply Paper 1990, 141p.

Simpson, T.R., 1948. Recharge by percolation wells, Excerpts from report on percolation, Feather River and tributaries, counties of Sutter and Yuba, California. California Div. Water Resources, 4 p.

Soyer, R., 1947. Recharge of aquifers. Technique Sanitaire et Municipal, vol. 42, 58-69.

Stakelbeek, A., Roosma, E., and Holzhaus, P.M., 1994. Deep well infiltration in the North-Holland dune area. In: Johnson, A.I. and Pyne, D.G., (eds.), Proceedings of the second international symposium on artificial recharge of ground water, 258-269.

Tayfur, G., Sen, Z., 2018. Groundwater Hydrology and Hydraulic, İstanbul, Turkey. Su Foundation Publications.

Thiem, G., 1923. Effect and purpose of recharge wells. Gesundheits- Ingenieur, vol. 46, no. 34, 331-333.

Todd, D.K., 1959. Annotated bibliography on artificial recharge of ground water through 1954. Geological Survey Water-Supply Paper 1477, 115 p.

Van Genuchten, M.Th., 1980. A closed form equation for predicting the hydraulic conductivity of unsaturated soils. Soil sci. soc. Am. J., vol. 44, 892-898.

Wang, H.F., and Anderson, M.P., 1982. Introduction to groundwater modeling: finite difference and finite element methods. W. H. Freeman and Company, USA, 237 p.

Wiese, B., and Nutzmann, G., 2007. Infiltration of surface water into ground-water under transient pressure gradients. IGB, 55-64.

Yazıcıgil, H., Doyuran, V., Karahanoğlu, N.,Yanmaz, M., Çamur, Z., Toprak, V., Rojay, B., Yılmaz K.K., Şakıyan, J., Süzen, L., Yeşilnacar, E., Gündoğdu, A., Pusatlı, T., and Tuzcu, B., 2000. "Investigation and Management of Groundwater Resources in Küçük Menderes River Basin under the scope of Revised Hydrogeological Studies", Final Report: Vol. I: Main Report, Vol. II: Meteorology and Hydrology, Vol. III: Geology, Vol. IV: Groundwater Database, Vol. V: Hydrogeology, Vol. VI: Groundwater Chemistry, Quality and Contamination, Vol. VII: Groundwater Flow Model Project, Project no: 98-03-09-01-01. Middle East Technical University, Ankara.

APPENDIX A

LABORATORY SOIL EXPERIMENT RESULTS

Table A.1. Sieve analysis results of SK-1

1	2	3			4			5	6	7
No	Sample No	Particle Dist.			Consistency Limit			Soil Class	Clay	Silt
		0.075	4.75	75						
		mm	mm	mm	LL	PL	PI			
		Passed %	Passed %	Passed %	%	%	%		%	%
1	SK-1 (0.00 – 10.00 m)	18.2	81.8	100,00	-	-	-	SP-SM	0.3	1.2
2	SK-1 (10.00 – 15.00 m)	13,4	86.6	100,00	-	-	-	SP-SM	0.00	0.00
3	SK-1 (15.00 – 25.00 m)	11.8	88.2	100,00	-	-	-	SP-SM	0.00	2.1
4	SK-1 (25.00 – 35.00 m)	10.6	89.4	100,00	-	-	-	SP-SM	0.00	0.00
5	SK-1 (35.50 – 45.00 m)	8.6	91.4	100,00	-	-	-	SP-SM	0.00	0.00
6	SK-1 (45.00 – 55.00 m)	9.3	100	100,00	-	-	-	SP-SM	0.00	0.00
7	SK-1 (55.00 – 60.00 m)	11.2	100	100,00	-	-	-	SP-SM	0.00	0.00
8	SK-1 (60.00 – 65.50 m)	7.2	99.7	100,00	-	-	-	SP-SM	0.00	0.00
9	SK-1 (65.50 – 68.50 m)	10.2	100	100,00	-	-	-	SP-SM	0.00	0.00
10	SK-1 (68.50 – 105.00 m)	9.3	91.7	100,00	-	-	-	SP-SM	0.00	0.00

Table A.2. Sieve analysis results of SK-2

1	2	3			4			5	6	7
No	Sample No	Particle Dist.			Consistency Limit			Soil Class	Clay	Silt
		0.075	4.75	75						
		mm	mm	mm	LL	PL	PI			
		Passed %	Passed %	Passed %	%	%	%		%	%
1	SK-2 (0.00 – 10.00 m)	18.2	81.8	100,00	-	-	-	SP-SM	0.3	1.2
2	SK-2 (10.00 – 15.00 m)	13,4	86.6	100,00	-	-	-	SP-SM	0.00	0.00
3	SK-2 (15.00 – 25.00 m)	11.8	88.2	100,00	-	-	-	SP-SM	0.00	2.1
4	SK-2 (25.00 – 35.00 m)	10.6	89.4	100,00	-	-	-	SP-SM	0.00	0.00
5	SK-2 (35.50 – 45.00 m)	8.6	91.4	100,00	-	-	-	SP-SM	0.00	0.00
6	SK-2 (45.00 – 55.00 m)	9.3	100	100,00	-	-	-	SP-SM	0.00	0.00
7	SK-2 (55.00 – 60.00 m)	11.2	100	100,00	-	-	-	SP-SM	0.00	0.00
8	SK-2 (60.00 – 65.50 m)	7.2	99.7	100,00	-	-	-	SP-SM	0.00	0.00
9	SK-2 (65.50 – 68.50 m)	10.2	100	100,00	-	-	-	SP-SM	0.00	0.00
10	SK-2 (68.50 – 135.00 m)	9.3	91.7	100,00	-	-	-	SP-SM	0.00	0.00

Table A.3. Sieve analysis results of SK-3

1	2	3			4			5	6	7
No	Sample No	Particle Dist.			Consistency Limit			Soil Class	Clay	Silt
		0.075	4.75	75						
		mm	mm	mm	LL	PL	PI			
		Passed %	Passed %	Passed %	%	%	%		%	%
1	SK-3 (0.00 – 10.00 m)	18.2	81.8	100,00	-	-	-	SP-SM	0.3	1.2
2	SK-3 (10.00 – 15.00 m)	13,4	86.6	100,00	-	-	-	SP-SM	0.00	0.00
3	SK-3 (15.00 – 25.00 m)	11.8	88.2	100,00	-	-	-	SP-SM	0.00	2.1
4	SK-3 (25.00 – 35.00 m)	10.6	89.4	100,00	-	-	-	SP-SM	0.00	0.00
5	SK-3 (35.50 – 45.00 m)	8.6	91.4	100,00	-	-	-	SP-SM	0.00	0.00
6	SK-3 (45.00 – 55.00 m)	9.3	100	100,00	-	-	-	SP-SM	0.00	0.00

Table A.4. Sieve analysis results of SK-4

1	2	3			4			5	6	7
No	Sample No	Particle Dist.			Consistency Limit			Soil Class	Clay	Silt
		0.075	4.75	75						
		mm	mm	mm	LL	PL	PI			
		Passed %	Passed %	Passed %	%	%	%		%	%
1	SK-4 (0.00 – 10.00 m)	18.2	81.8	100,00	-	-	-	SP-SM	0.3	1.2
2	SK-4 (10.00 – 15.00 m)	13,4	86.6	100,00	-	-	-	SP-SM	0.00	0.00
3	SK-4 (15.00 – 25.00 m)	11.8	88.2	100,00	-	-	-	SP-SM	0.00	2.1
4	SK-4 (25.00 – 35.00 m)	10.6	89.4	100,00	-	-	-	SP-SM	0.00	0.00
5	SK-4 (35.50 – 45.00 m)	8.6	91.4	100,00	-	-	-	SP-SM	0.00	0.00
6	SK-4 (45.00 – 55.00 m)	9.3	100	100,00	-	-	-	SP-SM	0.00	0.00
7	SK-4 (55.00 – 60.00 m)	11.2	100	100,00	-	-	-	SP-SM	0.00	0.00
8	SK-4 (60.00 – 65.50 m)	7.2	99.7	100,00	-	-	-	SP-SM	0.00	0.00
9	SK-4 (65.50 – 68.50 m)	10.2	100	100,00	-	-	-	SP-SM	0.00	0.00
10	SK-4 (68.50 – 105.00 m)	9.3	91.7	100,00	-	-	-	SP-SM	0.00	0.00

Table A.5. Sieve analysis results of SK-5

1	2	3			4			5	6	7
No	Sample No	Particle Dist.			Consistency Limit			Soil Class	Clay	Silt
		0.075	4.75	75						
		mm	mm	mm	LL	PL	PI			
		Passed %	Passed %	Passed %	%	%	%		%	%
1	SK-5 (0.00 – 10.00 m)	18.2	81.8	100,00	-	-	-	SP-SM	0.3	1.2
2	SK-5 (10.00 – 15.00 m)	13,4	86.6	100,00	-	-	-	SP-SM	0.00	0.00
3	SK-5 (15.00 – 25.00 m)	11.8	88.2	100,00	-	-	-	SP-SM	0.00	2.1
4	SK-5 (25.00 – 35.00 m)	10.6	89.4	100,00	-	-	-	SP-SM	0.00	0.00
5	SK-5 (35.50 – 45.00 m)	8.6	91.4	100,00	-	-	-	SP-SM	0.00	0.00
6	SK-5 (45.00 – 55.00 m)	9.3	100	100,00	-	-	-	SP-SM	0.00	0.00
7	SK-5 (55.00 – 60.00 m)	11.2	100	100,00	-	-	-	SP-SM	0.00	0.00
8	SK-5 (60.00 – 65.50 m)	7.2	99.7	100,00	-	-	-	SP-SM	0.00	0.00
9	SK-5 (65.50 – 68.50 m)	10.2	100	100,00	-	-	-	SP-SM	0.00	0.00
10	SK-5 (68.50 – 90.00 m)	9.3	91.7	100,00	-	-	-	SP-SM	0.00	0.00

Table A.6. Sieve analysis results of SK-6

1	2	3			4			5	6	7
No	Sample No	Particle Dist.			Consistency Limit			Soil Class	Clay	Silt
		0.075	4.75	75						
		mm	mm	mm	LL	PL	PI			
		Passed %	Passed %	Passed %	%	%	%		%	%
1	SK-6 (0.00 – 10.00 m)	18.2	81.8	100,00	-	-	-	SP-SM	0.3	1.2
2	SK-6 (10.00 – 15.00 m)	13,4	86.6	100,00	-	-	-	SP-SM	0.00	0.00
3	SK-6 (15.00 – 25.00 m)	11.8	88.2	100,00	-	-	-	SP-SM	0.00	2.1
4	SK-6 (25.00 – 35.00 m)	10.6	89.4	100,00	-	-	-	SP-SM	0.00	0.00
5	SK-6 (35.50 – 45.00 m)	8.6	91.4	100,00	-	-	-	SP-SM	0.00	0.00
6	SK-6 (45.00 – 55.00 m)	9.3	100	100,00	-	-	-	SP-SM	0.00	0.00

Table A.7. Sieve analysis results of SK-7

1	2	3			4			5	6	7
No	Sample No	Particle Dist.			Consistency Limit			Soil Class	Clay	Silt
		0.075	4.75	75						
		mm	mm	mm	LL	PL	PI			
		Passed %	Passed %	Passed %	%	%	%		%	%
1	SK-7 (0.00 – 10.00 m)	18.2	81.8	100,00	-	-	-	SP-SM	0.3	1.2
2	SK-7 (10.00 – 15.00 m)	13,4	86.6	100,00	-	-	-	SP-SM	0.00	0.00
3	SK-7 (15.00 – 25.00 m)	11.8	88.2	100,00	-	-	-	SP-SM	0.00	2.1
4	SK-7 (25.00 – 35.00 m)	10.6	89.4	100,00	-	-	-	SP-SM	0.00	0.00
5	SK-7 (35.50 – 45.00 m)	8.6	91.4	100,00	-	-	-	SP-SM	0.00	0.00
6	SK-7 (45.00 – 55.00 m)	9.3	100	100,00	-	-	-	SP-SM	0.00	0.00
7	SK-7 (55.00 – 60.00 m)	11.2	100	100,00	-	-	-	SP-SM	0.00	0.00
8	SK-7 (60.00 – 65.50 m)	7.2	99.7	100,00	-	-	-	SP-SM	0.00	0.00
9	SK-7 (65.50 – 68.50 m)	10.2	100	100,00	-	-	-	SP-SM	0.00	0.00
10	SK-7 (68.50 – 145.00 m)	9.3	91.7	100,00	-	-	-	SP-SM	0.00	0.00

Table A.9. Sieve analysis results of SK-9

1	2	3			4			5	6	7
No	Sample No	Particle Dist.			Consistency Limit			Soil Class	Clay	Silt
		0.075	4.75	75						
		mm	mm	mm	LL	PL	PI			
		Passed %	Passed %	Passed %	%	%	%		%	%
1	SK-9 (0.00 – 10.00 m)	18.2	81.8	100,00	-	-	-	SP-SM	0.3	1.2
2	SK-9 (10.00 – 15.00 m)	13,4	86.6	100,00	-	-	-	SP-SM	0.00	0.00
3	SK-9 (15.00 – 25.00 m)	11.8	88.2	100,00	-	-	-	SP-SM	0.00	2.1
4	SK-9 (25.00 – 35.00 m)	10.6	89.4	100,00	-	-	-	SP-SM	0.00	0.00
5	SK-9 (35.50 – 45.00 m)	8.6	91.4	100,00	-	-	-	SP-SM	0.00	0.00
6	SK-9 (45.00 – 55.00 m)	9.3	100	100,00	-	-	-	SP-SM	0.00	0.00
7	SK-9 (55.00 – 60.00 m)	11.2	100	100,00	-	-	-	SP-SM	0.00	0.00
8	SK-9 (60.00 – 65.50 m)	7.2	99.7	100,00	-	-	-	SP-SM	0.00	0.00
9	SK-9 (65.50 – 68.50 m)	10.2	100	100,00	-	-	-	SP-SM	0.00	0.00
10	SK-9 (68.50 – 95.00 m)	9.3	91.7	100,00	-	-	-	SP-SM	0.00	0.00

Table A.10. Sieve analysis results of SK-10

1	2	3			4			5	6	7
No	Sample No	Particle Dist.			Consistency Limit			Soil Class	Clay	Silt
		0.075	4.75	75						
		mm	mm	mm	LL	PL	PI			
		Passed %	Passed %	Passed %	%	%	%		%	%
1	SK-10 (0.00 – 10.00 m)	18.2	81.8	100,00	-	-	-	SP-SM	0.3	1.2
2	SK-10 (10.00 – 15.00 m)	13,4	86.6	100,00	-	-	-	SP-SM	0.00	0.00
3	SK-10 (15.00 – 25.00 m)	11.8	88.2	100,00	-	-	-	SP-SM	0.00	2.1
4	SK-10 (25.00 – 35.00 m)	10.6	89.4	100,00	-	-	-	SP-SM	0.00	0.00
5	SK-10 (35.50 – 45.00 m)	8.6	91.4	100,00	-	-	-	SP-SM	0.00	0.00
6	SK-10 (45.00 – 55.00 m)	9.3	100	100,00	-	-	-	SP-SM	0.00	0.00
7	SK-10 (55.00 – 60.00 m)	11.2	100	100,00	-	-	-	SP-SM	0.00	0.00
8	SK-10 (60.00 – 65.50 m)	7.2	99.7	100,00	-	-	-	SP-SM	0.00	0.00
9	SK-10 (65.50 – 68.50 m)	10.2	100	100,00	-	-	-	SP-SM	0.00	0.00
10	SK-10 (68.50 – 115.00 m)	9.3	91.7	100,00	-	-	-	SP-SM	0.00	0.00

Table A.11. Sieve analysis results of SK-11

1	2	3			4			5	6	7
No	Sample No	Particle Dist.			Consistency Limit			Soil Class	Clay	Silt
		0.075	4.75	75						
		mm	mm	mm	LL	PL	PI			
		Passed %	Passed %	Passed %	%	%	%		%	%
1	SK-11 (0.00 – 10.00 m)	18.2	81.8	100,00	-	-	-	SP-SM	0.3	1.2
2	SK-11 (10.00 – 15.00 m)	13,4	86.6	100,00	-	-	-	SP-SM	0.00	0.00
3	SK-11 (15.00 – 25.00 m)	11.8	88.2	100,00	-	-	-	SP-SM	0.00	2.1
4	SK-11 (25.00 – 35.00 m)	10.6	89.4	100,00	-	-	-	SP-SM	0.00	0.00
5	SK-11 (35.50 – 45.00 m)	8.6	91.4	100,00	-	-	-	SP-SM	0.00	0.00
6	SK-11 (45.00 – 55.00 m)	9.3	100	100,00	-	-	-	SP-SM	0.00	0.00
7	SK-11 (55.00 – 60.00 m)	11.2	100	100,00	-	-	-	SP-SM	0.00	0.00

Table A.12. Sieve analysis results of SK-12

1	2	3			4			5	6	7
No	Sample No	Particle Dist.			Consistency Limit			Soil Class	Clay	Silt
		0.075	4.75	75						
		mm	mm	mm	LL	PL	PI			
		Passed %	Passed %	Passed %	%	%	%		%	%
1	SK-12 (0.00 – 10.00 m)	18.2	81.8	100,00	-	-	-	SP-SM	0.3	1.2
2	SK-12 (10.00 – 15.00 m)	13,4	86.6	100,00	-	-	-	SP-SM	0.00	0.00
3	SK-12 (15.00 – 25.00 m)	11.8	88.2	100,00	-	-	-	SP-SM	0.00	2.1
4	SK-12 (25.00 – 35.00 m)	10.6	89.4	100,00	-	-	-	SP-SM	0.00	0.00
5	SK-12 (35.50 – 45.00 m)	8.6	91.4	100,00	-	-	-	SP-SM	0.00	0.00
6	SK-12 (45.00 – 55.00 m)	9.3	100	100,00	-	-	-	SP-SM	0.00	0.00
7	SK-12 (55.00 – 60.00 m)	11.2	100	100,00	-	-	-	SP-SM	0.00	0.00
8	SK-12 (60.00 – 65.50 m)	7.2	99.7	100,00	-	-	-	SP-SM	0.00	0.00
9	SK-12 (65.50 – 68.50 m)	10.2	100	100,00	-	-	-	SP-SM	0.00	0.00
10	SK-12 (68.50 – 90.00 m)	9.3	91.7	100,00	-	-	-	SP-SM	0.00	0.00

Table A.13. Sieve analysis results of SK-13

1	2	3			4			5	6	7
No	Sample No	Particle Dist.			Consistency Limit			Soil Class	Clay	Silt
		0.075	4.75	75						
		mm	mm	mm	LL	PL	PI			
		Passed %	Passed %	Passed %	%	%	%		%	%
1	SK-13 (0.00 – 10.00 m)	18.2	81.8	100,00	-	-	-	SP-SM	0.3	1.2
2	SK-13 (10.00 – 15.00 m)	13,4	86.6	100,00	-	-	-	SP-SM	0.00	0.00
3	SK-13 (15.00 – 25.00 m)	11.8	88.2	100,00	-	-	-	SP-SM	0.00	2.1
4	SK-13 (25.00 – 35.00 m)	10.6	89.4	100,00	-	-	-	SP-SM	0.00	0.00
5	SK-13 (35.50 – 45.00 m)	8.6	91.4	100,00	-	-	-	SP-SM	0.00	0.00
6	SK-13 (45.00 – 55.00 m)	9.3	100	100,00	-	-	-	SP-SM	0.00	0.00
7	SK-13 (55.00 – 60.00 m)	11.2	100	100,00	-	-	-	SP-SM	0.00	0.00

Table A.14. Sieve analysis results of SK-14

1	2	3			4			5	6	7
No	Sample No	Particle Dist.			Consistency Limit			Soil Class	Clay	Silt
		0.075	4.75	75						
		mm	mm	mm	LL	PL	PI			
		Passed %	Passed %	Passed %	%	%	%		%	%
1	SK-14 (0.00 – 10.00 m)	18.2	81.8	100,00	-	-	-	SP-SM	0.3	1.2
2	SK-14 (10.00 – 15.00 m)	13,4	86.6	100,00	-	-	-	SP-SM	0.00	0.00
3	SK-14 (15.00 – 25.00 m)	11.8	88.2	100,00	-	-	-	SP-SM	0.00	2.1
4	SK-14 (25.00 – 35.00 m)	10.6	89.4	100,00	-	-	-	SP-SM	0.00	0.00
5	SK-14 (35.50 – 45.00 m)	8.6	91.4	100,00	-	-	-	SP-SM	0.00	0.00
6	SK-14 (45.00 – 55.00 m)	9.3	100	100,00	-	-	-	SP-SM	0.00	0.00
7	SK-14 (55.00 – 60.00 m)	11.2	100	100,00	-	-	-	SP-SM	0.00	0.00
8	SK-14 (60.00 – 65.50 m)	7.2	99.7	100,00	-	-	-	SP-SM	0.00	0.00
9	SK-14 (65.50 – 68.50 m)	10.2	100	100,00	-	-	-	SP-SM	0.00	0.00
10	SK-14 (68.50 – 70.00 m)	9.3	91.7	100,00	-	-	-	SP-SM	0.00	0.00

Table A.15. SK-1 laboratory soil experiment results

Depth (m)	Water Content (%)	Natural Mass (g/cm^3)	Specific Gravity	Porosity
(0.00 – 10.00 m)	2.8	1.90	2.70	0.39
(10.00 – 15.00 m)	3.6	1.97	2.71	0.33
(15.00 – 25.00 m)	1.7	1.95	2.70	0.36
(25.00 – 35.00 m)	2.8	2.12	2.73	0.34
(35.50 – 45.00 m)	4.8	1.6	2.68	0.42
(45.00 – 55.00 m)	5.6	1.8	2.73	0.40
(55.00 – 65.00 m)	4.9	1.7	2.69	0.36
(65.00 – 70.50 m)	4.2	2.01	2.71	0.42
(75.50 – 78.50 m)	7.5	1.9	2.72	0.37
(78.50 – 80.00 m)	9.2	1.8	2.71	0.39

Table A.16. SK-2 laboratory soil experiment results

Depth (m)	Water Content (%)	Natural Mass (g/cm^3)	Specific Gravity	Porosity
(0.00 – 10.00 m)	2.9	1.90	2.71	0.39
(10.00 – 15.00 m)	4.6	1.97	2.71	0.34
(15.00 – 25.00 m)	1.5	1.95	2.71	0.36
(25.00 – 35.00 m)	2.8	2.12	2.73	0.36
(35.50 – 45.00 m)	5.8	1.6	2.7	0.41
(45.00 – 55.00 m)	6.6	1.8	2.73	0.40
(55.00 – 60.00 m)	4.9	1.7	2.69	0.38
(60.00 – 65.50 m)	5.2	2.01	2.7	0.42
(65.50 – 68.50 m)	8.5	1.9	2.72	0.39
(68.50 – 70.00 m)	9.2	1.8	2.71	0.39

Table A.17. SK-3 laboratory soil experiment results

Depth (m)	Water Content (%)	Natural Mass (g/cm^3)	Specific Gravity	Porosity
(0.00 – 10.00 m)	2.6	1.90	2.70	0.38
(10.00 – 25.00 m)	4.6	1.97	2.70	0.33
(25.00 – 35.00 m)	1.3	1.95	2.71	0.35
(35.00 – 45.00 m)	2.9	2.12	2.73	0.35
(45.50 – 50.00 m)	5.4	1.6	2.71	0.40
(50.00 – 55.00 m)	6.2	1.8	2.72	0.39
(55.00 – 55.50 m)	4.3	1.7	2.69	0.37
(55.50 – 65.50 m)	5.3	2.01	2.70	0.41
(65.50 – 75.50 m)	8.6	1.9	2.72	0.38
(75.50 – 85.00 m)	9.1	1.8	2.71	0.38

Table A.18. SK-4 laboratory soil experiment results

Depth (m)	Water Content (%)	Natural Mass (g/cm^3)	Specific Gravity	Porosity
(0.00 – 10.00 m)	2.9	1.90	2.71	0.39
(10.00 – 15.00 m)	4.6	1.97	2.71	0.34
(15.00 – 25.00 m)	1.5	1.95	2.71	0.36
(25.00 – 35.00 m)	2.8	2.12	2.73	0.36
(35.50 – 75.00 m)	5.8	1.6	2.7	0.41
(75.00 – 80.00 m)	6.6	1.8	2.73	0.40
(80.00 – 85.00 m)	4.9	1.7	2.69	0.38
(85.00 – 95.50 m)	5.2	2.01	2.7	0.42
(95.50 – 105.50 m)	8.5	1.9	2.72	0.39
(105.50 – 110.00 m)	9.2	1.8	2.71	0.39

Table A.19. SK-5 laboratory soil experiment results

Depth (m)	Water Content (%)	Natural Mass (g/cm^3)	Specific Gravity	Porosity
(0.00 – 10.00 m)	2.5	1.90	2.71	0.42
(10.00 – 15.00 m)	4.4	1.97	2.71	0.37
(15.00 – 25.00 m)	1.7	1.95	2.71	0.39
(25.00 – 35.00 m)	2.9	2.12	2.73	0.36
(35.50 – 45.00 m)	5.5	1.6	2.7	0.42
(45.00 – 55.00 m)	6.8	1.8	2.73	0.39
(55.00 – 60.00 m)	4.8	1.7	2.69	0.38
(60.00 – 75.50 m)	5.2	2.01	2.7	0.42
(75.50 – 80.50 m)	8.4	1.9	2.72	0.38
(80.50 – 90.00 m)	8.2	1.8	2.71	0.41

Table A.20. SK-6 laboratory soil experiment results

Depth (m)	Water Content (%)	Natural Mass (g/cm^3)	Specific Gravity	Porosity
(0.00 – 10.00 m)	2.9	1.90	2.71	0.39
(10.00 – 15.00 m)	4.6	1.97	2.71	0.34
(15.00 – 25.00 m)	1.5	1.95	2.71	0.36
(25.00 – 35.00 m)	2.8	2.12	2.73	0.36
(35.50 – 45.00 m)	5.8	1.6	2.7	0.41
(45.00 – 55.00 m)	6.6	1.8	2.73	0.40
(55.00 – 60.00 m)	4.9	1.7	2.69	0.38
(60.00 – 65.50 m)	5.2	2.01	2.7	0.42
(65.50 – 68.50 m)	8.5	1.9	2.72	0.39
(68.50 – 70.00 m)	9.2	1.8	2.71	0.39

Table A.21. SK-7 laboratory soil experiment results

Depth (m)	Water Content (%)	Natural Mass (g/cm^3)	Specific Gravity	Porosity
(0.00 – 10.00 m)	2.6	1.90	2.69	0.37
(10.00 – 15.00 m)	4.4	1.97	2.69	0.32
(15.00 – 25.00 m)	1.5	1.95	2.71	0.34
(25.00 – 35.00 m)	2.7	2.12	2.72	0.36
(35.50 – 45.00 m)	5.5	1.6	2.70	0.39
(45.00 – 55.00 m)	6.9	1.8	2.72	0.38
(55.00 – 60.00 m)	4.3	1.7	2.69	0.36
(60.00 – 65.50 m)	5.2	2.01	2.71	0.40
(65.50 – 68.50 m)	8.2	1.9	2.71	0.37
(68.50 – 70.00 m)	8.7	1.8	2.72	0.39

Table A.22. SK-8 laboratory soil experiment results

Depth (m)	Water Content (%)	Natural Mass (g/cm^3)	Specific Gravity	Porosity
(0.00 – 10.00 m)	2.8	1.90	2.71	0.39
(10.00 – 15.00 m)	4.4	1.97	2.71	0.34
(15.00 – 25.00 m)	1.5	1.95	2.71	0.36
(25.00 – 35.00 m)	2.8	2.12	2.73	0.36
(35.50 – 45.00 m)	5.8	1.6	2.7	0.41
(45.00 – 55.00 m)	6.6	1.8	2.73	0.40
(55.00 – 60.00 m)	4.9	1.7	2.69	0.38
(60.00 – 65.50 m)	5.2	2.01	2.7	0.42
(65.50 – 68.50 m)	8.5	1.9	2.72	0.39
(68.50 – 70.00 m)	9.2	1.8	2.71	0.39

Table A.23. SK-9 laboratory soil experiment results

Depth (m)	Water Content (%)	Natural Mass (g/cm^3)	Specific Gravity	Porosity
(0.00 – 10.00 m)	2.9	1.90	2.71	0.39
(10.00 – 15.00 m)	4.6	1.97	2.71	0.34
(15.00 – 25.00 m)	1.5	1.95	2.71	0.36
(25.00 – 35.00 m)	2.8	2.12	2.73	0.36
(35.50 – 45.00 m)	5.8	1.6	2.7	0.41
(45.00 – 55.00 m)	6.6	1.8	2.73	0.40
(55.00 – 60.00 m)	4.9	1.7	2.69	0.38
(60.00 – 65.50 m)	5.2	2.01	2.7	0.42
(65.50 – 68.50 m)	8.5	1.9	2.72	0.39
(68.50 – 70.00 m)	9.2	1.8	2.71	0.39

Table A.24. SK-10 laboratory soil experiment results

Depth (m)	Water Content (%)	Natural Mass (g/cm^3)	Specific Gravity	Porosity
(0.00 – 10.00 m)	2.9	1.90	2.71	0.39
(10.00 – 15.00 m)	4.6	1.97	2.71	0.34
(15.00 – 25.00 m)	1.5	1.95	2.71	0.36
(25.00 – 35.00 m)	2.8	2.12	2.73	0.36
(35.50 – 45.00 m)	5.8	1.6	2.7	0.41
(45.00 – 55.00 m)	6.6	1.8	2.73	0.40
(55.00 – 60.00 m)	4.9	1.7	2.69	0.38
(60.00 – 65.50 m)	5.2	2.01	2.7	0.42
(65.50 – 68.50 m)	8.5	1.9	2.72	0.39
(68.50 – 70.00 m)	9.2	1.8	2.71	0.39

Table A.25. SK-11 laboratory soil experiment results

Depth (m)	Water Content (%)	Natural Mass (g/cm^3)	Specific Gravity	Porosity
(0.00 – 10.00 m)	2.9	1.90	2.71	0.39
(10.00 – 15.00 m)	4.6	1.97	2.71	0.34
(15.00 – 25.00 m)	1.5	1.95	2.71	0.36
(25.00 – 35.00 m)	2.8	2.12	2.73	0.36
(35.50 – 45.00 m)	5.8	1.6	2.7	0.41
(45.00 – 55.00 m)	6.6	1.8	2.73	0.40
(55.00 – 60.00 m)	4.9	1.7	2.69	0.38
(60.00 – 65.50 m)	5.2	2.01	2.7	0.42
(65.50 – 68.50 m)	8.5	1.9	2.72	0.39
(68.50 – 70.00 m)	9.2	1.8	2.71	0.39

Table A.26. SK-12 laboratory soil experiment results

Depth (m)	Water Content (%)	Natural Mass (g/cm^3)	Specific Gravity	Porosity
(0.00 – 10.00 m)	2.9	1.90	2.71	0.39
(10.00 – 15.00 m)	4.6	1.97	2.71	0.34
(15.00 – 25.00 m)	1.5	1.95	2.71	0.36
(25.00 – 35.00 m)	2.8	2.12	2.73	0.36
(35.50 – 45.00 m)	5.8	1.6	2.7	0.41
(45.00 – 55.00 m)	6.6	1.8	2.73	0.40
(55.00 – 60.00 m)	4.9	1.7	2.69	0.38
(60.00 – 65.50 m)	5.2	2.01	2.7	0.42
(65.50 – 68.50 m)	8.5	1.9	2.72	0.39
(68.50 – 70.00 m)	9.2	1.8	2.71	0.39

Table A.27. SK-13 laboratory soil experiment results

Depth (m)	Water Content (%)	Natural Mass (g/cm^3)	Specific Gravity	Porosity
(0.00 – 10.00 m)	2.9	1.90	2.71	0.39
(10.00 – 15.00 m)	4.6	1.97	2.71	0.34
(15.00 – 25.00 m)	1.5	1.95	2.71	0.36
(25.00 – 35.00 m)	2.8	2.12	2.73	0.36
(35.50 – 45.00 m)	5.8	1.6	2.7	0.41
(45.00 – 55.00 m)	6.6	1.8	2.73	0.40
(55.00 – 60.00 m)	4.9	1.7	2.69	0.38
(60.00 – 65.50 m)	5.2	2.01	2.7	0.42
(65.50 – 68.50 m)	8.5	1.9	2.72	0.39
(68.50 – 70.00 m)	9.2	1.8	2.71	0.39

Table A.28. SK-14 laboratory soil experiment results

Depth (m)	Water Content (%)	Natural Mass (g/cm^3)	Specific Gravity	Porosity
(0.00 – 10.00 m)	2.9	1.90	2.71	0.39
(10.00 – 15.00 m)	4.6	1.97	2.71	0.34
(15.00 – 25.00 m)	1.5	1.95	2.71	0.36
(25.00 – 35.00 m)	2.8	2.12	2.73	0.36
(35.50 – 45.00 m)	5.8	1.6	2.7	0.41
(45.00 – 55.00 m)	6.6	1.8	2.73	0.40
(55.00 – 60.00 m)	4.9	1.7	2.69	0.38
(60.00 – 65.50 m)	5.2	2.01	2.7	0.42
(65.50 – 68.50 m)	8.5	1.9	2.72	0.39
(68.50 – 70.00 m)	9.2	1.8	2.71	0.39

APPENDIX B

HANTUSH MOUNDING SCENARIOS

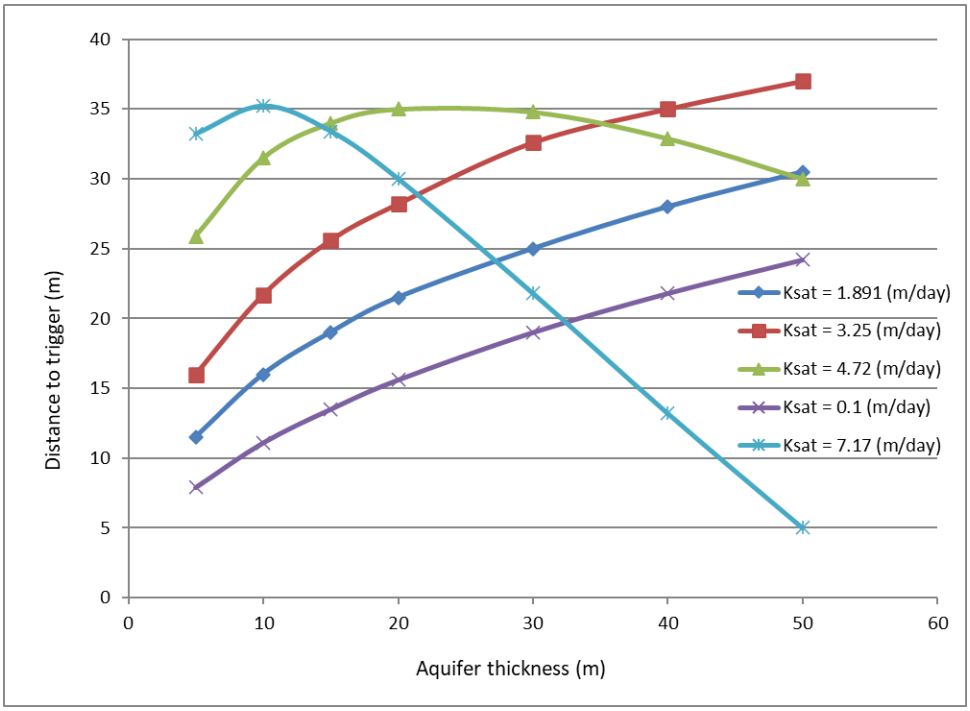

Figure B.1. Aquifer thickness vs. distance to triggered

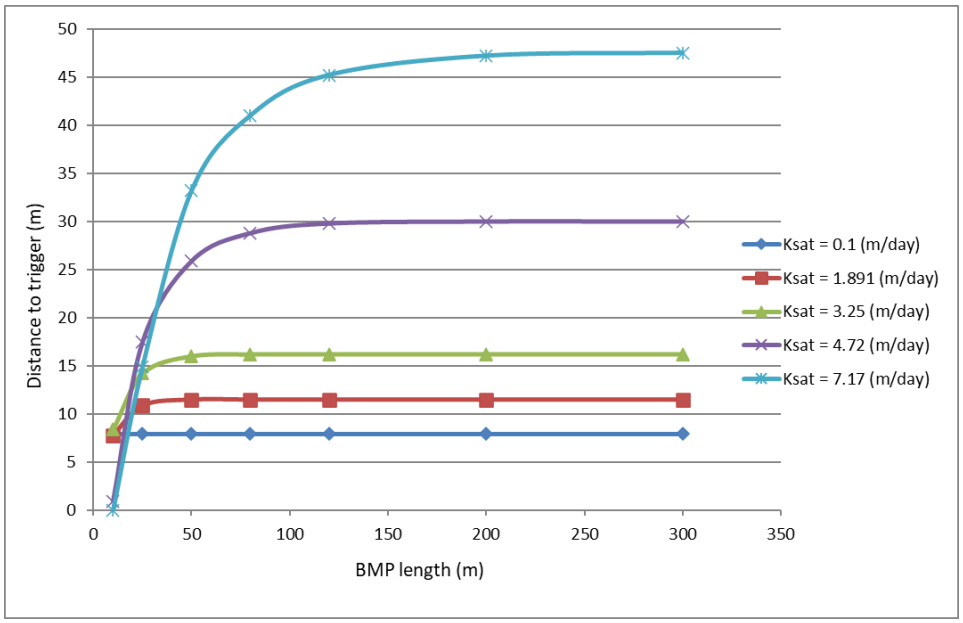

Figure B.2. Distance to triggered vs. basin length

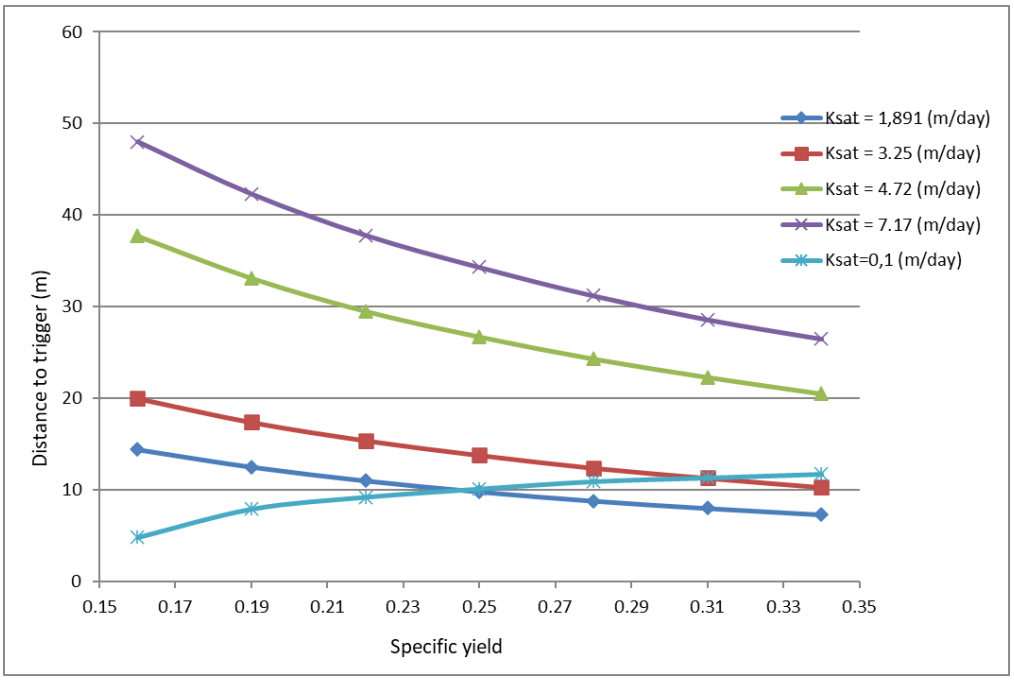

Figure B.3. Distance to trigger vs. specific yield

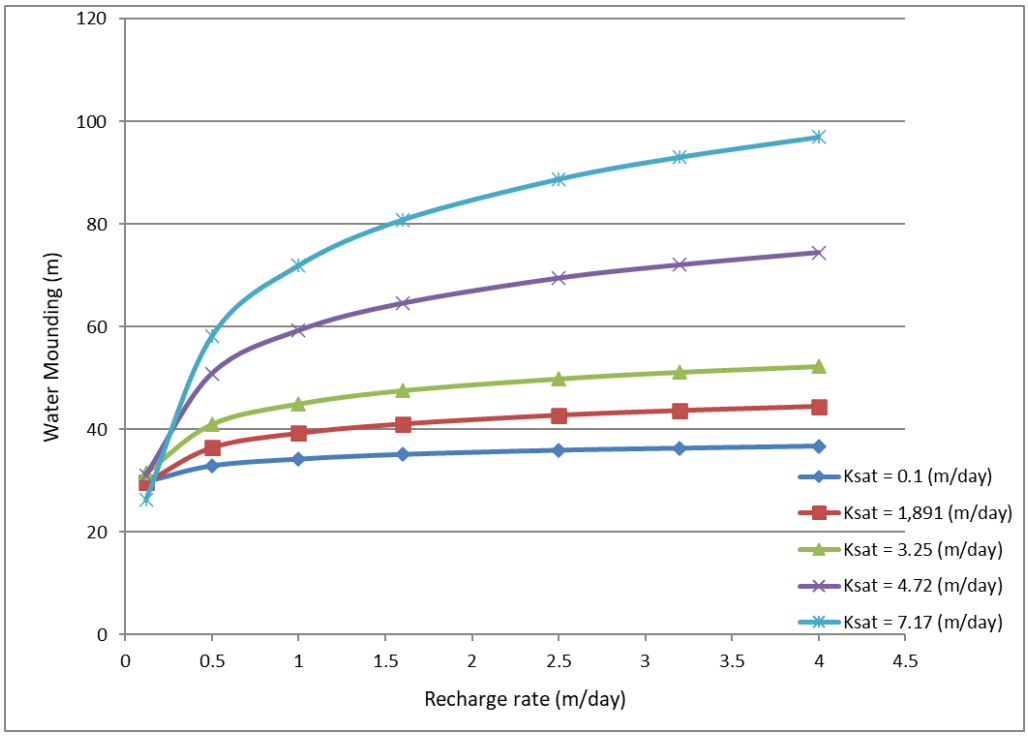

Figure B.4. Mounding vs. recharge rate

RECHARGE MODELING RESULTS

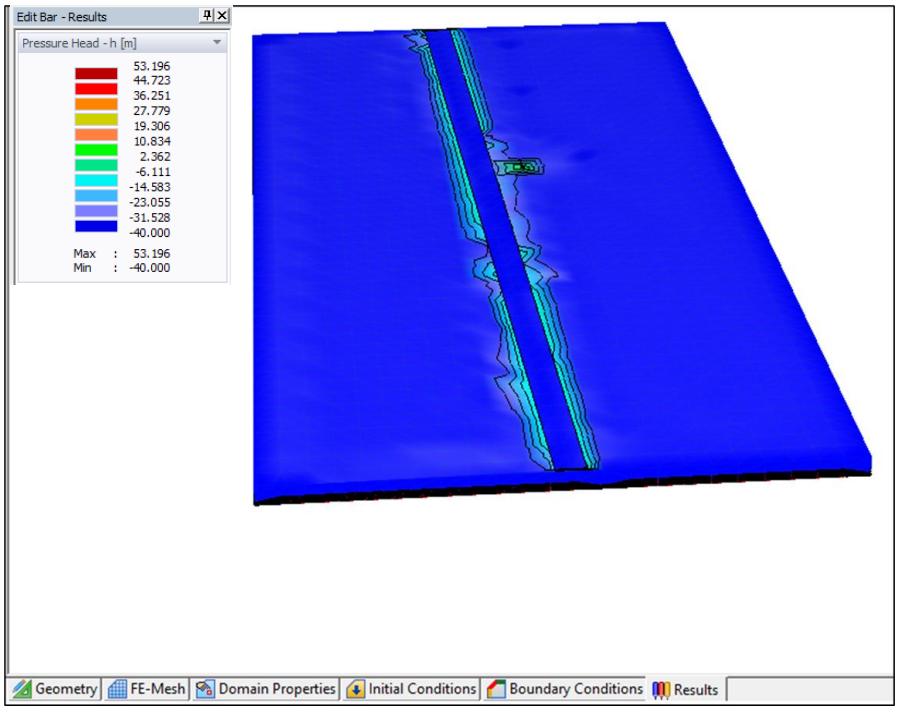

Figure B.5. Recharge model simulation (t= 60.day)

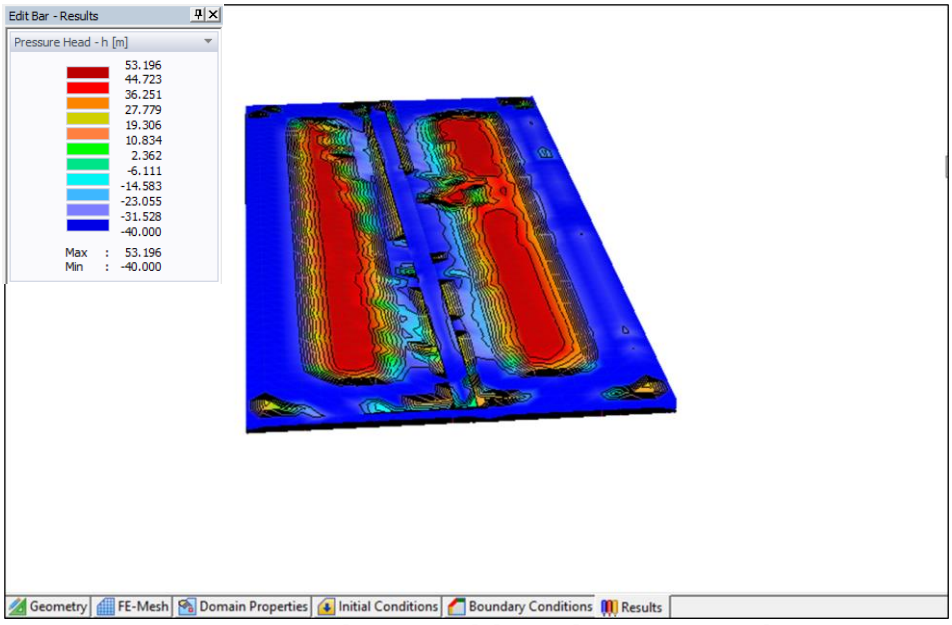

Figure B.7. Recharge model simulation (t= 180.day)

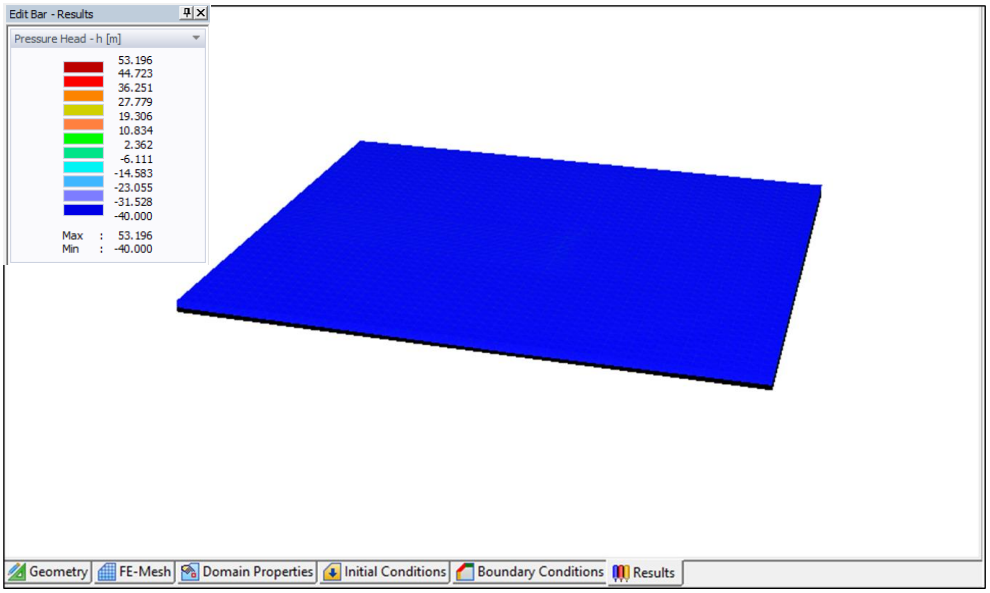

Figure B.8. Underground dam model simulation (t=0)

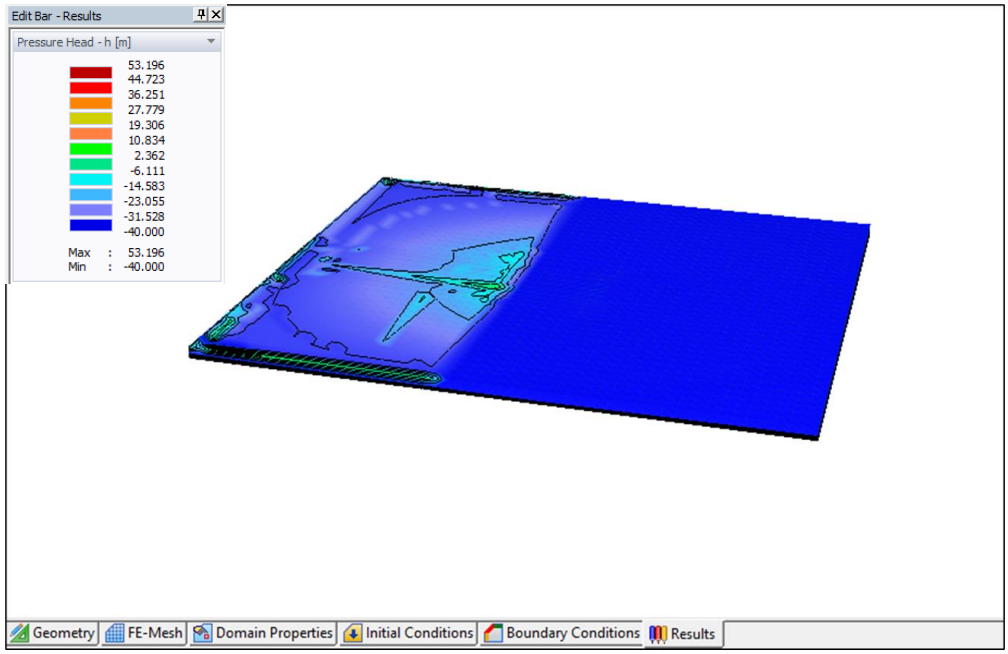

Figure B.9. Underground dam model simulation (t=60.day)

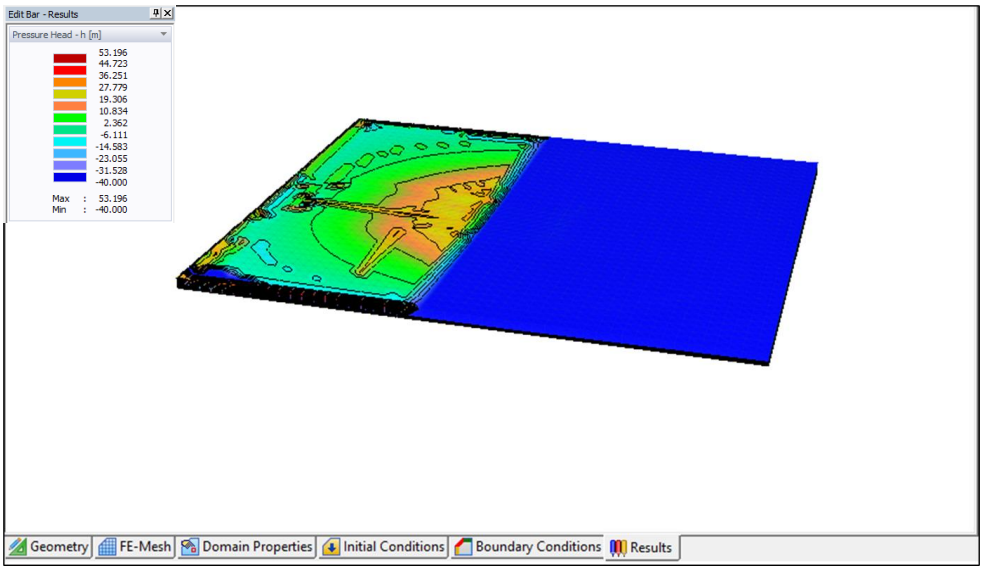

Figure B.10. Underground dam model simulation (t=120.day)

VITA

Yavuz Şahin

EDUCATION

M.Sc. in Civil Engineering **2013**
İzmir Institute of Technology, İzmir, Turkey
Title: Laboratory Tests To Study Stability Mechanism Of Rainfall Infiltrated Unsaturated Fine-Grained Soil Slopes Developing Into Shallow Landslides And Their Hydraulic Properties
Advisor: Prof. İsfendiyar Egeli

B.Sc. in Civil Engineering **2009**
Karadeniz Technical University, Trabzon, Turkey

CAREER EMPLOYMENT

Planning Engineer **2015 - Present**
Department of State Hydraulic Works

Research Assistant **2010 - 2013**
Civil Engineering Department
Izmir Institute of Technology

Project Assistant **2010 - 2013**
TÜBİTAK 109M635
Civil Engineering Department
IZTECH & METU

Site Engineer **2009 - 2010**
Gates Powertrain Company

PUBLICATIONS

PUBLISHED PAPERS

Sahin, Y., Baba, A., Tayfur, G., (2020). Dams of K. Menderes River Basin and Their Implications on The Agricultural Development. *İklim Değişikliği ve Çevre Dergisi, Su Vakfı.*

Sahin, Y., Baba, A., Tayfur, G., (2017). Küçük Menderes Havzası Su Kaynakları Sürdürülebilirliği. *DÜMF Mühendislik Dergisi.*

CONFERENCE PRESENTATIONS

Sahin, Y., Tayfur, G., Baba, A., (2017). Importance of Gördes Dam for İzmir Metropolitan City. 4th *International Water Congress 2-4 November,* İzmir, Turkey. (In Turkish)

Sahin, Y., (2017). Investigation of Surface and Groundwater Resources in Küçük Menderes River Basin. *9. Ulusal Hidroloji Kongresi*, Diyarbakır, Turkey. (In Turkish)

Sahin, Y., Tayfur, G., Baba, A., (2017). Sustainability of Water Resources in the K.Menderes River Basin. *9. Ulusal Hidroloji Kongresi*, Diyarbakır, Turkey. (In Turkish)